U.PORTO

FEUP FACULDADE DE ENGENHARIA
UNIVERSIDADE DO PORTO

NUMERICAL SIMULATION OF THE EFFECTS OF LIQUEFACTION IN SHALLOW FOUNDATIONS

PEDRO MELCHIOR MARQUES DE AGUIAR BARATA DE TOVAR

Dissertação submetida para satisfação parcial dos requisitos do grau de
MESTRE EM ENGENHARIA CIVIL — ESPECIALIZAÇÃO EM GEOTECNIA

Orientador: Professor Doutor António Viana da Fonseca

Coorientador: Doctor Ole Hededal

JULHO 2017

MESTRADO INTEGRADO EM ENGENHARIA CIVIL 2016/2017

DEPARTAMENTO DE ENGENHARIA CIVIL

Tel. +351-22-508 1901

Fax +351-22-508 1446

✉ miec@fe.up.pt

Editado por

FACULDADE DE ENGENHARIA DA UNIVERSIDADE DO PORTO

Rua Dr. Roberto Frias

4200-465 PORTO

Portugal

Tel. +351-22-508 1400

Fax +351-22-508 1440

✉ feup@fe.up.pt

http://www.fe.up.pt

To my family and A.M.D.G.

"But everyone who hears these words of mine and does not put them into practice is like a foolish man who built his house on sand. The rain came down, the streams rose, and the winds blew and beat against that house, and it fell with a great crash."
Matthew 7:26-27

ACKNOWLEDGEMENTS

Special thanks go to my supervisor Professor António Viana da Fonseca for giving me this opportunity and the wisdom and guidance during all the works. Along with all the technical support also the opportunity for this international and multicultural studying experience.

I am endlessly thankful to Ole Hededal and Giovanni Nicosia, my supervisors while at Lyngby COWI offices, for all the support and time given to make this possible and good for me. Learned a lot on the engineering practice and professional posture from you both.

I would like to acknowledge the valuable comments, discussions and motivation given by Professor Paulo Pinto, not only during this work but in all the last years of civil engineering study.

I also want to thank to all the people I met during the time of this work and that showed so different and important kinds of support and interests in the theme. The colleagues and friends at COWI/AS, the TOB group from St. Knud Lagard Church, the very multicultural barbecues group from the Hyrdevangen DTU residence, Fr. Richard and all the Malmö family, Eric and his great family and the party Venezuelan group. Also José Calejo at COWI/AS and Andres Fernandes who were critical supporters during my stay in Copenhagen.

I would like to thank to my friend Carlos Maria Azeredo, and colleague since ever, for all the motivation and assertiveness when I most needed it during all our time as students.

Eternal praise to my Lord and God who created the world and me with the desire and capacity to understand it.

ABSTRACT

Seismic hazards are one of the most powerful nature forces that threaten cities all across the globe. Specially when loose saturated sands underneath constructions are shaken and soil liquefaction is triggered. Although much research has been done in the field, numerical methods still show handicaps when soil-structure interaction has to be taken into account.

This project makes an overview of the current state of the art on the subject, focusing on the main works of the last decades and gathers recent case studies. A Christchurch building with settlements and tilting induced by soil liquefaction triggered by the February of 2011 earthquake is used as a case study. Structural and geotechnical information is gathered as well as observational data from before and after the seismic event.

A numerical simulation of soil and structure is made using PLAXIS®. The UBC3D-PLM is used to model the soil behaviour when liquefaction is triggered and deviatoric displacements take place induced by the presence of the structure. The soil model parameters are based on correlations with the SPT blow count number estimated from the cone penetration tests available as proposed by previous works on the field. Numerical simulation procedure and results are presented and comments are provided. The use of UBC3D-PLM for liquefaction simulation based only on CPT data has its limitations made clear and further developments are proposed.

KEY-WORDS: Liquefaction; Building settlements; Numerical modelling; Soil Dynamics; UBC3D-PLM soil Constitutive Model; Plaxis software; LIQUEFACT

RESUMO

Os sismos são uma das mais poderosas forças da natureza e ameaçam cidades dos quatro cantos do mundo. Em especial quando estas estão fundadas sobre depósitos de areias soltas e saturadas, que ao serem agitadas pelas ações sísmicas podem desencadear o fenómeno da liquefação dos solos. Embora muitos tenham sido os avanços feitos nesta área nos últimos anos, os métodos numéricos mostram limitações quando é necessário ter em conta a interação solo-estrutura.

Este trabalho faz uma revisão bibliográfica do atual estado da arte desta área, focando nos principais trabalhos das últimas décadas e reúne alguns casos de estudo recentes. Um edifício em Christchurch com assentamentos verticais e diferenciais consequência do despoletar do fenómeno de liquefação pelo sismo de Fevereiro de 2011 nesta cidade é usado como caso de estudo. Informação estrutural e geotécnica é reunida, bem como dados de observação local de antes e depois do sismo.

Um modelo numérico do solo e estrutura é criado com recurso ao software PLAXIS®. O UBC3D-PLM é usado como modelo constitutivo do comportamento do solo depois de despoletada a liquefação e inicio dos assentamentos como consequência da presença da estrutura. Os parâmetros do modelo constitutivo do solo são baseados em correlações com o número de pancadas do ensaio SPT, sendo este estimado através dos ensaios CPT disponíveis. O procedimento da modelação numérica e os seus resultados são apresentados e são feitos comentários. O uso do modelo UBC3D-PLM para simulação do fenómeno de liquefação de solos somente baseado em ensaios CPT tem as suas limitações que são apresentadas, sendo feitas propostas para desenvolvimento futuro.

PALAVRAS-CHAVE: Liquefação; Assentamentos de edifícios; Modelação numérica; Dinâmica de Solos; modelo constitutivo UBC3D-PLM; software PLAXIS

TABLE OF CONTENTS

FIGURES INDEX

TABLES INDEX

ABBREVIATIONS AND SYMBOLS

LATIN ALPHABET

a_{max}	Maximum horizontal acceleration at the ground surface
g	Acceleration of gravity
GPe	Elastic shear modulus
K^e	Elastic bulk modulus
k_B^e	Bulk moduli number at a reference stress level
k_G^e	Shear moduli number at a reference stress level
p_A	Atmospheric pressure (i.e. 100kPa)
p	Mean effective stress
p_W	Porewater Pressure
r_d	Depth-dependent shear stress reduction coefficient
R_U	Excess Porewater Pressure Ratio

GREEK ALPHABET

τ_{av}	Average cyclic shear stress
σ_v	Total vertical stress
$\sigma_v o$	Initial total vertical stress
$\sigma_v^{'}$	Effective vertical stress
$\sigma_{vo}^{'}$	Initial effective vertical stress
σ_{max}	Maximum principal total stress
σ_{int}	Intermediate principal total stress
σ_{min}	Minimum principal total stress
φ_p	Peak effective friction angle
φ_m	Mobilised friction angle
ψ_{mob}	Mobilised dilation angle

ABBREVIATIONS

CBD	Christchurch Business Center
CCCC	Christchurch Cathedral College
CSR	Cyclic Stress Ratio
CRR	Cyclic Resistance Ratio
CPT	Cone Penetration Test
CVR	Critical Void Ratio
FS	Factor of Safety
GWL	Ground Water Level
HS	Hardening Soil (soil constitutive model)
LS-I/II	Lismore Street Buildings I and II

LPI	Liquefaction Potential Index
LPI_{ISH}	Ishihara inspired liquefaction potential index”
LSN	Liquefaction Severity Number
M06	Analyses proposed by Moss and coleagues in 2006 in [33]
MSF	Magnitude Scalling Factors
NCEER	National Center for Earthquake Engineering Research
NZGD	New Zealand Geotechnical Database
PGA	Peak Ground Acceleration
RC	Reinforced Concrete
RW98	Analyses proposed by Robertson and Wride in 1998 in [30]
SSI	Soil-structure interaction
SPT	Standard Penetration Test

1
INTRODUCTION

1.1 INTRODUCTION AND OBJECTIVES

Liquefaction is a natural seismic-induced phenomena especially, but not only, triggered in loose and saturated sandy soils. When it happens the soil strength and stiffness are reduced and a wide spectrum of consequences are to be expected. Historical research shows that the phenomena was observed and documented trough history. Although observed before, the first substantial consequences were identified in the Western World after the 1755 Lisbon earthquake. [29]

In 1964 the well known Niagata and Alasca seismic events made high number of causalities and mass structural damage in the near cities. After the major building damages were attributed to the liquefaction phenomena, the technical community understood that to guarantee the cities earthquake-resilience it was necessary to mitigate the potential consequences of liquefaction on buildings. Global scale research started and empirical methods for liquefaction triggering and consequences assessment started to be accessible for practical engineering. Mitigation measures were also studied and enforced in critical projects.

On February 22nd 2011 a energetic M_w6.2 earthquake arrived to Christchurch, New Zealand. The consequences were catastrophic counting for 180 casualties, big economic losses and half of the Business Center buildings being closed for safety reasons. Again the substantial importance of this event for the scientific community because most of the damaged structures settled, slid, tilted, and collapsed partly due to liquefaction.

Present day procedures for liquefaction assessment are based on validated empirical and semi-empirical methods correlated to *in situ* tests. However this methods base their analyses on the likelihood of liquefaction being triggered and not on the consequences it might have on buildings. This fact makes the performance-based approach for structures impossible when using these methods. Besides this fact these practices only take into account the settlements due to volumetric-strain, that is consequence of the produced excess porewater pressure dissipation. Although volumetric mechanisms are the only ones

taken into account by these methods, research shows that the main mechanisms producing settlements and building failures are shear mechanisms.

Numerical modelling is presented as a possible solution for achieving results that are performace-based and consider shear mechanisms consequences. UBC3D-PLM soil constitutive model combines a relative overall simplicity and a powerfull approach to simulate liquefaction triggering and consequences on sandy and non-plastic silty soils. It uses isotropic and kinematic hardening rules for primary and secondary yield surfaces, in order to take into account the effect of soil densification and predict a smooth transition into the liquefied state during undrained cyclic loading. [40]

This work assesses the ability of a numerical code like PLAXIS®, with a soil constitutive model specifically for liquefaction simulation, the UBC3D-PLM, to correctly simulate liquefaction induced settlements on a building with shallow foundations. A substantially well documented case study of a building in Christchurch, New Zealand was numerically simulated using PLAXIS® software as it combines soil and structure numerical modelling. For the mentioned simulation, the UBC3D-PLM soil constitutive model is used and its parameters are computed solely based on CPT results using correlations proposed by Beaty and Byrne [26]. Empirical analyses on the available CPT results are performed and used for comparison with the observed building consequences. The study case building was founded on a peripheral strip footing, however for simulation simplicity the shallow foundation was considered constantly distributed bearing pressure, as a tipically rigid mat foundation.

1.2 THE FRAMEWORK

This work is divided into nine chapters where first three focus on giving an overview of the current state of the art and practice on the subject as well as state previous key information, as follows:

Chapter 2 makes an overview on the liquefaction phenomena throughout the human ages and what is now studied as a natural phenomena with the framework of soil mechanics. Also provides an insight on the problem of soil-structure interaction during and after the earthquake. The soil failure mechanisms due to liquefaction under structures are also described and studied and information from recent research is presented.

Chapter 3 serves as an information summary and explanation of the current practice on liquefaction assessment methods, specially focused on the use of the simplified procedure based on the cone penetration tests. Some methods for liquefaction consequences estimation are presented and their limitations stated.

Chapter 4 introduces the UBC3D-PLM soil constitutive model with its theoretical basis and correlation with the CPT results used in present work.

Chapter 5 describes the search and choosing of the study site used for the simulation and then reports the gathering of the available data on the soil layers, building structures and seismic loading.

Chapter 6 presents the simplified procedure analyses applied to the CPTs available and the results

are compared with the *in situ* observations after earthquake. Obtained results are then discussed and conclusions are made.

Chapter 7 outlines the needed procedure for the creation of the intended numerical simulation. The soil constitutive model parameters are computed, the structure is presented and damping values computation is explained. The specific PLAXIS® simulation phases are outlined and made assumptions justified.

Chapter 8 presents and discusses the numerical simulation results and compares the obtained results with the *in situ* observed ones.

Chapter 9 concludes with a brief summary of present dissertation and there the author tries to propose paths for further developments.

2
THE LIQUEFACTION PHENOMENA

Earthquake-induced liquefaction phenomena is of great concern for structures that are founded on relatively loose and saturated deposits of soils in seismically active regions. This has been proven by history, and specially in more recent years as more assessment capacity is made possible.

The present chapter makes an overview of the phenomena by firstly giving an historical perspective of building consequences when it is seismically induced. Secondly the scientific framework of soil mechanics is given to make possible the interpretation of the specific phenomena. The consequences in the built environment are then presented based on observational data from historical and recent years on the next section. Interesting conclusions from important works on the field are presented and discussed.

2.1 THE LIQUEFACTION INDUCED DAMAGE ON BUILT ENVIRONMENT

2.1.1 THE LISBON EARTHQUAKE

As Coelho presents in [29] the 1755 Lisbon earthquake seems to stand as the first seismic event after which earthquake-induced liquefaction was explicitly reported in the Western World. Although pointing the fact that the phenomenon had already been observed in Japan since 686.

The Lisbon earthquake took place in the first day of November of 1755 and is estimated to have magnitudes in the interval of 8.7 to 9.0 in the Ritcher scale. The combined effects of the earthquake induced tsunami and fire in the city downtown created large-scale damages. The so called large-scale damages can be observed in the pictures from Figure 2.1, and also the characteristic consequences of liquefaction triggering on buildigns tilting and settlements. Estimated consequences of 10.000 causalities, most of the capital city destroyed, as well as mass devastation on Southern Portuguese smaller cities.

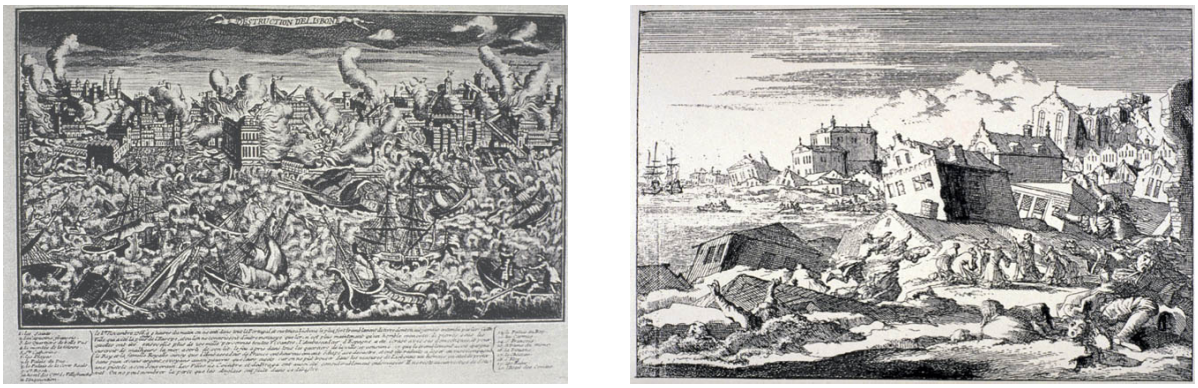

(a) (b)

Figure 2.1: Representation of the 1755 Lisbon earthquake damages.

As presented in [29] is a description by Rev. Charles Davy, a survivor of the upper cited earthquake:

"[...] I saw many large cracks and fissures in different parts; and one odd phenomenon I must not omit, which was communicated to me by a friend who has a house and wine-cellars on the other side of the river, viz., that the dwelling-house being first terribly shaken, which made all the family run out, [...], and immediately a great number of small fissures appeared in several contiguous pieces of ground, from whence there spouted out, like a jet stream, a large quantity of fine white sand to a prodigious height."

Another interesting description from a survivor is found in [9] and translated here, where liquefaction phenomena is clearly described:

"Terreiro do Paço [square in the Lisbon downtown] [...] as well as the drowning of the huge wharf made of stone close to this square [...] due to each of the strong shaking we were drowning; [...] and everywhere there were huge fissures, and from most of them there were water and sand coming out"

2.1.2 Recent consequences of liquefaction on buildings

With the focus on shallow founded buildings and based on the thesis of Zupan [18] some cases are presented in the following lines. The February 27th of 2010 M8.8 earthquake centered in Maule, Chile had its damaging effects on several cities, making more than 700 causalities and having big economic consequences.

A very peculiar consequence of this seismic event has big interest for this work: an hospital facility in Curanilahue, Chile. Opened only 2 years before and consisted on 10 structurally isolated wings with heights ranging from one to six stories, as shows the plant on figure 2.2. The taller wings being between the tallest buildings in the city. The foundation system consisted of shallow, isolated footings and strip footings beneath walls that were interconnected with grade beams [18].

Throughout the hospital site there is evidence of liquefaction around and adjacent to the structures. This becomes interesting given the fact that no liquefaction evidence was observed in the nearby areas with smaller buildings, which points out the importance of the structural inertial loads on the cyclic shear stresses

imposed on a buildings foundation soil. [18]

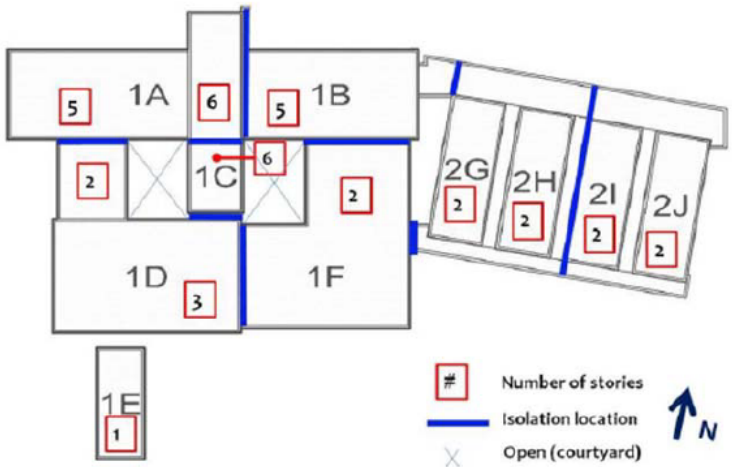

Figure 2.2: Plan view of the hospital where the isolation location and number of stories of each wing can be seen [18]

Two other relevant observed facts on [18]: the tallest wing settling the most and that structural damage was limited because of the isolation gaps between the wings.

Another case appears in Concepcion, Chile, as a consequence of the same seismic event, were [17] documented a group of four eight-story condominium buildings founded on shallow spread footings. For raising the ground level and make construction possible sandy fill was used across the site, being afterwards the earthquake observed liquefaction evidence of this same material through the site. As before, no evidence of liquefaction was observed in the street surrounding the site nor at an adjacent property with one to two-story residences.

Another case noted by [18] occurred as consequence of the 2011 M9.0 Tohoku, Japan earthquake in the Kanto plain region. Especially across the towns of Naka-Machi and Shin-Machi, in Tokyo that were a result of space reclaimed to the sea with sand excavated from Tokyo bay in 1964. Localised settlement depressions were observed around buildings, in addiction to broader uneven ground settlements, both observed in this reclaimed area and had no equal behaviour in the coastal area contemporary to 1964.

A detailed study [20] on this site led to the following relevant findings resumed by [18] as follows:

- in areas affected by liquefaction, settlements up to 60 cm were observed; settlements and tilts of buildings and foundations were pervasive as well as settlement of ground around pile-supported buildings damaged utilities;
- even when foundations settled and tilted, few superstructures atop rigid foundation systems were damaged;

- reinforced concrete houses and houses with RC flooring on the first floor tended to have larger settlements, likely because of higher contact pressure;
- buildings facing each other across a street tended to tilt away from one another, whereas buildings close to one another tended to tilt towards one another. This latter observation was attributed to the combined loads of adjacent buildings causing higher settlements on the shared side
- several pile foundations were damaged, and this was likely caused by permanent lateral ground displacement;
- in many of the reclaimed areas unaffected by liquefaction, ground improvement of some kind had been performed previously.

Figure 2.3 shows an iconic photograph after the 2011 M9.0 Tohoku, Japan earthquake event studied in [20] where different building settlements caused by soil liquefaction can be seen depending on their foundation characteristics or nonexistence of any structure. The soil around the building on the left, pile-founded, settles approximately 40 cm relatively to it, while the building on the right settles 30 centimetres relatively to the surrounding ground. This is a clear case of a shallow-founded building punching into the ground and experiencing more liquefaction-induced vertical settlement than the liquefaction-induced 1-D volumetric reconsolidation settlements of the surrounding level ground. [18]

Figure 2.3: Buildings supported on pile (left) and shallow foundation (right) after the 2011 M9.0 Tohoku, Japan earthquake event

In the more recent years is of major importance the 2010-2011 Canterbury earthquake sequence. That included 7 events with magnitudes above 5.5, together creating a very large number of casualties and economic losses [18]. This being a known critical seismic zone it was already under surveilance, and there is very high quality data on the earthquake event and building observed performance, making it a good case study and

base for many works and research on the field in the present days. Of special interest is the February 22nd, 2011 M6.2 event, that caused significant liquefaction and building damage in the Central Business District (CBD) of Christchurch. Where half the buildings were marked as restricted access because of potential safety issues. Based on what is stated above, this case will be the main focus of the present dissertation.

2.2 THE LIQUEFACTION PHENOMENA IN SOIL MECHANICS

The science objective is to create a framework to read the natural laws, and soil mechanics is no exception. In this work it becomes important to state how does soil mechanics understands and describes the liquefaction phenomena and how it is influenced.

Liquefaction is often described in the literature as the phenomena of seismic generation of excess porewater pressures and consequent softening of granular soils. [37]

Dry soil subjected to monotonic (i.e., unidirectional) shear loading may either decrease or increase in volume depending on its initial density and initial effective confining stress and on the levels of induced shear strain. Initially loose soil typically will tend to contract (i.e., decrease in volume and become denser) as it is sheared. Under the same confining pressure, initially dense soil will first contract but then dilate (i.e., increase in volume and become looser) as it is sheared. [37]

This can be observed in Figure 2.4 plots representing the paths of loose and dense soil specimens under perfectly drained or undrained loading. Also represented is the Critical Void Ratio (CVR) curve as it commands the different behaviours.

The CVR line describes the state toward which any soil specimen would migrate at large strains , whether by volume changes under drained conditions, changes in effective confining pressure under undrained conditions, or some combination under partially drained conditions. [22]

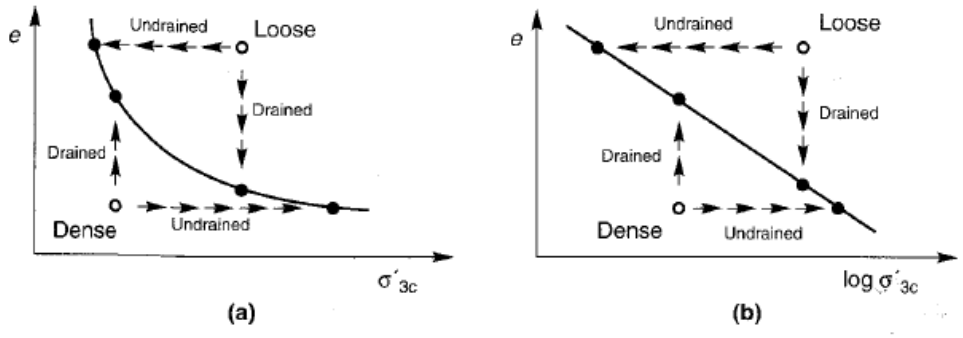

Figure 2.4: Behaviour of initially loose and dense specimens under drained and undrained conditions for (a) linear and (b) logarithmic effective confining pressure scales, by [22]

On the other hand, when initially loose or dense dry soils are subject to repeatedly reversing (cyclic) shear stress, they tend to decrease in volume, or contract, regardless of whether initially loose or dense. As the

monotonic loading induced liquefaction is not on the scope of this dissertation, but the earthquake induced liquefaction, the second one will be the one further studied.

When saturated soils are unable to contract due to water in the soil pores, the water pressure increases. If it reaches the level of the initial effective stress, liquefaction can be triggered. The extent to which a soil tends to contract or dilate during shearing dominates liquefaction behaviour. [37]

Figure 2.5 shows a sequence of three pictures by Ishiara in [19] that present the mechanical principles behind the liquefaction triggering in a chronological order from (a) to (c). The scheme is a virtual triaxial test where the soil total and effective stresses as well as the porewater pressure measures are taken in very perceptible ways. After the static phase in (a), (b) is the seismic intermediate phase where the porewater pressure increased due to contractive and undrained soil behaviour. This undrained behaviour is the consequence of the very quick loading created by the earthquake, not making possible to dissipate de porewater pressure as it is created inside the soil layers. When the consolidation phase takes place (c) the porewater pressure comes to an equilibrium creating a vertical settlement in the sample.

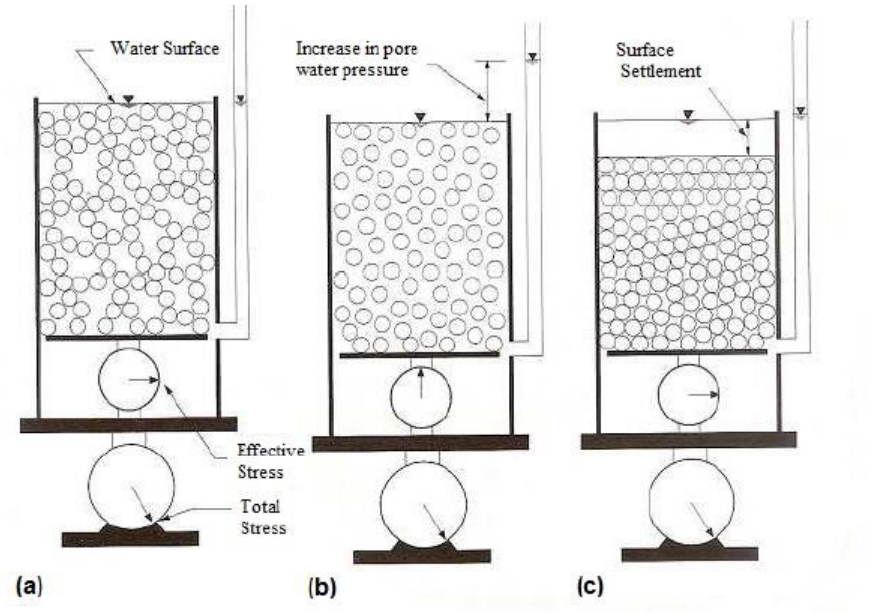

Figure 2.5: The Ishiara [19] scheme to explain the liquefaction triggering mechanism

The most complete form of liquefaction is triggered when the porewater pressure reaches the total value of vertical stress. However intermediate values of water pressure produce soil softening and must be taken into account as they are of vital importance. Because of this the following ratio is used in the literature as follows:

$$r_U = \frac{p_W}{\sigma_v} \tag{2.1}$$

where r_U is the excess porewater pressure ratio, p_W is the porewater pressure and σ_v is the total vertical stress.

Liquefaction is perfectly triggered when r_U equals the unit value. However substantial ground softening and possible colapse is reached for values of 0.8, or even lower values for specific soil characteristics. [37] Moreover [27] considers zones with a maximum r_U greater than 0.7 to be liquefied.

2.3 The liquefaction phenomena and its consequences on built environments

2.3.1 The soil failure mechanisms due to liquefaction under structures

Based on the literature review made by Shideh Dashti on [35], Joshua Zupan in [18] summarises the key findings on the soil failure and settlement mechanisms. The key findings on shallow founded buildings are here summarised in the following paragraphs, this being the main focus of this work.

Based on the consequences of the 1964 M_w 7.6 Niigata earthquake and of the 1990 M_w 7.7 Luzon, Philippines seismic event in Dagupan City, it was concluded that partial or complete bearing failures happened mostly in two- to four-story buildings shallow founded on relatively thick and uniform deposits of clean sand. Building with similar conditions but wider foundations generally settled less. [38] [42].

The data from these two sources was then plotted in [23], normalising the average foundation settlement and the the building width by the liquefied layer thickness. Good correlations were achieved as observed in Figure 2.6

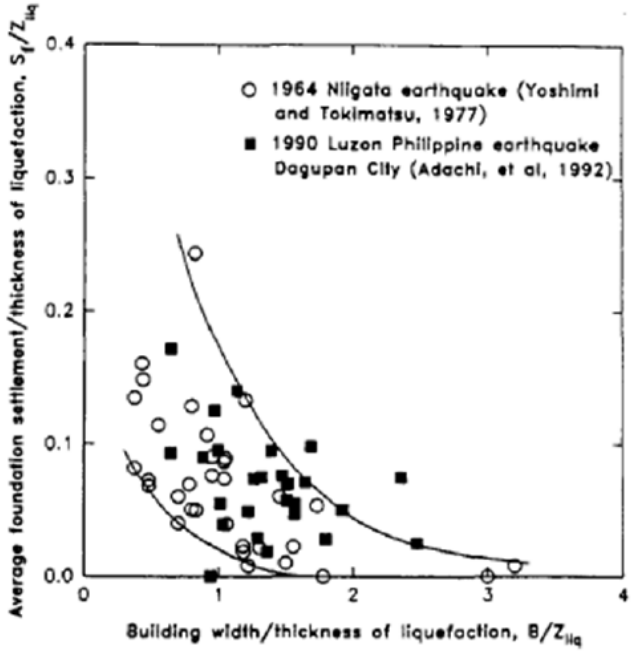

Figure 2.6: Achieved correlation of the normalised foundation settlement and building width by the liquefied layer thickness from [23]

From the data of the 1964 Niigata, Japan earthquake, [41] concluded that if the ratio of the building width to the thickness of the liquefiable soil layer is less than 3, the structures will settle more than the free-field soil.

During the 1999 Mw 7.4 Kocaeli earthquake buildings in Adapazari, Turkey punched into the ground, tilted and underwent horizontal movements due to liquefaction or cyclic softening of shallow and relatively thin layers of silts of low to medium plasticity, as ilustrated by Figure 2.7. Some conclusions are made by Zupan in [18] as follows.

Many of the Adapazari buildings where three- to six-stories of reinforced concrete (RC) frame structures and mat foundations at depths of about 1.5 meters. The groundwater level was between 1 and 2 meters depth and the PGA value was estimated to be in the 0.35 to 0.45g interval. The ground failures were observed to happen near structures and less when far from them. Building settlements were found to be directly proportional to the building's contact pressure, and its ratio of height to width was seen to influence the amount of building tilt.

Figure 2.7: Adapazari building that overturned due to liquefaction

A series of 1g horizontally loaded shaking table tests performed by Yoshimi and Tokimatsu in [42] of a rigid model structure on saturated Toyoura Sand with different relative density values led to some interesting conclusions: the excess pore water pressure ratios under the center of the structure were smaller than away from the structure and the excess pore water pressure ratio, R_U, decreased as the weight of the structure increased. When the R_U reached 0.6, the structure settlement increased and it decreased with the increasing of the footing width for a given thickness of liquefiable soil layer.

Dashti [35] advances some conclusions based on the centrifuge experiments on rigid circular footings on

liquefied or cyclic softened soil by [34] and [23]: the excess pore water pressure ratios were smaller beneath the model structures than at locations far from them and building settlements occurred mainly during shaking and not during the pore pressure dissipation.

Liu and Dobry [23] in the above cited experiments observed that increasing the relative density of the foundation soil decreased the settlements of the structures.

After this set of conclusions from past experiments and in-field observations, there is substantial interest in understanding the mechanisms presented in [32], specially the ones related to settlements created by deviatoric ground movements. Figure 2.8 schematically reproduces these mechanisms, which explanations follows.

Seed in [32] presents this cases divided into three different groups based on the causes for the mechanism: Figures 2.8 (a) and (b) account for mechanisms consequence of soil volumetric reduction or loss; Figures 2.8 (c) through (f) represent failure mechanisms due to deviatoric ground movements and Figures 2.8 (g) through (i) illustrate structural settlements due to full or partial bearing failures.

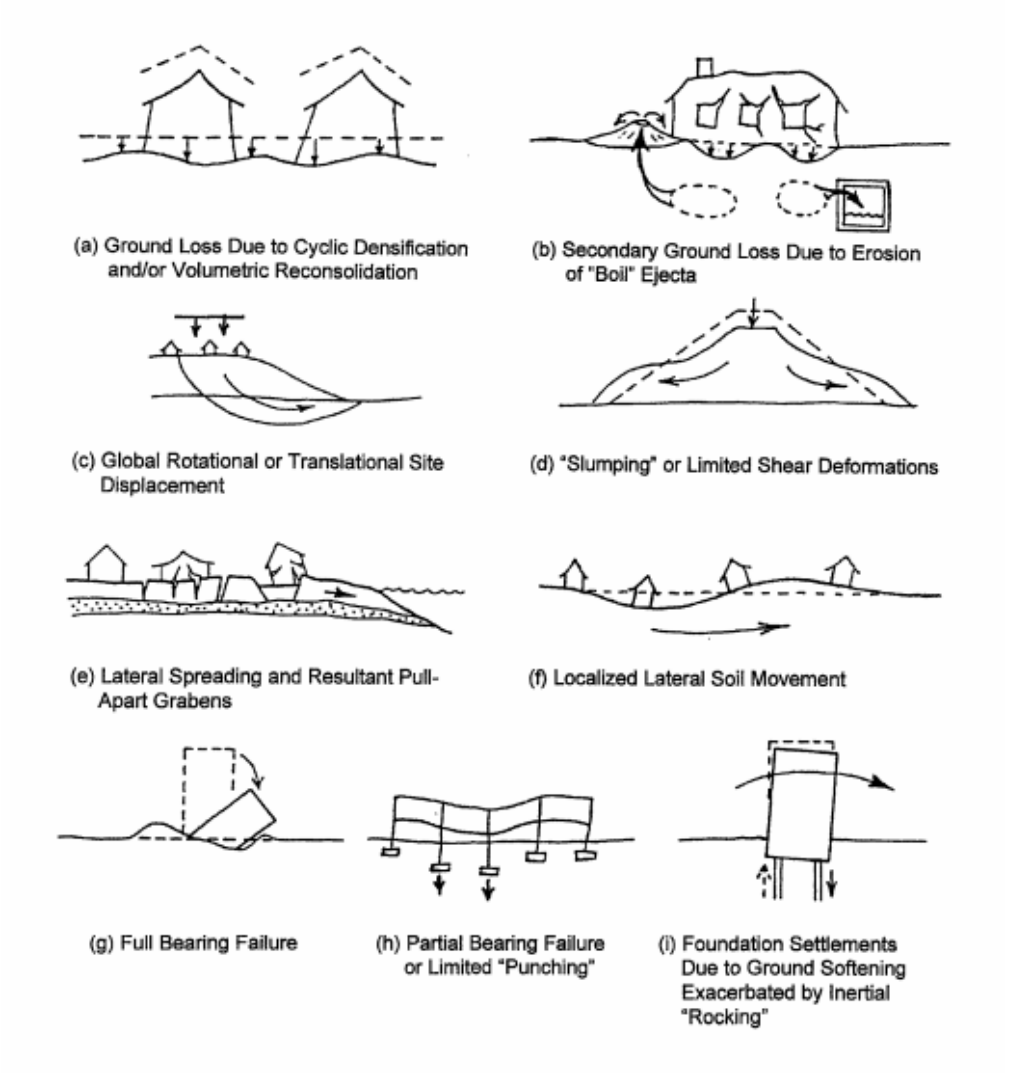

Figure 2.8: Liquefaction-induced vertical settlements mechanisms as [32]

Figure 2.8 (a) represents an "apparent ground loss" causing soil surface to settle with a differential distribution. This "apparent ground loss" is consequence of one or a combinations of both two different phenomena: the cyclic densification of the non-saturated soil and the volumetric reconsolidation of liquefied (or partially liquefied) soils as cyclically-induced pore pressures escape by drainage. Although the overall magnitude of these settlements can be reasonably well predicted by several methods (Tokimatsu and Seed 1987 and Ishiara and Yoshimine, 1992), the locally differential settlements magnitude and distribution cannot be reliably predicted.

Figure 2.8 (b) shows a mechanism of ground loss because of the erosion of soil particles carried by water escaping through cracks and fissures (often referred to as "sand boils") as excess pore water is dissipated to reach the hydrostatic equilibrium. This "soil transportation" can occur in two directions: to the ground

surface or to accessible buried voids as basements, culverts and sewers. It is essentially impossible to predict and creates locally differential settlements. Two mitigation measures often implemented are: to ensure sufficient lateral continuity of foundations as to be able to "bridge" or cantilever over localized subsidences and construct deep foundation support (piles or piers) extending beneath the depth of potential ground loss.

Figure 2.8 (c) and (d) show two mechanisms of slope failure due to liquefaction: the global rotational or translational site displacement and the "slumping" of the embankment due to large shear deformations. Both this ground movements produce settlements at the crests or heels of the slopes or embankments. When these types of potential liquefaction-induced deformations and displacements are "large", higher than 1 meter, then they are amenable to engineering prediction. However, for small to moderate (approximately 0.05 to 0.75 meters) levels of deformation the current methods are not capable of displacement estimation. Therefore, significant judgement is currently required to asses the likely deformations, and their impact on structures and other engineered facilities. The lack of reliable and well-calibrated analyses tools here often results in the need for conservative assumptions, and often leads to implementation of conservative hazard mitigation measures.

Figure 2.8 (e) and (f) represent very similar mechanisms that can produce surface settlements. Figure (e) illustrates the creation of grabens as consequence of the soil lateral spreading that creates potentially damaging local differential settlements on surface. Figure (f) represents localised lateral soil movement that produces both heaving and settlements as the overall soil volume is mainly conserved. As the previous analysed pair of mechanisms, these two are also difficult to predict, and again, conservative assumptions and mitigation measures must be taken into account whenever these mechanisms are considered potentially serious hazards for a constructed site.

Figure 2.8 (g) shows the case when the liquefaction-induced loss of strength and stiffness of the soil is sufficiently severe to produce a full bearing capacity failure. This can produce very large "punching" settlements (tens of centimetres or more) and in the case of slender structures, can even lead to toppling.

Figure 2.8 (h) illustrates partial bearing failure or limited "punching" settlements that can happen at one or more isolated footings, or can occur at mat and raft foundations (especially at corners and edges). These settlements are associated with situations where post-liquefaction shear strength is still sufficient to prevent a full bearing capacity failure, but as a result of the cyclic softening some settlements may appear. These settlements are further complicated to estimate because of the interaction between the soil and the structure on surface, as the structure increases the cyclic vertical loads due to inertial "rocking" with cyclic softening, as also seen on Figure 2.8 (i). The mechanisms presented in these two picture are especially important given the fact that no reliable settlements estimation is currently available and being this one of the most common settlements mechanisms due to soil liquefaction .

3
LIQUEFACTION ASSESSMENT METHODS

Two seismic events created major consequences due to liquefaction triggering in 1964. Those were the 9.2 magnitude earthquake that struck Prince William Sound, in southern Alaska, US, causing severe damage in the form of liquefaction (as cited in [29]). And a few months later, another strong tremor in Niigata, Japan, resulted in 36 causalities and 3500 houses destroyed due to severe liquefaction-induced damage to numerous structures and produced some of the most notable illustrations of the potential effects of liquefaction [29].

Certain that most of the structural damage was observed to be due to the liquefaction phenomena, it became clear that further investigation on this subject was needed [39].

3.1 THE SIMPLIFIED PROCEDURE

Professors Seed and Idriss made the first important work with the objective of creating a normalised procedure for assessment of liquefaction potential for given soil and seismic loading. Published in 1971 and often referred to as the "Simplified Stress-Based Procedure", or simply "Simplified Procedure". Since that year this has been the most used and widespread liquefaction assessment method for practical engineering [37] and the one and only included in design codes [25].

During the past years and since 1971 this method has been object of continuous modification for improvement. Although its framework never changed and it is this framework which this chapter tries to present and then its use based on CPT data. The very basis of the framework has a lot in common with other security assessment methods used in engineering practise by appealing to a Factor of Safety (FS), in this case against liquefaction triggering, that is defined as the following quotient:

$$\mathrm{FS} = \frac{\mathrm{CRR}}{\mathrm{CSR}} \tag{3.1}$$

where CSR - Cyclic Stress Ratio is the seismic demand at a given depth due to earthquake shaking and CRR - Cyclic Resistance Ratio is the CSR value that triggers liquefaction. So to speak CRR is the capacity of the soil to resist to liquefaction.

3.1.1 THE CYCLIC STRESS RATIO

For sites where ground slope is less than 6% the earthquake-induced shear stresses are assumed to be solely due to the vertical propagation of the shear waves [39] and can be computed by one-dimensional dynamic response analysis of the soil deposit [14].

Because of the difficult and time-consuming computation of the soil dynamic response, due to the necessity of good soil characterisation and ground motions input, [14] proposed the following simplified equation for CSR estimation:

$$\mathrm{CSR} = \frac{\tau_{av}}{\sigma'_{vo}} = 0,65 \cdot \left(\frac{a_{max}}{g}\right) \cdot \left(\frac{\sigma_{vo}}{\sigma'_{vo}}\right) \cdot r_d \tag{3.2}$$

where the quotient between the average cyclic shear stress τ_{av} and the initial effective vertical stress σ'_{vo} is a normalised value for measuring the imposed loading to the ground by a given earthquake: this quotient being the basis for the following formula. The $0,65$ value accounts for reducing this maximum value, that otherwise would happen only one time during the earthquake to a more frequent value, so it can be considered a cyclic loading; a_{max} is the maximum horizontal acceleration at the ground surface; g is the acceleration of gravity; σ_{vo} and σ'_{vo} are the initial total and effective vertical stresses, respectively and r_d is a depth-dependent shear stress reduction coefficient that takes into account the flexibility of the soil deposit as it behaves with a nonrigid response and which explanation follows.

As observed in figure 3.1b there are various curves to estimate the evolution of r_d in depth: The curve named "Cetin and Seed (2004)" from [21] is based on 50 study sites and 42 different input motions combined using SHAKE91 software. Plus 53 well-characterised real sites responses that have liquefied in previous earthquakes, this procedure creates a database of 2153 site responses ploted in Figure 3.1a. This relation is considered more representative of the cyclic shear stress at liquefaction sites than other $\mathrm{r_d}$ curves. [37].

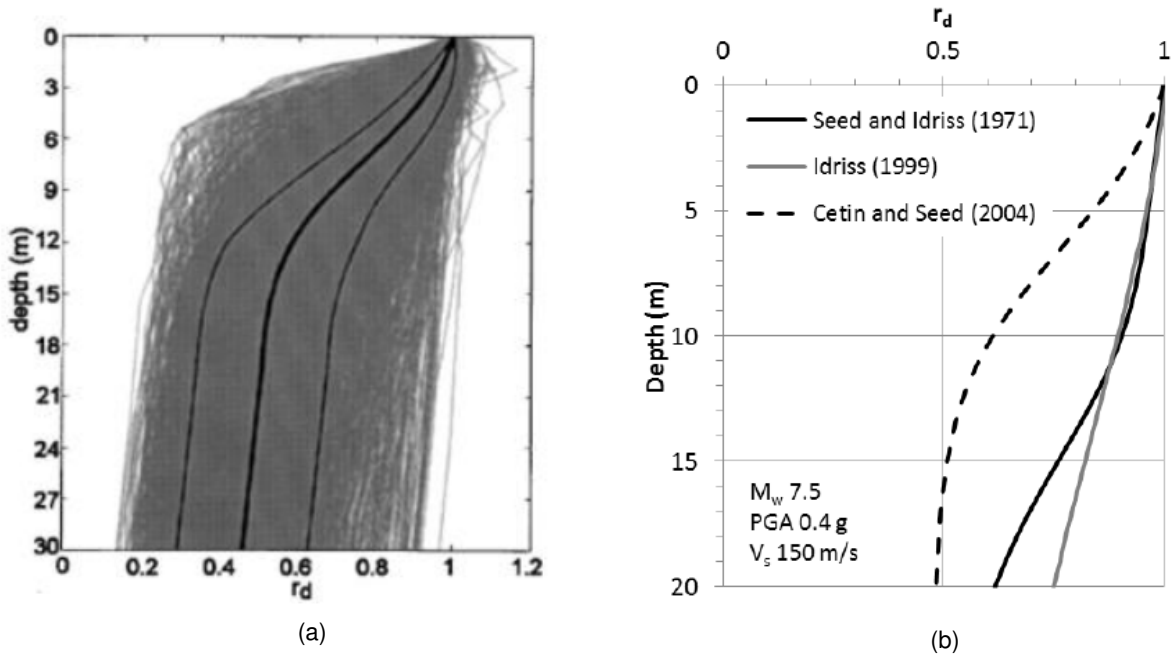

Figure 3.1: (a) the r_d curve by [21] with the mean and standard deviation curves in solid and (b) proposed r_d variation in depth from different researchers

Given the usage complexity of the ”Cetin and Seed (2004)” curves and the fact that the ones from [15] are more conservative and suitable for routine practise and non-critical projects [37] this are the ones described and further used in this work.

This shear stress reduction coefficient curve proposed by [15] is the result of continuous improvement from previous works, although still highly simplified, and which equation follows:

$$\begin{aligned} r_d &= exp[\alpha(z) + \beta(z)] \\ \alpha(z) &= -1.012 - 1.126sin\left(\frac{z}{11.73} + 5.133\right) \\ \beta(z) &= 0.106 + 0.118sin\left(\frac{z}{11.28} + 5.142\right) \end{aligned} \tag{3.3}$$

3.1.2 THE CYCLIC RESISTANCE RATIO

The CRR cannot be measured reliably in the laboratory for most liquefiable soils, largely because obtaining high-quality samples from the field for laboratory testing is expensive for most projects or even technically impossible [37]. Representative *in situ* test parameter as SPT, CPT, shear waves velocity and BPT must then be used to develop relationships to figure the soil CRR.

Figure 3.2 compares features of the four major *in situ* tests used for the assessment of liquefaction resistance [39].

Feature (1)	Test Type			
	SPT (2)	CPT (3)	V_s (4)	BPT (5)
Past measurements at liquefaction sites	Abundant	Abundant	Limited	Sparse
Type of stress-strain behavior influencing test	Partially drained, large strain	Drained, large strain	Small strain	Partially drained, large strain
Quality control and repeatability	Poor to good	Very good	Good	Poor
Detection of variability of soil deposits	Good for closely spaced tests	Very good	Fair	Fair
Soil types in which test is recommended	Nongravel	Nongravel	All	Primarily gravel
Soil sample retrieved	Yes	No	No	No
Test measures index or engineering property	Index	Index	Engineering	Index

Figure 3.2: Comparison of advantages and disadvantages of various field tests for assessment of liquefaction resistance from [39]

Despite the specific differences and advantages of every test, the CPT has clear advantages, as presented in [39]: the most important being the nearly continuous profile that allows a more detailed definition of the soil layers than any other tool and the generally more consistent and repeatable results. Also pointed in [39] is the fact that the CPT based interpretations must be verified with few well-placed boreholes (preferably with SPT), to confirm soil type and further verify liquefaction resistance interpretations.

Based on what is stated on the previous paragraph and given the main objective of this work and its time limitations, the cone penetration test is assumed to be the preferential tool to estimate the soil CRR and will be the only one presented. The interested reader may find the usage description of the other three tools very well gathered in the [39] document.

3.1.3 THE CPT USAGE FOR CRR ESTIMATION

The framework to estimate CRR values from CPT test is the plot of coordinates that relate the normalised CPT tip resistance to the CSR measured or estimated on the soil for sites with seismic history for a given seismic event. Each of these coordinated points is associated with a binary Yes/No for if there was liquefaction phenomena triggered or not. The CRR curve will be the one created that can separate the plot area in two distinct areas: the one with the liquefied sites and the one with no liquefaction observed.

This curve designing is not something objective as it depends on the used sites database; what is considered to be “liquefaction positive” and if it can be perceived or not and also the variability on the direct correlation between CPT tip resistance and the soil resistance to liquefaction as this is a phenomena conditioned by lots of different factors.

The most commonly used relationships to predict CRR form CPT tip resistance are the ones developed by [30], [33] and [15]. With some differences in the frameworks used to construct each curve: Robertson and Wride 1998 (RW98) uses curves based on SPT blow count converted to CPT tip resistance. When comparing this curve with real CPT data from binary liquefaction triggered sites it has shown to be consistent with this field data The ”Moss et all (2006)” and ”Idriss and Boulanger (2008)” curves are obtained directly from CPT data from 200 case histories. M06 is a probabilistic relationship. The three curves are shown in the image, one must note that the one referred as Moss et al. (2006) is in fact the curve for the probability of 15%, the one proposed in [37] to be used for a deterministic approach.

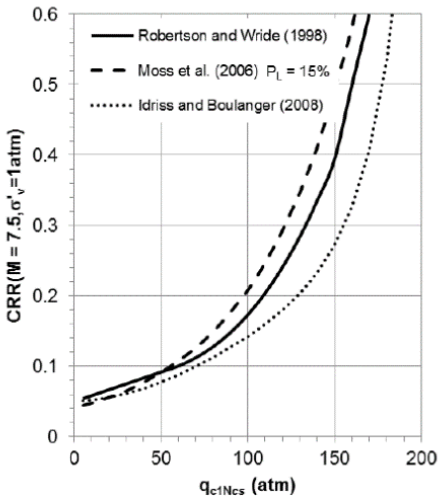

Figure 3.3: Comparison of CPT based predictive relationsips [37])

3.1.4 THE IMPORTANCE OF THE NUMBER OF CYCLES

The CRR, i.e., the cyclic stress ratio required to initiate liquefaction, decreases with the increasing of the number of cycles of a given seismic event, which means that these both cyclic ratios must be associated with the number of cycles of the studied earthquake.

Earthquake magnitude is used as a proxy for the number of cycles because the duration of shaking and the associated number of loading cycles very well correlate with the earthquake magnitude [37]. Firstly proposed by [13] the magnitude scaling factors (MSFs) are used to adjust the CRR curve upper or down for earthquakes with magnitude different from 7,5. The inverse of this factor is called "magnitude weighting factors" and can be used to correct the CSR for a given magnitude, either way the same result is reached.

The new factor of safety formula can be written as follows:

$$FS = \frac{CRR_{7.5}}{CSR} \cdot MSF \tag{3.4}$$

where CRR is determined from the curves drawn in Figure 3.3; CSR is the cyclic stress ratio generated by earthquake shaking and MSF value defined differently by different investigators.

Figure 3.4 presented in [37] plots MSFs curves from various works. Speciall attention is made to the values range proposed by the consensus described in [39]. Table 3.1 presents the MSF values recommended for engineering practice in the [39] document, shown in Figure 3.4.

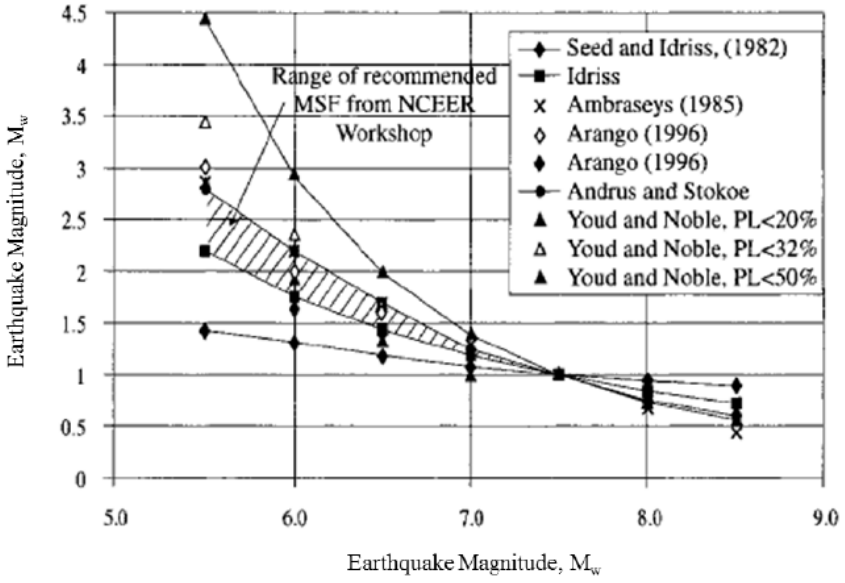

Figure 3.4: Recommended magnitude scaling factors from [39] and MSFs proposed by other previous works

Table 3.1: The MSF values proposed by [39]

Magnitude, M	MSF value
5.5	2.20 - 2.80
6.0	1.76 - 2.10
6.5	1.44 - 1.60
7.0	1.19 - 1.25
7.5	1.00
8.0	0.84
8.5	0.72

3.2 CURRENT APPROACH FOR THE ASSESSMENT OF LIQUEFACTION CONSEQUENCES ON STRUCTURES

The uncertain behaviour of the liquefaction phenomena and its complexity in the interaction with near structures created an engineering field where empirical methods and correlations where created along the recent years to make building consequences estimation possible.

The up-to-date 2006 NASEM [37] document divides these screening procedures into three types: **(1)** a procedure that establishes a threshold ground motion below which liquefaction damage is expected to be inconsequential; **(2)** a procedure to screen sites for damage potential based on the appearance of surface manifestations of liquefaction and **(3)** procedures that use results from liquefaction triggering evaluations to compute a numerical index for the severity of triggering, which is presumed to correlate with liquefaction damage potential.

3.2.1 THRESHOLD GROUND MOTIONS

This criterion is used to eliminate unnecessary analyses and is commonly used among federal, state and local American public agencies. [37]. This is especially used in bridge designing, based on Federal Highway Administration (FHWA) guidance documents and American Association of State Highway and Transportation (AASHTO) specifications, then being used in others parts of the world. This is based on maximum earthquake magnitude and/or peak ground acceleration values, below which there is no need for specific liquefaction analyses, and also in in situ tests that estimate soil resistance to liquefaction (cone penetration test, soil penetration test and shear wave velocity), and considering the soil to have inconsequent consequences if a minimum value of those parameters is reached.

3.2.2 APPEARANCE OF SURFACE MANIFESTATION

This way of assessing liquefaction consequences is based on the assumption that the severity of the surficial manifestations of liquefaction serves as a proxy to the liquefaction damage potential on structures. This assumption is likely valid for shallow foundation systems and surficial or near-surface infrastructure, but it may not be valid for deep foundation systems.

Based on field performance data and firstly quantified by Ishihara (1985) was the influence of non-liquefiable capping soil layer on the suppressing of the surficial manifestation of liquefaction of an underlying liquefiable layer. Using field performances from the 1976, Tangshan, China, earthquake, the May 26, 1983, M 7.3 Nihonkai-Chubu earthquake and professional judgement, Ishihara (1985) plotted coordinated points relating the depths of the two above-mentioned layers and giving each point the binary conditions of whether ground manifestations were observed or not, as seen on Figure 3.5a. Then adjusting curves to separate the two distinct areas of surficial manifestation and defining a value for when the curve becomes vertical. This value represents the minimum thickness of the above non-liquefiable layers that ensures no ground manifestations, as observed for the 3 meters values on figure. Figure 3.5b shows three plotted generalized curves for different PGA values also by Ishihara in [19].

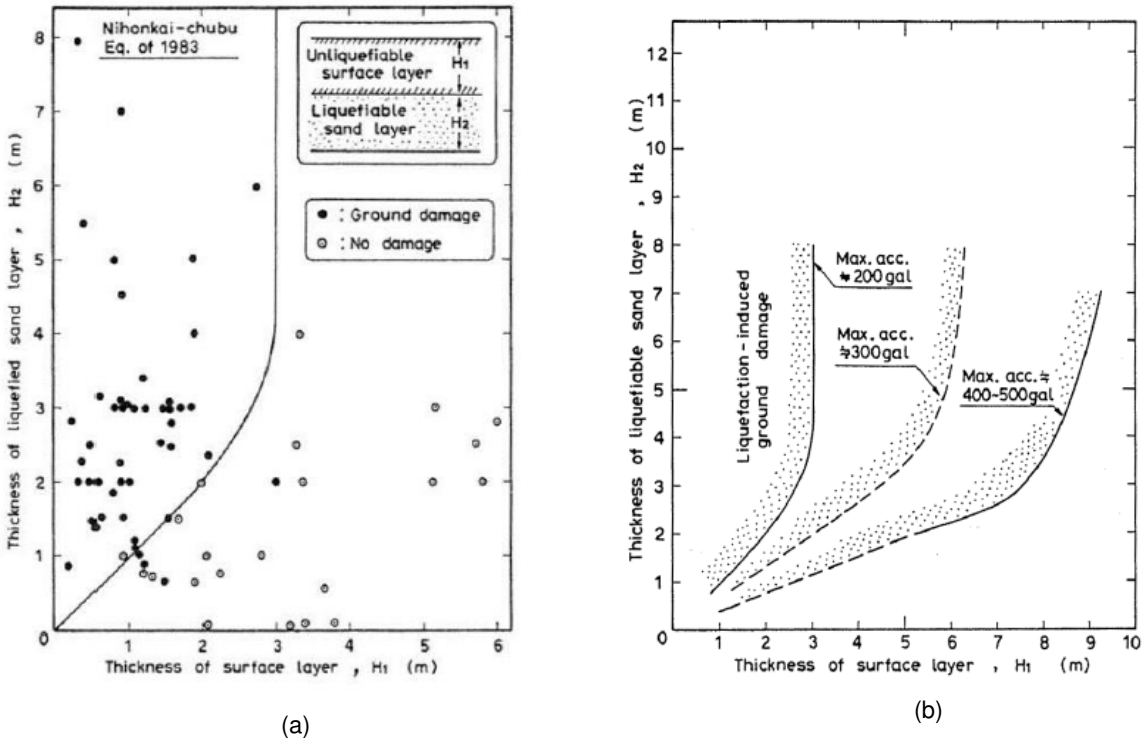

Figure 3.5: The Ishihara curves. (a) Chart showing thickness of non-liquefying capping surface layer required for surface manifestation based on data from the 1983 Nihonkai-Chubu earthquake and PGA of 0.2 g and (b) a generalized chart showing boundary thickness of surface layers for other PGA values from [37].

3.2.3 LIQUEFACTION SEVERITY INDICES

With the objective of providing a measure of the surface damage expected from soil liquefaction, some liquefaction severity indices were created during the past decades. Not being this the main focus of this work, only the two most used frameworks are further explained: The Liquefaction Potential Index, LPI, from Iwasaki et al. (1978) and its improved Ishihara inspired LPI, or LPIISH, added by Maurer et al. (2015) and the Liquefaction Severity Number, LSN, from van Ballegooy et al. (2012).

3.2.3.1 The liquefaction potential index – LPI

The LPI, proposed by Iwasaki and colleagues in 1978, provides a depth-weight index of the potential for triggering of liquefaction at a site. (NASEM, 2016) Being computed as follows:

$$LPI = \int_0^{20m} F \cdot w(z) dz \tag{3.5}$$

where $F = 1–FS$ for $FS \leq 1$ and $F = 0$ for $FS > 1$ (FS is the factor of safety against liquefaction, obtained from a simplified stress-based liquefaction evaluation procedure) and $w(z)$ is a linear depth weighting function given by

$$w(z) = 10–0,5z$$

and $w(z) = 0$ for $z < 20m$ (z is the depth in meters below the ground surface)

The resulting index value increases therefore with: the thickness of liquefiable layers in the uppermost 20 meters; the proximity of the liquefiable layers to the ground surface and with the how much the FS is lower than 1. LPI can range from the minimum of 0, when there are no layers with FS lower than 1 in the uppermost 20 meters, to a maximum of 100, when FS to liquefaction is zero in all the uppermost 20 meters of soil.

Site data analyses make possible to correlate LPI values with expected liquefaction consequent damage. Liquefaction hazard maps have been developed using the LPI framework for many seismic regions in the world.

In the recent work by Maurer et al. in [8] some improvements are made while maintaining this same framework. A power-law depth weighting function has been employed instead of the linear one used in the original framework and made the procedure accountable for the limiting thickness of the non-liquefiable capping layer. The result of this "Ishihara inspired liquefaction potential index", or LPI_{ISH}, was a reduction in the number of false-positive predictions (i.e., where damage was predicted but not observed) in a big historical database while keeping the capacity to predict true positive liquefaction cases. Also granted is the capacity to measure multiple liquefiable layers above a non-liquefiable one, opposed to the limitations of the 1985 Ishiara approach in [19].

Although LPI_{ISH} shows better prediction capacities over LPI, it can still yield incorrect predictions of liquefaction consequences. Therefore, there is still a need for further development of liquefaction damage indices

if they are to be considered reliable [37].

3.2.3.2 Liquefaction severity number – LSN

LSN uses a power law depth-weighting factor to determine the cumulative liquefaction response of a profile and includes contributions from all layers that have an FS ≤ 2 and is determined as follows:

$$LSN = 1000 \int \frac{\varepsilon_v}{z} dz \tag{3.6}$$

where ε_v is the calculated post-earthquake volumetric strain at depth z (in meters) expressed in decimal form and computed with the method implemented by Zhang in [12] for CPT data. LSN has shown to be fairly well correlated with the surface damage manifestations observed during the 2010-2011 Canterbury, New Zealand earthquake sequence. Both liquefaction severity indices are useful in engineering practice for prioritizing sites for more detailed investigation and for regional hazard mapping, but they are not a substitute for more detailed analyses, and they do have limitations.

3.2.4 Current approach to building settlements due to liquefaction

As presented in the beginning of this chapter, since the work of [14] and its improvements by [39], this has been the almost universal procedure for liquefaction triggering assessment used in engineering practice.

If the probability and possible consequences of liquefaction triggering is above acceptable then the usage of empirical methods gives an estimative on the settlement due to post-liquefaction reconsolidation. This methods typically assume free-field and one-dimensional conditions. [37] but, as the only option available, they have been used to predict building settlements in the past years and in current time.

Although this is the most commonly applied approach to estimate liquefaction-induced building settlements, [35], among many others, argues that this neglects the importance of other settlement mechanisms that could damage the structure and its surrounding utilities. [37].

From experimental evidence of the damage induced in several buildings, [35] states that beside volumetric-induced settlement mechanisms, which are prevalent in free-filed conditions, the development of shear-induced settlements is one of the pivotal mechanisms driving the deformation of the liquefied soil, especially in the presence of structures near the ground surface.

4

NUMERICAL MODELLING OF LIQUEFACTION PHENOMENA

As stated in Chapters 2 and 3, the liquefaction phenomena and its consequences on built environment has been addressed in the last decades by empirical methods that improved the design against liquefaction and generally helped the decision-making process concerning liquefaction, but there are two handicaps on these methods. The first is the known issue of empirical methods that different researchers with the same case studies and data come to different conclusions. Second is the impossibility to perform real full-scale experiments which limits the development of databases to support empirical methods. [3]

Researchers require proper numerical tools for improving the understanding on earthquake- induced liquefaction and for developing new mitigation techniques, as element testing and physical modelling have their own limitations. In the first case, it is challenging to predict the behaviour of a complex problem from the behaviour of a small soil element, especially if the mechanism of failure and/or deformation is inadequately established. In the second case, constraints associated with the costs of centrifuge testing and the limited geometry of centrifuge models hamper the use of this tool to clarify every aspect of the problem. [29]

As numerical modelling is a time-efficient and cost-effective technique for a broad range of problems, it is an ideal tool to perform liquefaction analyses, but it is still a very challenging task for current numerical tools. [29]

PLAXIS® is a very well-known and wide spread commercial software in the current engineering practice. This will be the numerical tool used for the present work as it allows for both soil and structure simulation. The UBC3D-PLM soil constitutive model can be easily added to PLAXIS® as a ”user defined soil model”.

The present chapter aims to present a simple description of the UBC3D-PLM constitutive model framework, assumptions and list the input parameters. In the end of the chapter the model correlations with *in situ* tests are described and the parameters computation is shown.

4.1 THE UBC3D-PLM MODEL

The UBC3D-PLM model name stands for three intrinsic characteristics:

- UBC as University of British Columbia
- 3D for the three dimensional yield function by Tsegaye in [5]
- PLM standing for the addiction of a post liquefaction factor to the previous constitutive model

The UBC3D-PLM is one of the most commonly used constitutive models for liquefaction problems in practice. Even though it is an advanced model, it is relatively simple to apply, since it has a reasonable number of parameters that can be extracted from laboratory or *in situ* tests. The model was initially developed for sand-like soils having the potential for liquefaction under seismic loading. [3]

A brief explanation of the model principles follows in the next sections. The interested reader can further understand the model framework in the specific chapters of the works [4] [40] and [1].

4.1.1 GENERALIZED EFFECTIVE STRESS FRAMEWORK

Coelho [29] states that the framework difference between the models to describe soil behaviour (in general) and other materials that can be studied as single-phase materials is as follows:

Few exceptions are the particular case of drained loading where a single-phase approach is valid, or the contrasting particular case of undrained loading, where the single-phase solution is acceptable if the pore-pressure generation can be linked in a unique manner to the deformation of the solid material, as it sometimes happens in static loading. But as earthquake phenomena are usually not included in these categories, a full effective stress-based framework is required to properly model soil behaviour under those circumstances.

This creates the necessity for the UBC3D-PLM soil constitutive model.

4.1.2 THE YIELD SURFACE

To model the boundary between the elastic and the plastic material behaviours, a soil model must have a defined yield function. In first place, the yield function of the UBCSAND is explained and then the generalisation for the UBC3D-PLM model is presented, as this being the main difference from the original to the updated UBC3D-PLM model.

To make the existence of a densification rule possible, there are two Mohr-Coulomb based yield surfaces implemented, as represented in a p'-q plot in Figure 4.1.

When loading from an isotropic stress state, both primary and secondary yield surfaces expand according to the same hardening rule. [40] When unloading and reloading, the behaviour is controlled by the secondary yield surface.

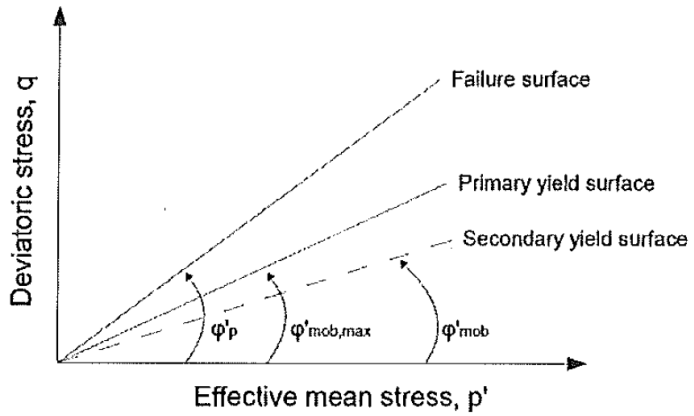

Figure 4.1: Liquefaction-induced vertical settlements mechanisms as [32]

For the UBC3D-PLM model the critical yield function implementation follows Equation 4.1.

$$f_m = \frac{\sigma_{max} - \sigma_{min}}{2} - \left(\frac{\sigma_{max} + \sigma_{min}}{2} + c \cot \varphi_p \right) \sin \varphi_m \tag{4.1}$$

where σ_{max} and σ_{min} are the maximum and minimum principal total stress, respectevely; φ_p is the peak effective friction angle and φ_m is the mobilised friction angle during hardening. The yield surface in the three dimentional stress space is not influenced by the intermediate stress, as pointed in [40].

As defined by Equation 4.1, when all the 6 planes are combined in one figure and only the part with $\sigma_{min} \leq \sigma_{int} \leq \sigma_{max}$ is shown, a general 3D surface of the Mohr-Coulomb criterion is obtained as in Figure 4.2. [5]

Tsegaye in [5] also represents the projection of the Mohr-Coulomb yield surface in a deviatoric plane as therefore presented in Figure 4.3.

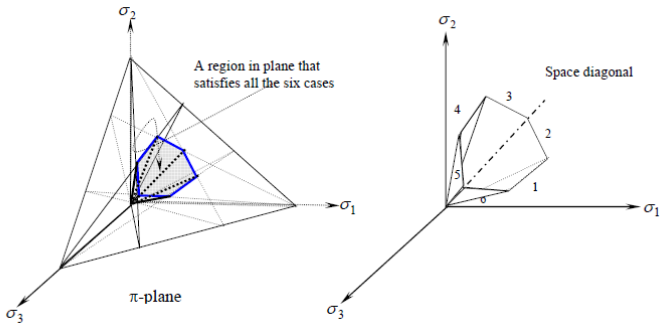

Figure 4.2: The six arrangements of the minimum, intermediate and maximum principal stresses

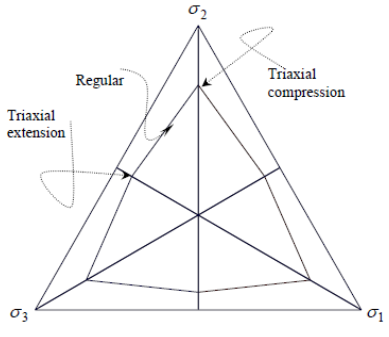

Figure 4.3: Projection of the Mohr-Coulomb yield criterion in π plane

4.1.3 Elastic behaviour

Within the secondary yield function the elastic behaviour is modeled by two stress dependent modulus defined by the following equations:

$$K^e = k_B^e \cdot p_A \cdot \left(\frac{p}{p_{ref}}\right)^{me} \tag{4.2}$$

$$G^e = k_G^e \cdot p_A \cdot \left(\frac{p}{p_{ref}}\right)^{ne} \tag{4.3}$$

where K^e is the elastic bulk modulus and G^e is the elastic shear modulus; k_B^e and k_G^e are bulk and shear moduli numbers at a reference stress level, respectively. p_{ref} is the reference stress level, that is commonly taken as the atmospheric pressure (i.e. $p_A = 100 \quad kPa$) and p is the mean effective stress. The exponents me and ne are two parameters to define the rate of stress dependency of stiffness.

4.1.4 Hardening rules

To govern the amount of plastic strain resulting from the mobilization of the yield surfaces, two hardening rules are implemented in the model. The primary yield function has its isotropic hardening rule defined by Tsegaye in [5] and is generalisation written as follows in Equation 4.4 and schematically presented in Figure 4.4.

$$d \cdot \sin\varphi_m = 1.5 K_G^p \left(\frac{p}{P_A}\right)^{np} \frac{P_A}{p_m} \left(1 - \frac{\sin\varphi_m}{\sin\varphi_p} R_f\right)^2 d\lambda \tag{4.4}$$

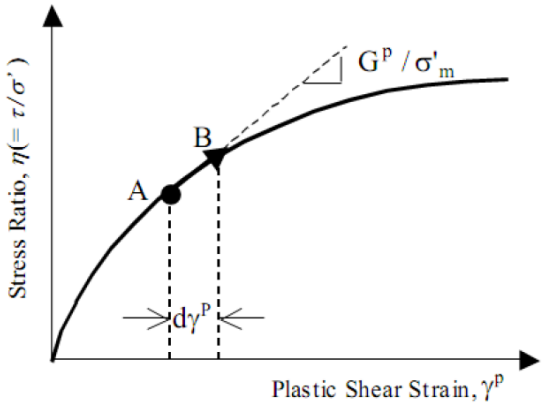

Figure 4.4: Representation of the hardening rule adopted from the UBCSAND model

where K_G^p is the plastic shear modulus number, np is the model parameter for non-linear stiffness dependency of the plastic shear modulus; p is the mean normal stress , p_A is the atmospheric pressure in stress units and $d\lambda$ is the plastic strain increment multiplier. [5]

The secondary yield surface is introduced and is added an hardening rule for proper simulation of gradual development of excess porewater pressures. It allows for modelling the generation of porewater pressures under lower rate in the cycles just before liquefaction onset, phenomenon known as soil densification. This rule is named as "densification rule" by some literature and is described by Equation 4.5.

$$k_G^p = k_{G,initial}^p \left(4 + \frac{n_{rev}}{2}\right) \cdot k_{dens} \cdot fac_{hard} \tag{4.5}$$

where $k_{G,initial}^p$ is the initial k_G^p value given as input by the user; n_{rev} is the number of shear stress reversals from loading to unloading or vice versa; fac_{hard} is an input parameter to calibrate the densification rule; k_{dens} is a factor between 0.5 and 1.0 to correct the densificatiion rule for loose and non-cohesive soils, depending on the $(N_1)_{60}$ value.

4.1.5 Plastic potential function and flow rule

Plastic shear strains will start developing if the stress state reaches the defined yield surface. The plastic potential function specifies the direction of the plastic strain. A non-associated flow rule based on the Drucker-Prager plastic potential function is used in the UBC3D-PLM [40] and is formulated as:

$$g = q - \frac{6 \sin \psi_{mob}}{3 - \sin \psi_{mob}} p' \tag{4.6}$$

$$\sin \psi_{mob} = \sin \varphi'_{mob} - \sin \varphi'_{cv} \tag{4.7}$$

where g is the plastic potential function; ψ_{mob} is the mobilised dilation angle computed from the flow rule in Equation 4.7; q is the deviatoric stress and p' is the mean effectivestress.

4.1.6 Post-liquefaction and cyclic mobility

The upper cited flow rule definition does not allow for proper capturing of the soil stiffness degradation related to post-liquefaction behaviour of loose sands and cyclic mobility of dense sands. [16]

This occurs because when the primary yield surface touches the peak stress state (governed by the peak friction angle) the secondary yield surface is deactivated. After the deactivation of the secondary yield surface the primary loading surface is used again. A new input parameter is defined at this stage in order to include the post-liquefaction behaviour of the soil. If a non zero multiplier fac_{post} is specified, from that stage in the primary yield surface a modified plastic shear modulus will be used based on the following equation: [40]

$$K_G^p = K_{G,initial}^p \cdot fac_{post} \tag{4.8}$$

where $K_{G,initial}^p$ is the initial value given as input by the user.

4.1.7 MODEL PARAMETERS

Table 4.1 summarises the model input parameters as well as it respective units, brief description and determination method. As made clear by the stated Determination method in Table 4.1 a substantial number of model parameters have no physical meaning.

Table 4.1: UBC3D-PLM model parameters summarized

Parameter	Unit	Description	Determinantion Method
ϕ_{cv}	(degrees)	Constant volume friction angle	Drained Triaxial Compression
ϕ_p	(degrees)	Peak friction angle	Drained Triaxial Compression
c	kPa	Soil cohesion	Drained Triaxial Compression
K_B^e	-	Elastic bulk modulus number	Empirical curve fitting
K_G^e	-	Elastic shear modulus number	Empirical curve fitting
K_G^p	-	Plastic shear modulus number	Empirical curve fitting
me	-	Elastic bulk modulus exponent	Empirical curve fitting
ne	-	Elastic shear modulus exponent	Empirical curve fitting
np	-	Plastic shear modulus exponent	Empirical curve fitting
R_f	-	Failure ratio	-
fac_{hard}	-	Densification factor	Fitting parameter
$(N_1)_{60}$	-	Corrected SPT value	-
fac_{post}	-	Post-liquefaction factor	Fitting parameter
P_A	kPa	Reference stress	-

4.1.8 MODEL PARAMETERS COMPUTATION

Makra [3] states that UBC3D-PLM is a descriptive model and the parameters are determined by curve fitting, preferably from cyclic undrained direct simple shear (DSS) tests.

Proposed in [26] is a set of equations based on the SPT blow count value normalised to the $(N_1)_{60}$ for the initial generic calibration of the model.

In this work, as follows in Chapter 5, the case study site has no lab tests made available and the cone penetration tests are the ones considered to give best results, compared with SPT, and are used for parameters correlation.

The upper stated option for the CPT result is based on the fact that this test takes a continuous set of values from site, as SPT is not capable of. For the specific liquefaction phenomena studied in this work it is of great advantage to have a continuous set of data. The Robertson correlation in [31] will be used to convert CPT to SPT blow count values.

Presented are the correlations defined in [26] and implemented by Makra in [3] and further used in present work:

$$\phi_p = \phi_{cv} + \frac{(N1)_{60}}{10} + max\left(0; \frac{(N1)_{60} - 15}{5}\right) \tag{4.9}$$

$$K_G^e = 21.7 \cdot 20 \cdot (N1)_{60}^{0.3333} \tag{4.10}$$

$$K_B^e = 0.7 \cdot K_G^e \tag{4.11}$$

$$K_G^p = K_G^e \cdot (N1)_{60}^2 \cdot 0.003 \cdot +100 \tag{4.12}$$

$$R_f = 1.1 \cdot (N1)_{60}^{-0.15} \tag{4.13}$$

5
CASE STUDY DESCRIPTION

One main objective established in the beginning of this work was to model an historical case of liquefaction-induced building settlements and compare the computed results with the measured values, in order to test the numerical modelling of such a complex phenomena. Given the few well documented historical cases, where building settlements occurred due to liquefaction phenomena, this was the first big task of this work.

5.1 CASE STUDY SITE SELECTION

Christchurch was assumed as a good source of case studies, given the recent earthquake events with induced liquefaction under built environments and the fact that considerable information is available, as well as many works that have been developed based on this site.

Some criteria were set as minimum for a site to be considered a possibility:

- Location with liquefiable layers and proved to have liquefied in a well documented seismic event;
- Proper geotechnical characterization of the layers;
- Presence of a well defined structure in the area above;
- Proper after seismic event observational data from ground and structural behaviour;
- Trustable earthquake information from nearby and correlatable to site.

Based on Zupan work [18] vast Christchurch data collection on buildings that suffered from liquefaction consequences, as well as after seismic event observation of these buildings. This very complete work was used as data source for the present dissertation. To simplify the analyses of all these different criteria and sites and make the comparison possible the following table presented in figures 5.1 and 5.2 was constructed.

SITE	SITE description	DATA SOURCE	CHARACTERIZATION (IS and LAB)									HISTORY DATA								
			SPT	CPT	Vs	SOURCE/OBS	PSD (partic	FC	WC	Attem berg	SOURCE/OBS	L Trig FF	L Trig STR	L Sett FF	L Sett STR	Sett OBSERVED	STR DAM. OBSERVED	SOURCE/OBS	EQ info	SOURCE/OBS
LX	Benavente, Lisboa, data from LIQUEFACT/FEUP project	NO STR	1	1	1	2 excel docs sent by prof Viana	-	-	-	-		-	-		-				-	
PARK. LOT	Armagh street and Madras street parking lot	NO STR (ZUPAN, 2014 - page 139)																		
CTUC Bling		ZUPAN, 2014 page 149	-	1	-	page 402	-	-	-	-		1	- (?? pssrible paper??)	1	- (??- possible)	1	1	page 158 beyond	1	4 earthquakes (?)
SA Bling		ZUPAN, 2014 page 157	-	1	-							1	-	1	-	1				
PILE-6 and FTG-7/4		ZUPAN, 2014 page 162	-	1	-	+ bore hole	-	-	-	-		1		1		1	1		1	
PwC Bling	lateral spreading vs. 2D	ZUPAN, 2014 page 168	-	1	-	+ cable tool boreholes	-	-	-	-		1	-	1	-	1	1		1	
VT&VSA Bling	VT on mat found and VSA on piles	ZUPAN, 2014 page 188	-	1	-	+ 4 cross section maps	-	-	-	-		1	-	1	-	1	1		1	
SCH Bling		ZUPAN, 2014 page 209	1	1	-	4 + 5 CPT; SPT data??	-	-	-	-	good soil units description by layers	1	-	1	-	1		settlement by cpt depths	1	
CTH Bling	page 228-248	ZUPAN, 2014 page 213	1	1	-	T&T (2013) ZUPAN page 450	1	1	-	1	(lab only for critical layer) 2 near piezometers	1	-	1	-	1	1		1	
LS-I & II Buildings		ZUPAN, 2014 page 239	1	1	-		1	1	-	1	(possible assume 100m sample test)	1	-	1	-	1	1		1	

Figure 5.1: Site choosing tables #1

STRUCTURE		OBSERVATIONS
STR. CHARATERISTICS	FOUNDATION CHARACT.	
six-story, RC, frame str	complex shallow foundation pressure 100-200 KPa at the	demolished!
less data (mas pode-se ir usar mais do que aqui está apresentado) and smaller settlements		
3 buildings; pile and 2 with shallow foundation (big and small)		
mat basement bigger to south and tilt	250 Kpa	
As with the PWC building, advanced SSI numerical models will likely be able to provide more insight into the complex performance of the VT and the VSA buildings, and these analyses are underway by researchers at the University of California at Berkeley and the University of Canterbury.	VT: 120 Kpa	
pos-liq sett and struct damages very well documented (see bibliography)	BAD: complex structure for modeling	layer by layer description (Tonkin and Taylor, 2013)
Consequently, the shear induced building settlement mechanisms described by Dashti et al. (2010a) were important for this case.	shallow vs. deep liquefiable soils	

Figure 5.2: Site choosing tables #2

After the gathering and comparison of all the information, LS-I and LS-II buildings where the ones chosen as consequence of the fulfilment of all the criteria above and having some specific characteristics that where considered as an advantage, such as:

- The presence of a shallow founded building, which exemplifies the actual problem with liquefaction-induced settlements on buildings, because of buildings that were constructed before liquefaction awareness and that are still in use;
- It is structurally simple which makes it possible for numerical simulation;
- Sufficiently isolated from other buildings, so making it is reasonable to consider that they have no interaction during the liquefaction phenomena;
- The geotechnical characterisation was performed with CPT tests, what was assumed to be a more reliable source of soil information and five where available on site, as well as two SPT tests with stratigraphy analyses.

5.2 Report on site data

5.2.1 Site location

New Zealand is situated near Australia and surrounded by the South Pacific Ocean as shown in Figure 5.3a. Christchurch is its largest city in the South Island of New Zealand with a population of almost 400.000 inhabitants as observed in Figure 5.3b. Near the Christchurch Business District (CBD) in the number 19 of Lismore street are the LS-I and LS-II buildings shown in 5.3c.

(a) (b) (c)

Figure 5.3: Christchurch location (a) in the world; (b) in New Zealand and (c) Lismore street buildigs I and II location

5.2.2 Buildings structural information

Figure 5.4 presents building plant where it is made clear the relative position to the Lismore Street and also some structural characteristics are highlighted and described in following paragraphs.

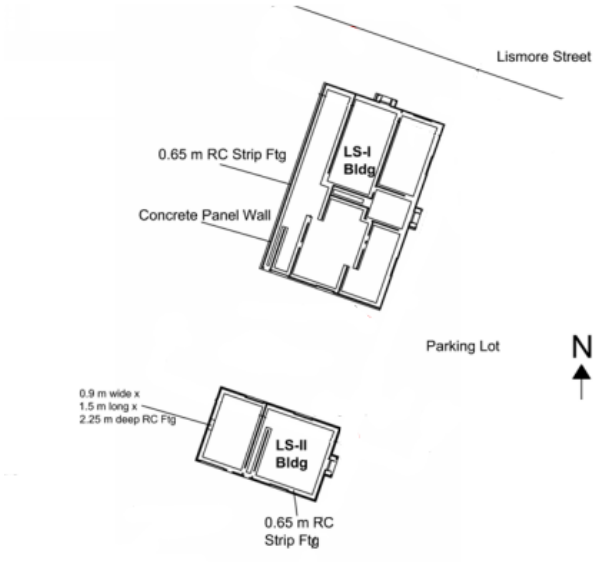

Figure 5.4: LS-I and LS-II buildings structural plant from [18]

Based on the information of [18] and the 2007 buildings design drawings, both the LS-I and LS-II buildings were two-story concrete panel buildings, with some distinct properties:

- **LS-I:** Plan dimentions of 28 by 18 meters. The shallow foundation consisted of 1.2 m wide by 0.65 m deep RC strip footings beneath the concrete panel walls with a 0.125 m thick concrete slab spanning between the wall footings.
- **LS-II:** Plan dimensions of 18 by 11 meters. The shallow foundation was nearly identical, with the exception being a 0.9 m wide by 1.5 m long by 2.25 m deep RC footing beneath a concrete encased steel column located at the center of the westernmost wall.

The second floors of both buildings consisted of 7.5 cm of cast in place concrete atop permanent timber formwork. The floors were supported by precast concrete beams that connected to the panel walls with steel angles. Timber trusses supported 0.4 mm Zincalume Trimdeck roofing for both buildings. The LS-II building consisted of both office space and an adjoining warehouse. The office space was divided into a first and second floor and comprised approximately 60% of the floor plan on the east side of the building; the warehouse space was not divided into a first and second floor and comprised the west side of the building. The spaces were separated by a transverse concrete panel wall (see plan)

5.2.3 GEOTECHNICAL DATA AVAILABLE

As referred in [24], the New Zealand Geotechnical Database (NZGD) is an online database that provides a searchable repository for new and existing geotechnical information. It builds on the success of the Canterbury Geotechnical Database (CGD), which was developed for the Christchurch rebuild following the 2010/2011 Canterbury earthquake sequence. It also incorporates data previously held on the Auckland Geotechnical Database, which was initially set up by Watercare.

The NZGD is primarily aimed at providing more efficient access to geotechnical information. It can also be used for more strategic purposes such as assisting with natural disaster recovery, increasing resilience around New Zealand, catastrophe loss modelling, and informing land planning and regulatory processes." [28]

Given the access to the NZGD it was possible to gather high quality data on the site geotechnical information taken in different time:

- 5 CPTs tests very close and around to the two chosen buildings, made after the four major earthquakes sequence;
- 2 boreholes with stratigraphy analyses and N_{SPT} blow count;
- In a 150 meters radius there are two lab tested samples with particule size distribution, fines content and water content;
- One piezometer localized 150m away and recording accessible data.

In Figure 5.5 the next picture the CPT and SPT tests locations and refusal depth in meters inside brackets can be observed. For the present dissertation, it is of particular interest the *in situ* tests performed near the LS-II building.

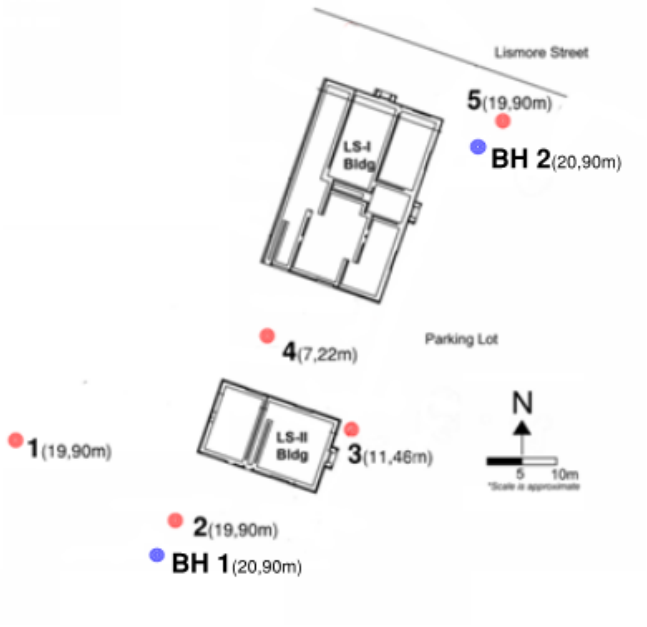

Figure 5.5: Building plant with CPT and SPT tests locations and depth of refusal

5.2.4 Earthquake

There were 4 major seismic events in this area on a relative short period of time (less than one year). In Figure 5.6, presented by Zupan [18], is shown the date, magnitude and PGA for these 4 main seismic events. The PGA for the 26 DEC 2010 event is estimated as the median geo-mean PGA recorded at the four strong ground motion recording stations within the CBD. The remaining PGAs were estimated using the work of [7] as assumed by Zupan in [18]. Where PGA_{50} is the median PGA value and PGA_{16} and PGA_{84} are the 16 and 84 percentiles, respectively, of the lognormal distribution proposed by Bradley in [7]. In this work PGA_{50} will be the one used value.

Given Zupan's abbreviations in [18] and previously used, RW98 stands for the Robertson and Wride CPT-based correlations for liquefaction triggering assessment proposed in 1998 as in [30].

Event	M_w	PGA_{16} (g)	PGA_{50} (g)	PGA_{84} (g)
4 SEP 10	7.1	0.17	0.23	0.31
26 DEC 10	4.8	0.22		
22 FEB 11	6.2	0.37	0.50	0.68
13 JUN 11	6.0	0.20	0.29	0.43

Figure 5.6: Magnitude and PGA values for RW98 analyses [30] from [18]

Over a period of many months, the Canterbury earthquake sequence developed from a relatively standard aftershock sequence following the M_W7.1 Darfield earthquake into a complex and long-lasting series of damaging earthquakes. This sequence will transform the thinking of seismic hazard in New Zealand and internationally for decades to come as these earthquakes are characterised by complex soil and structural ruptures and high accelerations records. [18]

Of particular note is the destructive power of the M_W6.2 Christchurch earthquake of 22nd February 2011, in which a number of factors, including the earthquake's proximity to the city and probable directivity effects, resulted in levels of damage higher than expected for the size of the earthquake. Understanding the reasons for the high levels of damage is vital to estimate the hazards posed by similar earthquakes near other New Zealand or international cities. A combination of aftershock studies and geodetic and strong motion source modelling utilising high-quality data is important for understanding the source mechanisms and rupture processes of the major earthquakes of the Canterbury sequence.

The presence of the GeoNet seismic networking in the region, and throughout New Zealand, and the deployment of additional, temporary instruments, has provided an unparalleled data set that will enhance our understanding of this earthquake sequence and inform the earthquake hazard in similar (low strain rate) environments. To make best use of this data, the complete lifecycles of these earthquakes, their source mechanics and rupture processes, seismic path effects as modified by local crustal and basin structures, and the various site effects that enhanced the damaging potential of the earthquakes all need to be understood. Progress has already been made but much more is left to be done.

Given the various seismic events and observational data taking place on site along the years a time-line was drawn to have a clear sight and make the information understanding possible, as presented in 5.7 and followed by its description and justification.

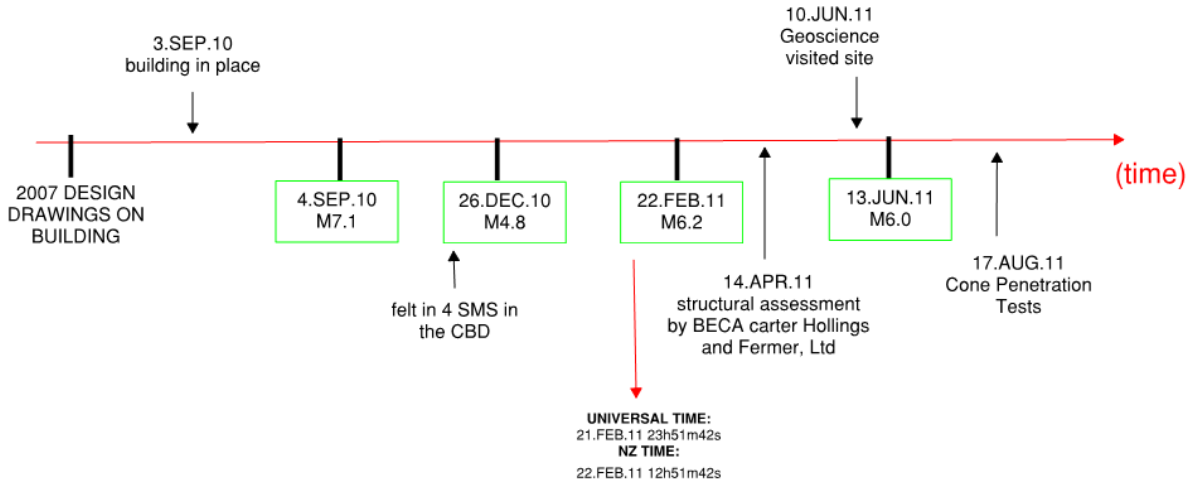

Figure 5.7: Timeline of the events on the site

The four seismic events stated on figure 5.6 are made clear troughout the time-line along with date and magnitude values.

Based on google maps photos archive, on the 3rd of September of 2010 the buildings were already constructed and in use.

In the 26.FEB.2011 event significant amount of sediment ejecta was observed around the LS-I and LS-II buildings. [24] Building vertically surveys were conducted by Beca Carter Hollings and Ferner Ltd on the month of April of 2011. All the 5 CPT tests available were conducted on the 17.AUG.2011, one month after the 13.JUN.2011 earthquake.

The February 22nd of 2011 M_w6.2 event was the most damaging from all the events in terms of loss of life and economic damage, with 185 causalities and half the buildings in the CBD marked as restricted access because of potential safety issues.

But in this day there are three main events with high magnitudes: 6.2, 5.5 and 5.6. [11] and [6] observe that many of the ground motion recordings from the 22.FEB.11 event display characteristics of ground motions recorded on liquefied soils. These characteristics include the presence of large amplitude acceleration "spikes" associated with cyclic mobility, a reduction in the high-frequency content after strong shaking commenced, and long period spectral amplification. Figure 5.8 illustrates the recorded acceleration histories along azimuth 271 at station CBGS during the 4 SEP 10 and 22 FEB 11 earthquakes. Qualitative evidence of soil liquefaction is observed in the acceleration time history during the Christchurch event but not during the Darfield event, calling for the awareness on the liquefaction phenomena in the big difference on magnitude values.

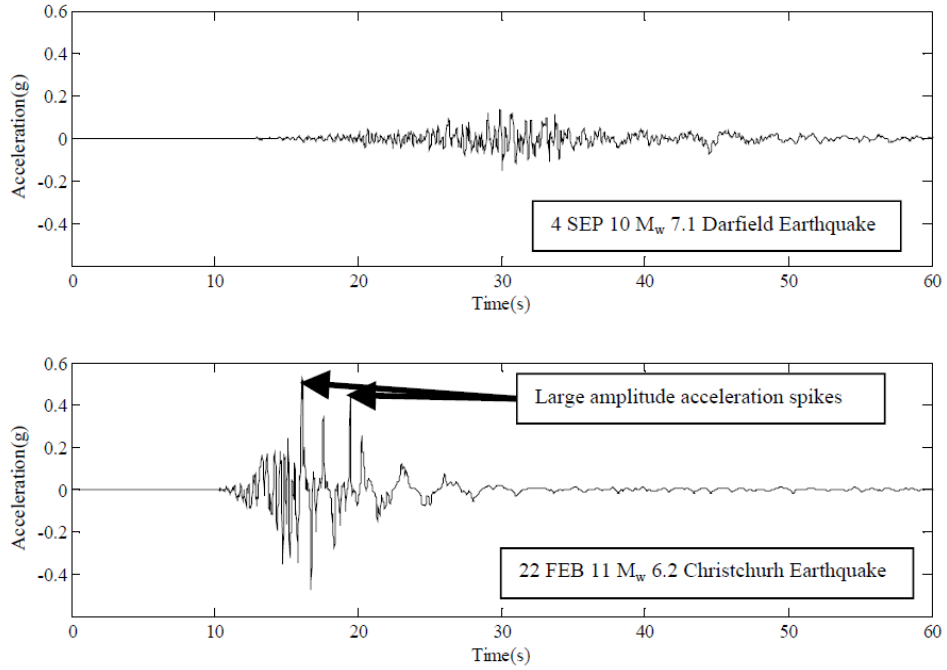

Figure 5.8: Observational evidence on the liquefaction triggering from [18]

Based on all the information stated above and other further presented, the 22.FEB.2011 M_w6.2 earthquake was the one event chosen to be used in the numerical simulation. This decision is made based on some factors:

- It is the one event creating most damage in this sequence;
- Event associated with major liquefaction phenomena, as stated with Figure 5.8;
- Good observational data about building behaviour after the earthquake, further presented;
- Earthquake properties very susceptible of liquefaction triggering;
- Available data on the earthquake from Seismic Station (SS) correlatable to site, as further expressed.

As in geotechnical engineering the study object is not totally understood, when a decision in made some assumptions must be taken into account:

- The observational data results of the building behaviour on April of 2011 is manly caused by this earthquake and not the previous ones, this should not be far from reality, but must be stated as assumption;
- The CPT tests performed at 17.AUG.2011 are assumed to have the same results as if they were taken before the earthquake. This is a critical assumption, given that the soil in known to densify and reduce its liquefaction susceptability when exposed to an earthquake;

- The earthquake data measured in the CCCC seismic station are assumed to be representative of the seismic waves arriving to the study site. Following this path arises some questions, further discussed;
- The layers above SS did liquefy.

In the 22nd February of 2011 there were three major magnitude seismic events throughout the day. The one with higher magnitude happened on the 21st February of 2011 at 23h 51m 42s universal time, or in the 22nd February of 2011 at 12h 51m 42s as in New Zealand time zone. This must be stated as different databases use different time zones.

During this seismic event several seismic stations (as ilustrated in Figure 5.9) were recording data in Christchurch. The Christchurch Cathedral College Seismic Station (CCCC SS) is the one closer to the buildings (approximately 800 meters as observed in figure 5.10) and the one with higher quality geotechnical information on the soil layers underneath.

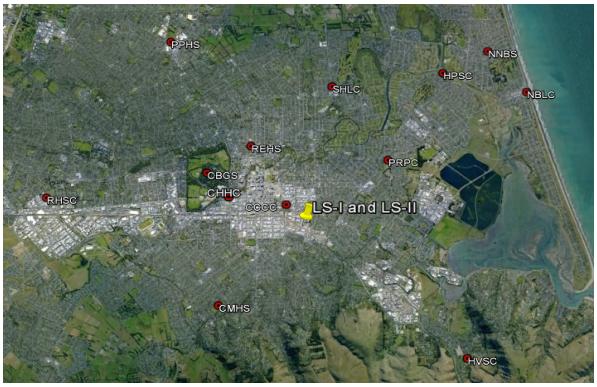

Figure 5.9: Seismic stations in the city of Christchurch

Figure 5.10: Relative location of SS and case study

The stratigraphy of the soil layers under the CCCC SS is made acessible by GeoNet [10] and presented in Appendix B. As the underneath soil layers are generally characterised by soft and loose sand and gravel soils, in the shallower more than 30 meters. Being theses soil type the most susceptible to liquefaction. Also knowing the substantial influence that soil liquefaction has in the soil dynamic response (see Figure 5.8), then this upper cited document shows clearly that the SS data is very susceptible of being influenced by the liquefaction phenomena triggering.

Although the upper mentioned disadvantages of the geology of the underneath soil for the use of this SS as seismic data source, it is the finest data available and will be the one assumed in this work.

5.3 OBSERVED BUILDING CONSEQUENCES

These observations, although not exclusive, are focused on the LS-II building, as it is the building of particular interest to this work. All the observations on the building presented here were made between the 22.FEB.2011 and 13.JUL.2011 seismic events. And, as stated above, it is assumed that earthquakes prior to 22.FEB.2011 had no effects on building behaviour. This statement must not be far from reality as there are no previous observation reports on the site, so no previous major damages are expected. The LS-II building appeared more damaged after the earthquake, tilting to North. This is contrary to the empirical analyses performed by Zupan [18], so it concludes: *This reinforces the fact that, while volumetric settlements due to liquefaction of deeper materials (i.e., greater than 4 times the width of the strip footings for this case) should contribute to the overall building settlement, the shear-induced building settlement mechanisms described previously govern the performance of shallow founded buildings atop shallow liquefiable soils.*

The LS-II horizontal movements at the top of the concrete wall panels was up to 91 mm towards the north. While only hairline cracks were observed in the concrete wall panels, the concrete floor slab was uneven throughout the unit and sediment ejecta was observed in the interior of the unit. Partition walls were damaged and there were areas where ceiling tiles collapsed. While both buildings appeared to have settled relative to the surrounding ground, LS-II appeared to have settled more than LS-I. Measurements suggest that LS-I settled approximately 8 cm relative to the surrounding ground at the NE corner and the north side of LS-II settled approximately 12 cm more than the south side of LS-I. Tilt measurements were performed along the concrete panel walls of both buildings and were generally consistent with the Beca verticality surveys [24] presented in Figure 5.11.

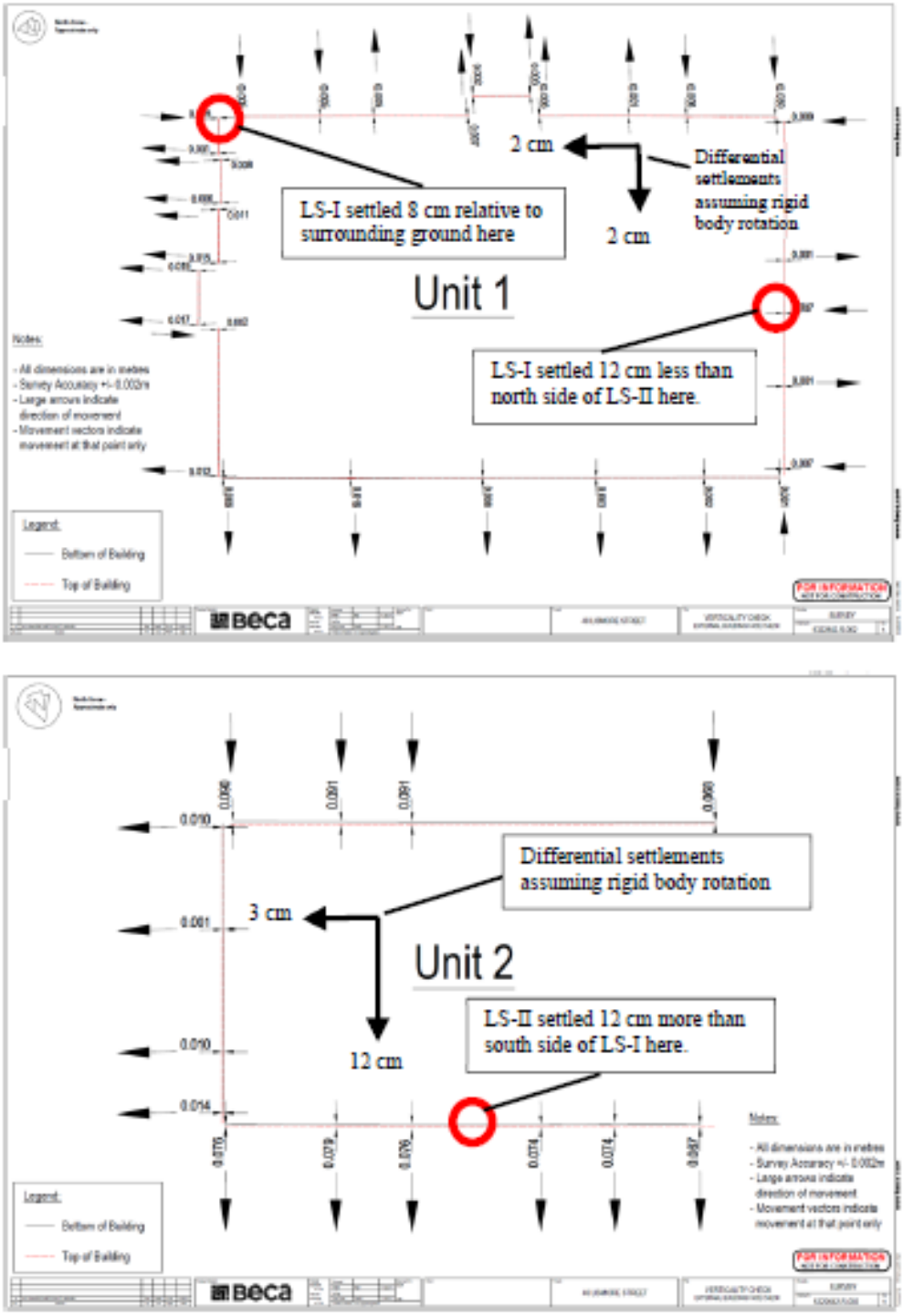

Figure 5.11: Observed settlements on LS buildings from Beca vertical survey after earthquake

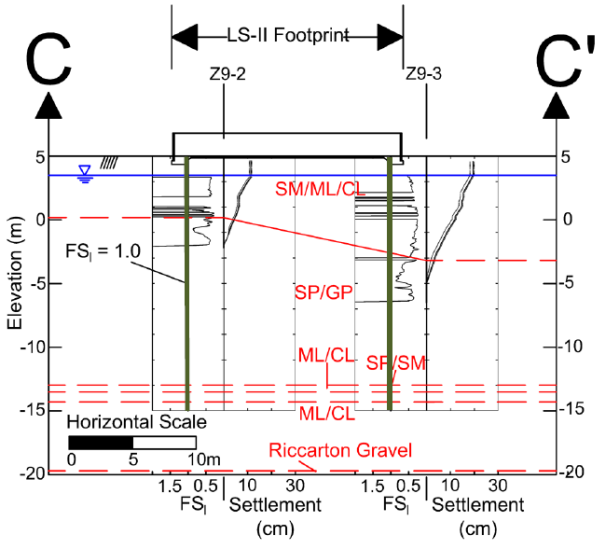

Figure 5.12: Observed settlements on LS buildings from Beca vertical survey after earthquake

Figure 5.12 shows the stratigraphy underneath LS-II building as studied by Zupan in [18]. As observed by Zupan: *the shallow liquefiable SM/ML layer may be the one critical one to the settlements. These materials, located immediately beneath the shallow strip footings that supported the building walls, appear to be present beneath the groundwater level throughout the site. Consequently, the shear induced building settlement mechanisms described by [36] were important for this case.*

Figure 5.13 focus on the observed movements of the LS-II building oriented towards North.

Given the registered observations, the Northeast side of the LS-II building settles in total 18 cm relative to the surrounding ground. (This arrises from the observation that Northeast corner of LS-I settles 8 cm relatively to the surrounding ground; LS-I has a differential settlement assuming rigid body movement of 2 cm to North and the Northeast side of LS-II settles 12 cm more than the South side of LS-I)

Zupan [18] concludes: *As described previously, the LS-II building was more severely damaged than the LS-I building. Given that both buildings were founded on strip footings with the same geometry, it would seem that foundation width has not played a role in the relative performance of these buildings. However, the distribution of structural loads appears to be more even throughout the building footprint of the LS-I building (as stated by the foundation strips distribution shown in figure 5.4), whereas the loads appear to be concentrated around the perimeter of the LS-II building, with the exception being the two footings that cut across the building footprint near the center of the building in the transverse direction. One hypothesis, therefore, would be that the relatively more even distribution of structural loads has led to relatively more even foundation settlements at the LS-I building. This is consistent with the observation that the LS-II strip footings underwent punching settlement, thereby causing the ground floor slab to deform and appear to bulge in the center relative to the perimeter.*

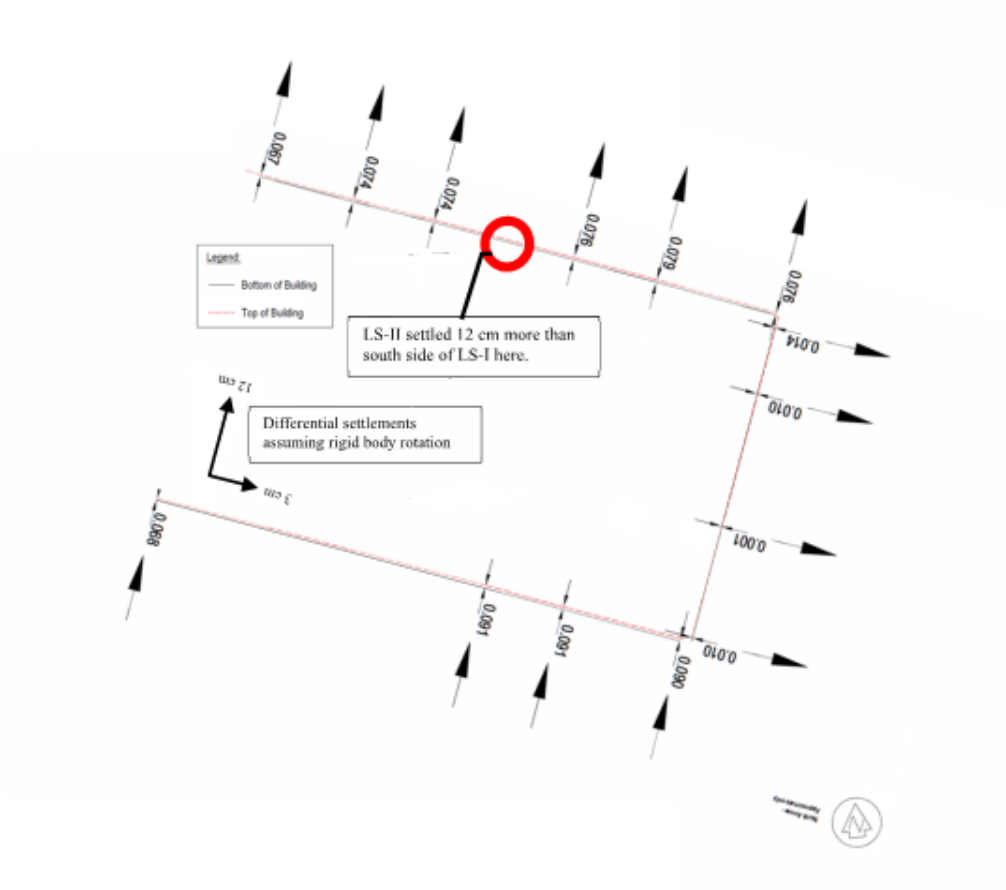

Figure 5.13: Observed settlements only on the LS-II building from Beca vertical survey after earthquake and north oriented

Differences in the SSI could have also played a significant role in the relative performance of the two buildings. As described previously, the second floor of the LS-II building was only present within the office portion of that building (i.e., the eastern 60% of the floor plan). The presence of a floor mass over the east side of the building but not the west side would have likely caused uneven superstructure inertial forces to be transferred to the building foundation, and this could have caused differential settlements due to non-uniform SSI-induced ratcheting. As indicated on Figure 5.13 the horizontal movements of the top of the concrete panel walls in the north-south direction were slightly greater on the eastern side of LS-II than the western side.

As shown by present chapter, substantial information is available on the observed consequences on LS-II building. This makes the analyses on further chapters conceivable and possible to be validated.

6
SIMPLIFIED PROCEDURE ANALYSIS

Based on the State of the Art given in Chapter 3, where liquefaction assessment methods are covered and discussed, and based on the initial objectives for this work, the present chapter makes the liquefaction assessment for the case study based on the simplified procedure. These results will then be useful for comparison with the observational data and serve as reference for the following numerical simulations.

The simplified procedure is applied through the commercial software CLIQ® for liquefaction analyses based on CPT results. The approach is based on the NCEER(1998) consensus summarised in [39] and presented in the introductory chapters.

The five CPTs to which Chapter 5 refers are given as CLIQ® input, other parameters are summarised on Table 6.1.

Table 6.1: CLIQ® input parameters values

Magnitude - M_w	PGA	GWL [from surface]
6,2	0,5 g	1,5 m

Figure 6.2 illustrates the usual conventional CLIQ® output where general soil information is presented in five plots, result of the method application to CPT 1. Analyses specifically related to liquefaction triggering and consequences are further mentioned and presented. The complete CLIQ® analyses report of all five CPTs is presented in Appendix C.

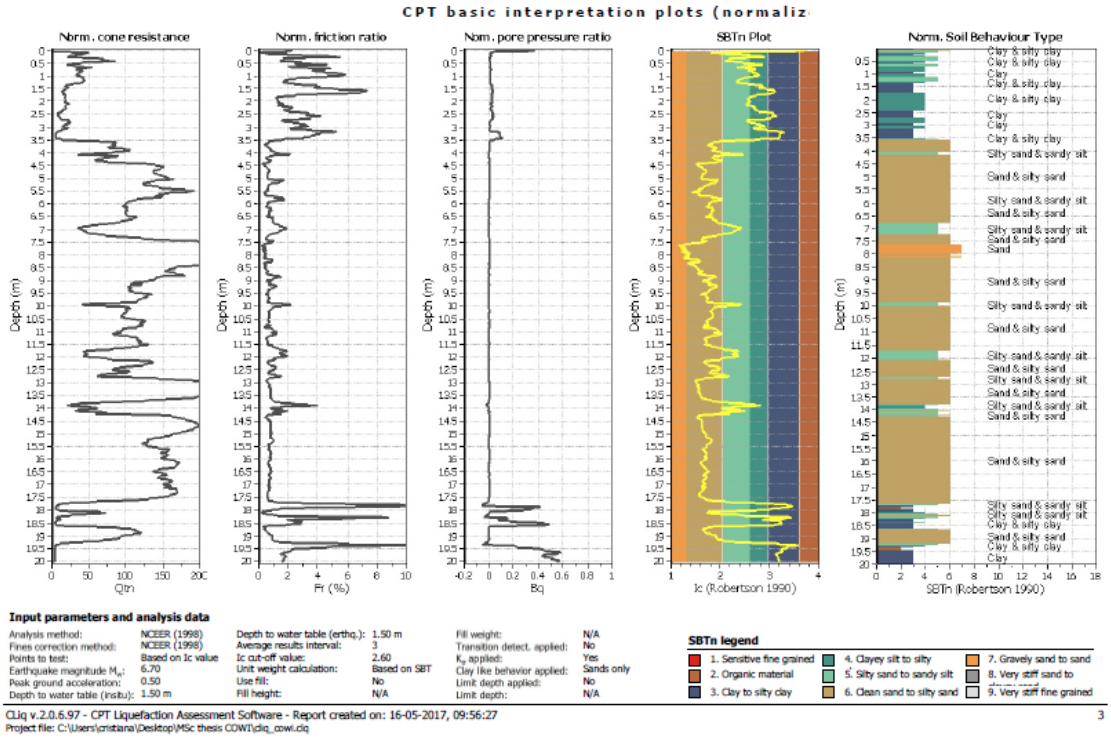

Figure 6.1: CLIQ® conventional output

6.1 CONE PENETRATION TESTS AVAILABLE AND GENERAL ANALYSES

Each of the 5 CPTs was referenced with an identification (ID) number as in Figure 5.5 and summarised in Table 6.2. Included is their identification in [28] and [18], as main data souces for the present work, and the test depth of refusal. The coordinates presented in the last column are justified and used in the subsequent section.

Table 6.2: CPT identification number, depth of refusal and coordinates

ID number	ID in [28]	ID in [18]	Refusal depth [m]	Coordinates [m]
1	CPT_34336	Z9-4	19,90	(0 ; 11,5)
2	CPT_34337	Z9-5	19,90	(22,8 ; 0)
3	CPT_34335	Z9-3	11,46	(48,4 ; 12,5)
4	CPT_34334	Z9-2	7,22	(36,1 ; 25,4)
5	CPT_34333	Z9-1	19,90	(72,4 ; 57,6)

Figure 6.2 shows the 5 CPT analyses side by side and the two with lower depth of refusal are proportionally reduced so that comparison is made easier, as for the same vertical scale. The first conclusion is that the CPTs are in good agreement, even though two of them do not reach the 20 meters of study depth. Special attention will be given to the first 4 because they are closer to each other. Consequently more accuracy is expected as they can describe reliably the soil under the LS-II building, consequence of the CPT locations presented in 6.8.

This soil can be divided in two different layers: one with clay, silty clay and sandy silt in depths between 0,5 and 5 to 7 meters; and another layer beneath this first one to the end of the studied depth of 20 meters, mainly with sand and silty sand. The presented analyses also depict that this second layer is intermittent with thin bands of more fine materials.

CPTs 1, 2 and 5 all agree on a different layer after the 18 meters depth of more fine particles. However at this depth, liquefaction is probably not a problem, specially as main focus is on soil-structure interaction of shallow founded buildings, so this soil constitutive difference will not be considered. This soil simplified characterisation will be further used for the numerical modelling.

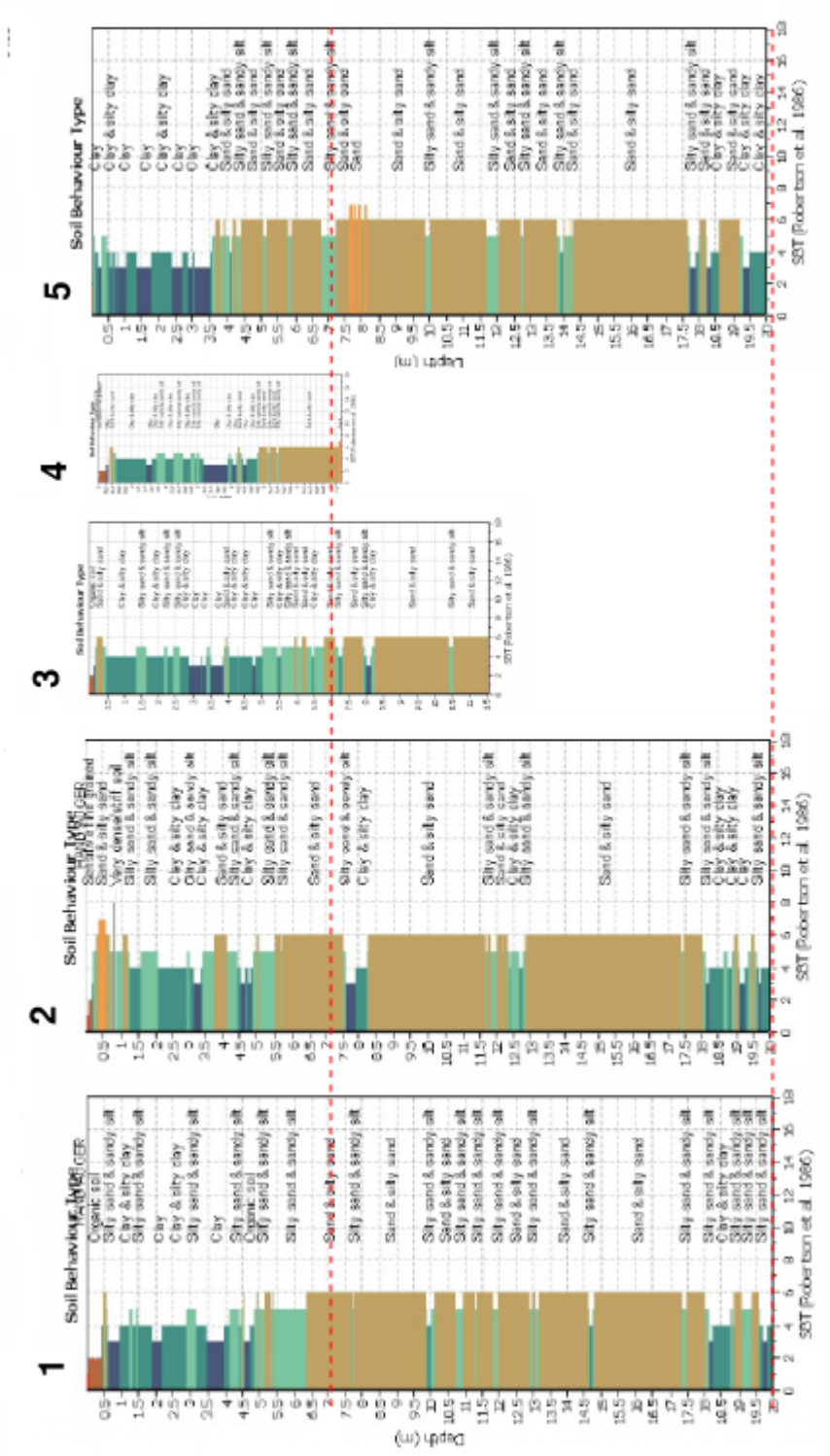

Figure 6.2: Behaviour Index analyses for the 5 CPTs and side-by-side comparison

6.2 CLIQ® SOFTWARE ANALYSES

Based on the simplified procedure presented in Chapter 3, CLIQ® estimates values for the liquefaction induced settlements considering a free-field (FF) approach. This assumes the data given by the 5 CPT to characterize the soil profile and assumes that no structure is present above it. This correlation is based on the work by Zhang [12]. The estimated values are presented in two plots, for vertical settlement and lateral displacement, shown as an integral along the CPT test depth.

Presented in figures 6.3 to 6.7 are the CLIQ® output estimative for each CPT and side-by-side are shown the expected vertical settlement and lateral displacement .

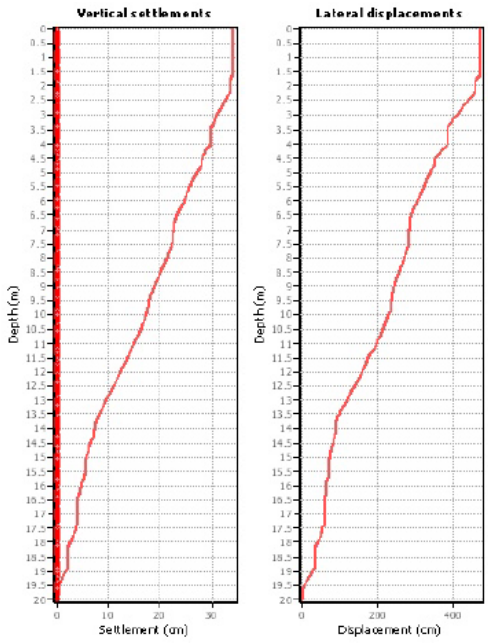

Figure 6.3: Vertical and lateral displacements CPT 1

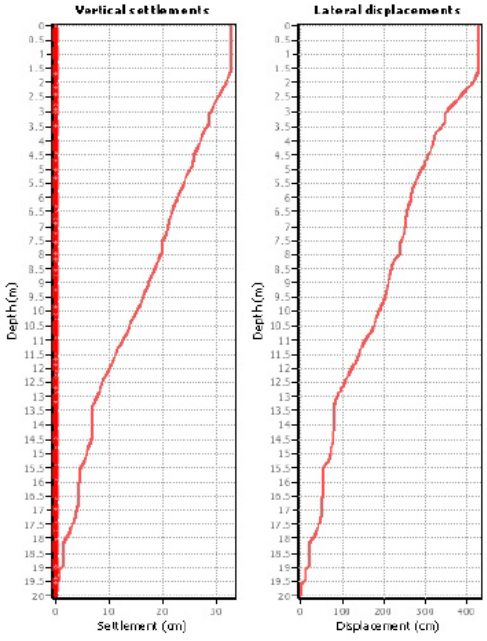

Figure 6.4: Vertical and lateral displacements CPT 2

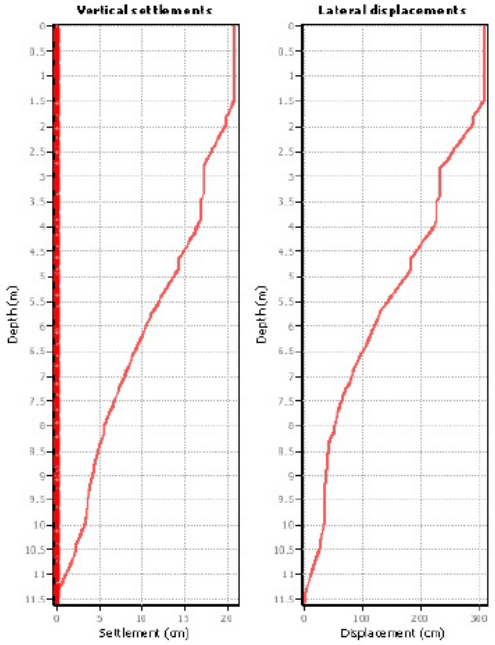

Figure 6.5: Vertical and lateral displacements CPT 3

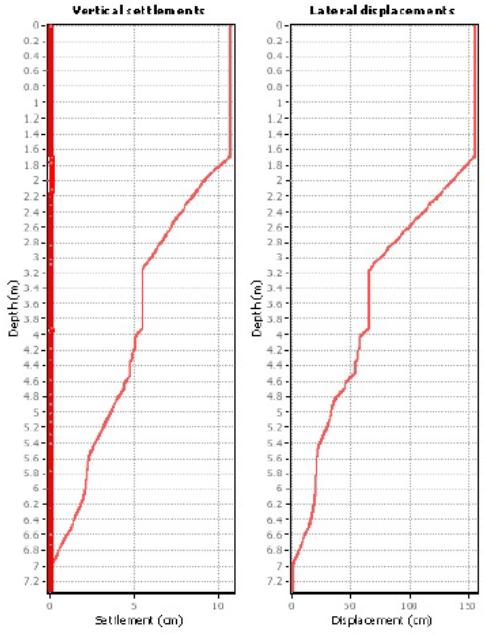

Figure 6.6: Vertical and lateral displacements CPT 4

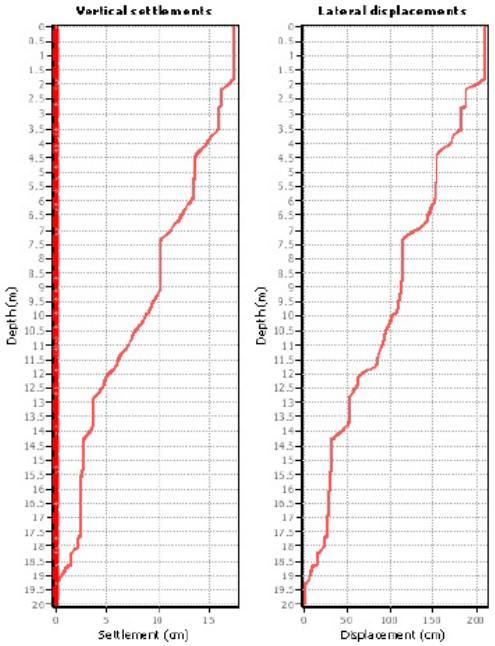

Figure 6.7: Vertical and lateral displacements CPT 5

From the CLIQ® analyses presented in Figure 6.2 where behaviour index is estimated and the vertical and lateral displacements predicted in the output of figures 6.3 to 6.7, some conclusions are presented:

- It is universal to the 5 CPTs that the layers between the depth interval of 2 to 14 meters are the substantial cause of settlements.
- The presence of fine layers of finer materials in the CPT 5 location has clear influence in the vertical and lateral displacements.

Assuming the CPT locations as in Figure 6.8 and designating the referential origin location, 2D coordinates in meters are associated to each CPT analyses.

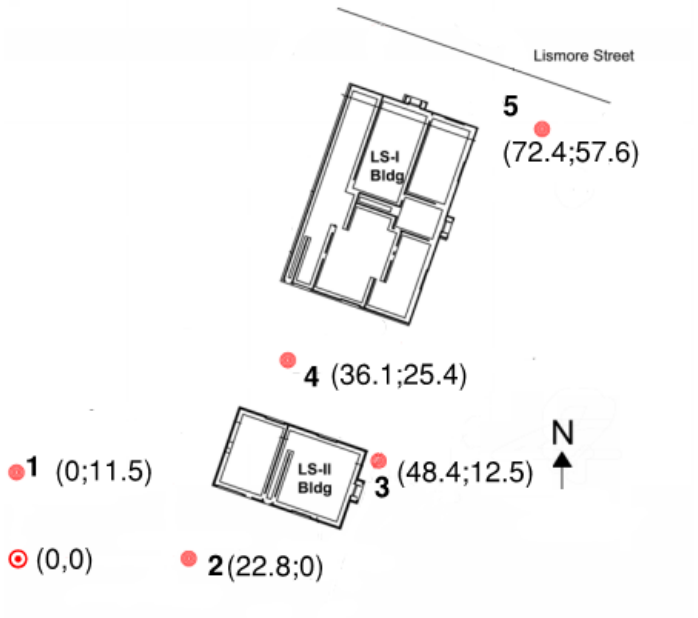

Figure 6.8: CPTs location relative to buildings and coordinates computation

This coordinates are summarised in Table 6.2. With this input information and using CLIQ®, the 2D plan distribution of liquefaction induced vertical settlements is drawn as outlined and color scaled in Figure 6.9.

Despite Figure 6.9 being a valuable way of results interpretation, the fact that there are three different depths of refusal for all 5 CPTs, makes this kind of representation possibly misleading. Therefore this plan analyses must be done considering each depth interval, so comparison is made layer by layer and more accuracy is reached.

The three different depths of refusal results are put together in Figure 6.10 as a way to simplify the results analyses.

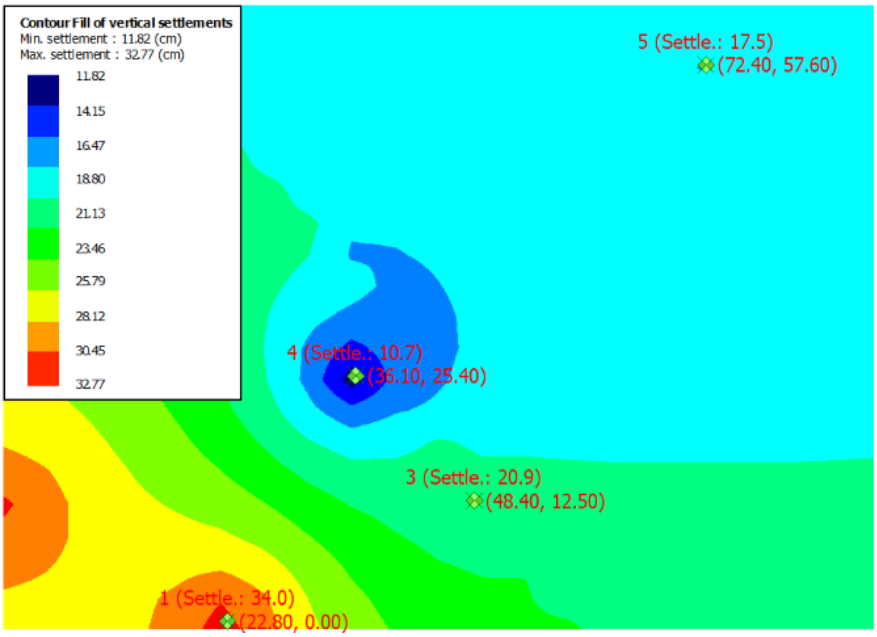

Figure 6.9: The 2D plan distribution of liquefaction induced vertical settlements outlined and color scaled

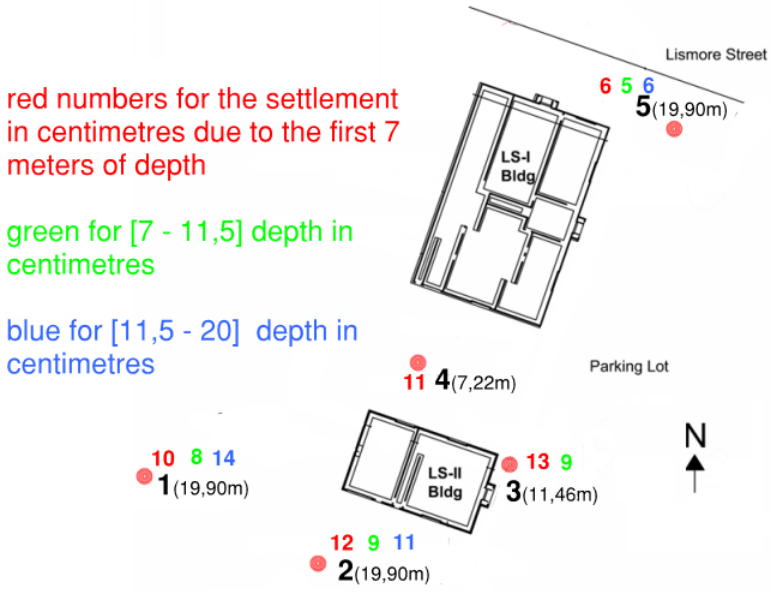

Figure 6.10: Empirical assessment of the liquefaction induced settlements assuming free-field behaviour

In Figure 6.10 three soil depth intervals are used: 0,5 to 7 meters; 7 to 11,5 meters and 11,5 to 20 meters. The vertical settlements associated to each interval is computed and associated to a color in the plan.

This results are computed considering FF soil behaviour, so that the building presence is not taken into account. Special attention to the CPTs 1 to 4, the ones around LS-II building that show a tendency of this

building for tilting towards East due to liquefaction induced differential settlements of the upper 7 meters of soil and a substantially low contribution of the [7 - 11,5] depth interval.

Another interesting analysis is made by using the surface manifestation approach proposed in [19] and presented in Section 3.2.2. CLIQ® output on this approach is presented in Figure 6.11. This approach does not take into account the building presence on surface, but only the free field.

The approach consists on the continuous sum of surface layers not susceptible to liquefaction, then related with an analogue process for the underneath liquefiable layers. The observation of estimated vertical and lateral displacements along depth and comparison with this total values makes clear the Ishiara method implemented in CLIQ®.

As the estimated PGA values is 0.5 and all CPT cordinate points are inside the proposed curve with substantial margin, it is expected considerable surface manifestation. Given the high estimated PGA value it would only be possible to have capping influence for much thicker surface layers, as there is not enough capping capacity compared with the liquefaction potential.

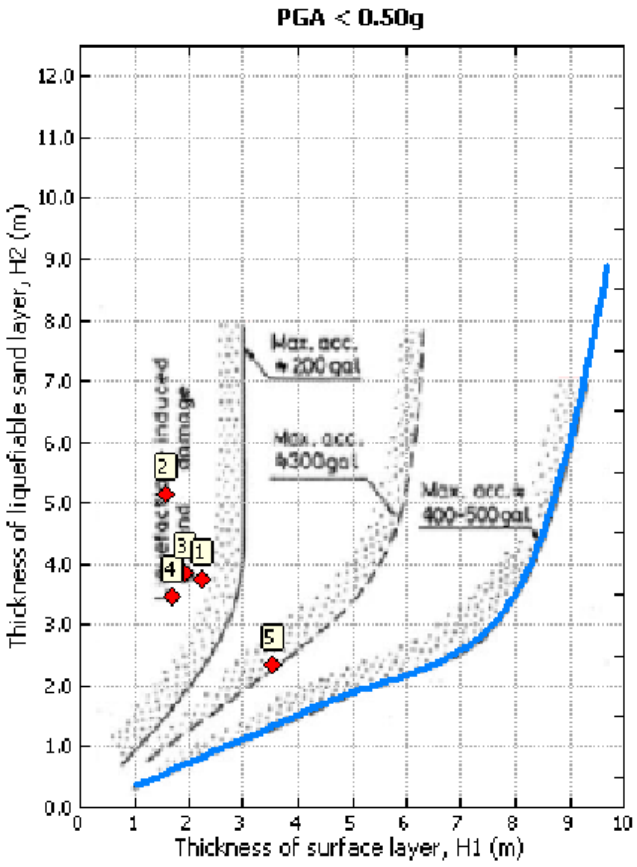

Figure 6.11: Surface manifestation analyses by CLIQ® using the approach in [19]

6.3 Comparison with observed results

The observed building performance stated in Chapter 5 is now compared with the CLIQ® analyses. Figures 6.12 to 6.14 are site plans based on the CLIQ® analyses mentioned previously for different considered depth analyses and the building foundation is schematically included without scale.

Figure 6.12 shows the vertical settlements considering only the top 7 meters of soil. A clear tendency for the building to tilt towards the Southeast direction is observed. Vertical settlements around 11 centimetres are also to be expected through all the foundation area. This tilting tendency is probably related to liquefaction of the saturated SM/ML layer described in [18] that is present in this 7 meters depth and shown in Figure 5.12.

Figure 6.13 considers the top 11,5 meters of soil, so CPT 4 location as no data after the 7 meters of depth refusal. Although not considering CPT 4 results, substantial homogeneity is found in the other CPT locations, where a uniform vertical settlement of 21 centimetres is to be expected.

Figure 6.14 contemplate the analyses of all CPTs to respective depth of refusal, so that maximum settlement values are reached. Special attention to CPTs 1 and 2 that show settlements higher than 30 centimetre.

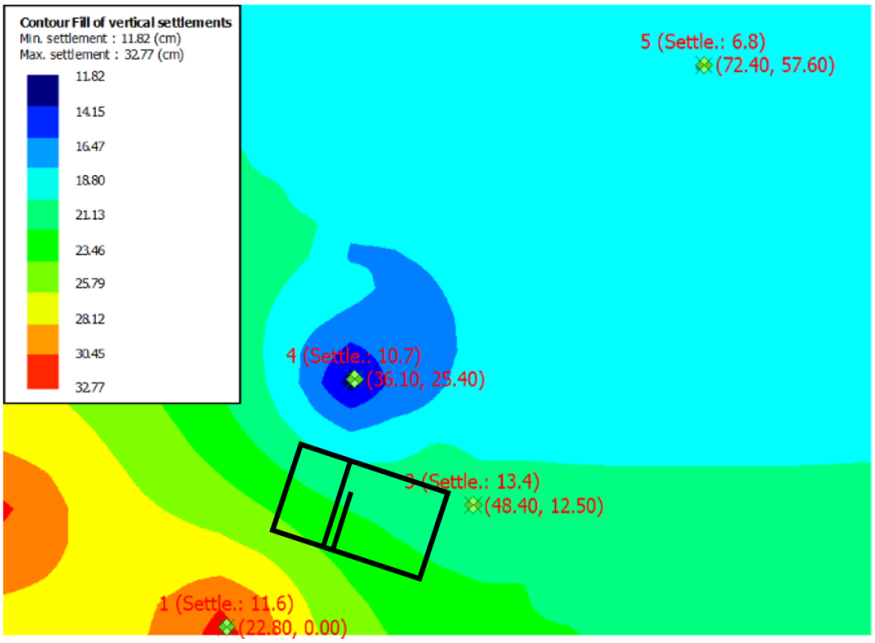

Figure 6.12: Site plant with color scaled vertical settlements due to liquefection in the top 7 meters

Figure 6.13: Site plant with color scaled vertical settlements due to liquefection in the top 11,5 meters

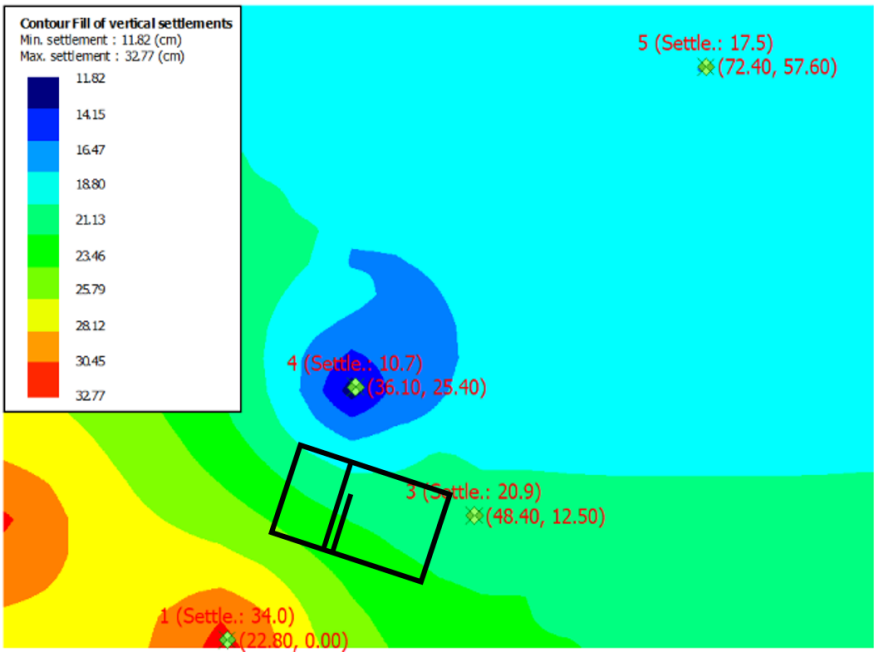

Figure 6.14: Site plant with color scaled vertical settlements due to liquefection in the 20 meters depth

Given all the above results from CPT analyses and the observed data presented in Chapter 5, it is concluded that:

- The 12 centimetre building tilting towards the north-northeast direction observed after earthquake has no substantial correlation to the tilting estimated through CPT analyses considering FF.
- The 6 centimetres building vertical settlement relative to surrounding ground that was observed is substantially low when compared with the computed 32 and 34 cm of CPTs 1 and 2, respectively.

These conclusions are in substantial agreement to other research on the subject as their possible explanation lays on SSI consequences and are not comparable to a FF analyses. Some specificities of the LS-II building might have contributed for the SSI consequences having substantial importance for final results:

The differential loads inside the building as presented in Chapter 5. The building first floor does not occupy all the plan view of the building, but only 60% of it, the west side. This differential loading in combination with soil softening due to liquefaction is the possible cause of the building tilting towards North-East, also pointed by Zupan [18].

The foundation design might also have its contribution as the loads appear to be concentrated around the perimeter and not distributed along all the foundation area. The opposite is true in the LS-I as easily observed in the plan on Figure 5.4 where LS-I structural loading is distributed in a major area when compared with LS-II. The upper mentioned higher bearing pressure and the heave observed on the foundation slab inside the building [18] makes this a possible cause of the higher vertical settlements on this strucure.

Other factor that might influence the size of the post-liquefaction settlements is the ratio between the width of foundation and the thickness of the liquefiable layer. CPT results might mislead interpretation as liquefiable layer is difficult to measure.

7
NUMERICAL SIMULATION

Current chapter presents all the numerical modelation process, stating the assumptions made. As justified in above chapters, PLAXIS® is the software used for this works numerical simulations, as it is capable of modelling both soil and structure, as well as their interaction.

7.1 INPUT GROUND MOTION

From the NZGD [28] it was possible to access data from the CCCC Seismic Station, described in Chapter 5. The data is made available with a time step of 0.02 seconds, recording acceleration, velocity and displacements in three directions: N00E; N90W and vertical. For simplicity N90W was assumed as the most descriptive direction as it is the one with higher acceleration values. The data was given as input to PLAXIS® as a table of accelarations and *baseline correction* option is activated. Final dynamic multiplier input plot on is shown in Figure 7.1.

By selecting the upper mentioned *drift correction*, PLAXIS® corrects the possible drift in the displacements (i.e. non null final displacements in the signal), caused by the integration of the accelerations and velocities. The correction is made by applying a low frequency motion from the begining of the phase of the calculation and by correcting the acceleration accordingly. For a correct *drift correction*, the time interval of the phase and of the input signal should be the same, as further shown. [2]

The simulation dynamic time is set to 40 seconds, this is assumed based on user experience, as strong seismic shaking peaks without little ones at the beggining and end of the seismic signal may cause converging complications. On the other hand PLAXIS® cannot simulate soil drainage during dynamic phase. The consequence of creating a 40 seconds time interval of strong shaking during which there is no drainage is the high usage of a total stress analyses on a case where drainage is likely to take place. This evidence has effects on the settlements and strain estimation, further acknowledged.

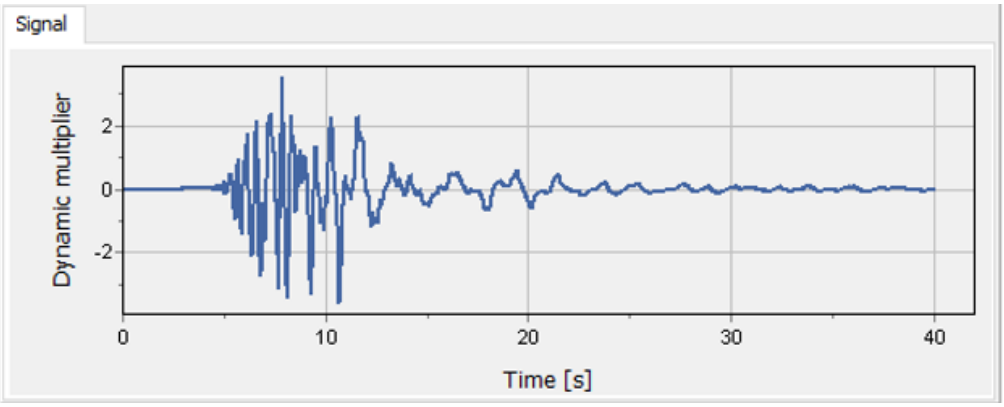

Figure 7.1: Dynamic multiplier (as factor of the acceleration) for earthquake signal input on PLAXIS®

7.2 Soil profile

Figure 6.2 shows the 5 CPT side by side for comparison. As stated in Chapter 5, the CPTs 1 to 4 will be the ones used for modelling as they are the ones around the LS-II building, so more accuracy is made possible. As stated in Chapter 6 this soil will be generally divided in two different layers: the above one with clay, silty clay and sandy silt for depths between 0,5 and 5 to 7 meters; and another layer from the bottom of this first one to the end of the studied depth of 20 meters, mainly with sand and silty sand constituents.

The deepest introduced layer is used as bedrock of the model as proposed by the PLAXIS® manual. [2] Figure 7.2 schematically shows the simulated soil profile with the three uppermentioned layers and the 1 meter ground water level.

7.3 Materials parametrization

As proposed in PLAXIS® manual [2] and common practice engineering the numerical simulation must be made using phases, as explained in further section. Different phases will require specific soil constitutive models and in this work UBC3D-PLM and Hardening Soil will be the ones used and its parameters calculation is shown in this section.

Parameters for the first 7 meters layer (unit A) are computed solely based on CPT 4, as the one with more properties homogeneity in this area. The soil underneath (unit B) has its parameters computed through an arithmetic mean and combination of CPTs 2 and 3 considering that no thin materials layers are present, meaning that all material is Sand and Silty Sand.

7.3.1 UBC3D-PLM soil constitutive model parameters

UBC3D-PLM parameters are calculated based on the equations proposed in [3] and stated in Chapter 3. These equations are based on the normalised SPT blow count number, $(N_1)_{60}$.

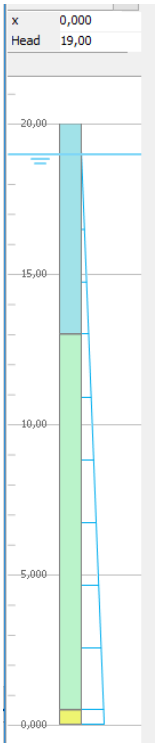

Figure 7.2: Soil profile used for PLAXIS® input

Although there are other options available, this work assumes the CPT to be the best *in situ* test for liquefaction assessment as a continuum results spectrum is possible. The chosen path was to convert the CPT values into SPT ones using the CLIQ® framework and use the layers mean value as descriptive of all layer. This assumption has clear advantages and disadvantages acknowledged by the author but not much discussed here for simplicity. Main advantage being the fact that CPT tests a virtually continuous soil profile while SPT only assesses soil on discrete depths. This is specially important as liquefaction vast consequences may be caused by a thin layer possibly undetectable to the SPT. The correlation of CPT values to SPT ones has its own limitations as many parameters are estimated from from only one parameter, the SPT normalised blow count number and are assumed to characterize a complex soil layer.

The average SPT blow count values for each layer are presented in Table 7.1 as well as estimated relative density ($D_r$in percentage) value.

Table 7.1: Equivalent SPT blow count number used as representative of the soil layers

Layer	Depth [m]	$(N_1)_{60}$	D_r [%]	V_S velocity [m/s]
Unit A	0 - 7	11,6	34	150
Unit B	7 - 20	23,8	40	215

The relative densities announce a loose to medium loose soil, very susceptible to liquefaction triggering. Ap-

plying the correlations presented in Chapter 4 and proprosed by [26], the parameters values were computed and final values are shown in Table 7.2. It must be taken into account that this correlations are proposed for use in the UBCSAND model and not in the UBC3D-PLM. For simplicity they will be assumed as valid for present model, as Makra [2] proposes.

Table 7.2: UBC3D-PLM constitutive model parameters

Parameter	A unit	B unit
ϕ'_{cv}	37	38
ϕ'_{p}	41	42
c'	0	0
K^e_G	1188	1217
K^p_G	1603	1883
K^e_B	831	852
me	0.5	0.5
ne	0.5	0.5
np	0.4	0.4
R_f	0.69	0.69
$p_{ref}(kN/m^2)$	100	100
$\sigma_t(kN/m^2)$	0	0
fac_{hard}	0.45	0.45
$(N1)_{60}$	11,6	23,8
fac_{post}	0.02	0.02
K_0	0.5	0.5

The parameters me, ne and np have their values taken from the ones proposed by [2]. A parametrization study would be needed for good accuracy on the values of fac_{hard} and fac_{post}. As this is out of the scope of the present work and based on the values proposed by Makra in [3] these were assumed to be as presented in Table 7.2.

7.3.2 HARDENING SOIL CONSTITUTIVE MODEL PARAMETERS

The Hardening Soil (HS) model is not extensively explained here as it is not the main focus of this work and only used to create the initial stress level. Further understanding might be useful from [3]. The assumed values are achieved as a combination of CPT data and equations for correlation used in similar works by Borozan [16] and Makra [3].

Table 7.3: Hardening Soil constitutive model parameters

Parameter	A unit	B unit
$\phi(^\circ)$	37	38
$\psi(^\circ)$	41	42
c' (kPa)	0	0
E_{50}^{ref} (kPa)	33724,3	67556,6
E_{oed}^{ref} (kPa)	33724,3	67556,6
E_{ur}^{ref}	101172,8	202669,7
m	0,5	0,5
K_0	0.5	0.5

7.4 STRUCTURE

The structure is modelled based on the available construction plans (Figure 7.3); general description from Zupan [18] and local photographs (Figure 7.4).

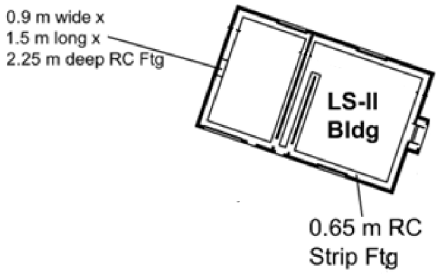

Figure 7.3: Building structural plan [18]

Figure 7.4: LS-II building photo [18]

Based on the foundation illustrated in the building structural plans shown in Figure 7.3 the concrete volume was approximately assessed to be of 61.8 m^3, as shown in the following calculations:

$$(1,2 * 0,65) * (18 * 2 + 11 * 2) = 45 \quad m^3$$

$$(18 - 1,2 * 2) * (11 - 1,2 * 2) = 16,8 \quad m^3$$

$$45 + 16,8 = 61,8 \quad m^3$$

where the building measures 18 per 11 meters long and scaling was used to assess the foundation strip width of 1,2 meters. The two floors and roof were assumed to have the 10 kPa loading and considering concrete to be 25 KN/m^3, the pressure imposed by the building in the foundation layer is approximately about 38 kPa, as follows:

$$3 * 10 + 61,8 * 25/(11 * 18) \approx 38 \quad kPa$$

As aiming for a 2D numerical model, the modelled structure was a building section on the transverse direction as this is the direction of most of the observed tilting movements, as mentioned above. The input structure is presented in Figure 7.5 wich explanation follows.

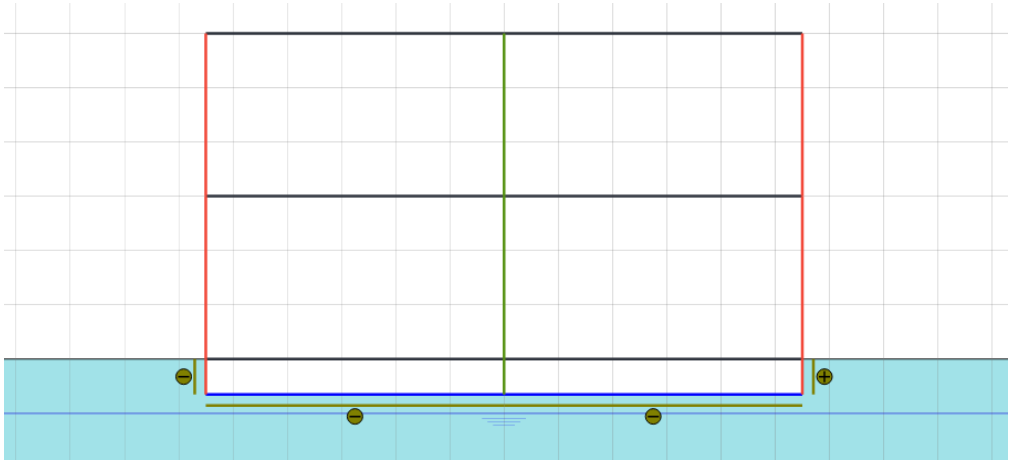

Figure 7.5: Structure simulation for PLAXIS® input

All structural components were modelled with plates, except for the middle column that uses a node-to-node anchor (NtN anchor). This exception is made for proper model functioning and as no extra weight is added by this component.

The linear-elastic isotropic behaviour is assumed and average Rayleigh damping coefficients for concrete structures are assigned as shown in Table 7.4. "The stiffness is given per unit width in out-of-plane direction, while weight is given as force per unit of length per unit width in the out-of-plane direction." The parameters values are presented in Table 7.4

Table 7.4: Structure components parameters

Parameter	Vertical	Horizontal	Foundation	NtN anchor
Color	RED	BLACK	BLUE	GREEN
Weight - w [KN/m/m]	0	10	8	0
Normal stiffness - EA [KN7M]	9 x 10^6	9 x 10^6	1,2 x 10^7	2,5 x 10^6
Flexural stiffness - EI[KNm^2/m]	6,75 x 10^4	6,75 x 10^4	1,6 x 10^5	–
Poisson ratio - ν	0	0	0	0
Rayleigh coefficients - α/β	0.232/8· 10-3	0.232/8· 10-3	0.232/8· 10-3	0.232/8· 10-3

To model the relative displacement and interaction between soil and structure PLAXIS® allows the introduction of an interface in the soil-structure boundary as seen in Figure 7.5.

7.5 DAMPING

Strain levels above 10^{-4} - 10^{-2} %, are considered high and most Plaxis models are capable of campturing their consequent damping. Still small vibrations create small strain levels that are responsible for irreversible soil behaviour, that must be taken into account for soil representation close to reality. To take the small strain associated damping into account it is suggested in [2] to define Rayleigh damping coeficients.

The Rayleigh damping is expressed through damping matrix [C], constituted by a portion of mass [M] and stiffness [K] matrixes, defined by the Rayleigh coeficients α and β, as follows:

$$[C] = \alpha[M] + \beta[K] \tag{7.1}$$

These two coefficients are calibrated following the procedure by [2]. The used Fourier Acceleration spectrum is presented in Figure 7.6; V_S waves velocity is assumed equal to the respective layer mean value, presented in Table 7.1 and the thickness of the soil layer is assumed to be 50 meters, regarding CCCC seismic station geology in Appendix B.

The graphic representation of the computatiion procedure used by PLAXIS® follows in Figure 7.7 and final values are then summarised in Table 7.5.

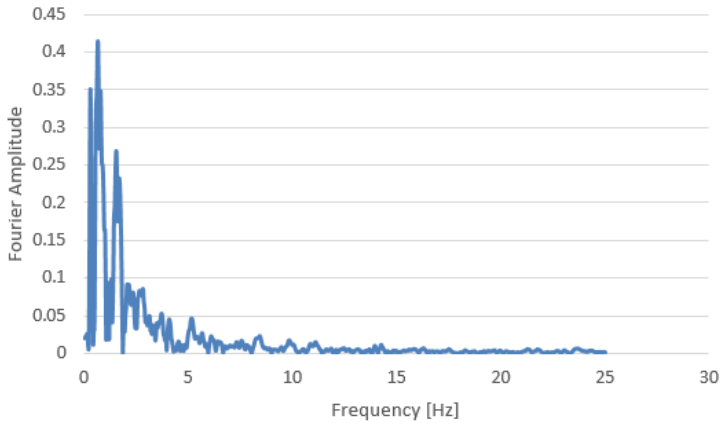

Figure 7.6: Fourier acceleration spectrum of the assumed earthquake

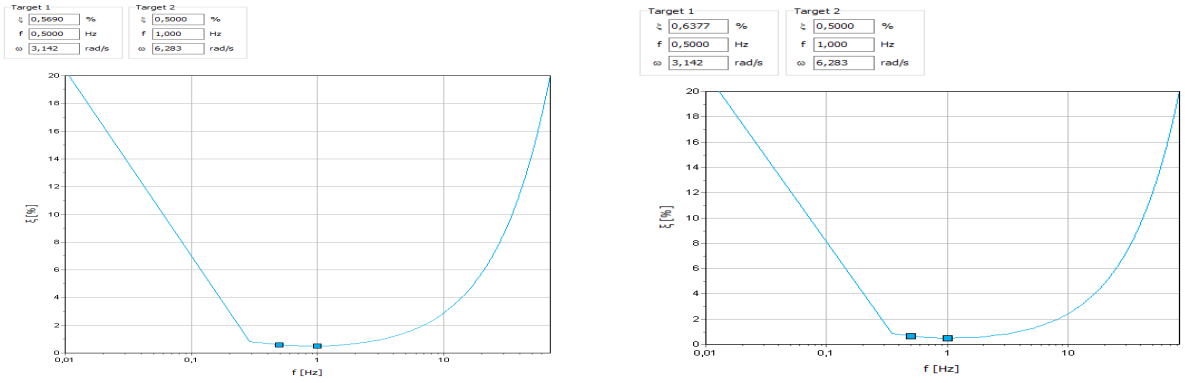

(a) (b)

Figure 7.7: Rayleigh damping ratios computation in PLAXIS® for (a) Unit A and (b) Unit B

Table 7.5: Input Rayleigh damping coeficient values

Unit	α	β
A	0.02672	$0.9147 \cdot 10^{-3}$
B	0.03248	$0.7689 \cdot 10^{-3}$

7.6 MESH

The mesh generation is fully automatic and based on a robust triangulation procedure [2], that produces a mesh with its average element size equal or less than one-eight of the wavelenght associated with the maximum frequency component f_{max} of the input wave, following the equation:

$$AES \leq \frac{\lambda}{8} = \frac{\mathrm{v}_{s,min}}{8 \cdot f_{max}} \tag{7.2}$$

where AES stands for the Average Element Size; $\mathrm{v}_{s,min}$ for the lowest wave velocity and f_{max} for the maximum frequency component.

As the main focus of this work is the seismic induced liquefaction mechanisms under shallow founded structures and given that those mechanisms take place in the top level of the soil profile, around the building foundation: a more coarse mesh was set to this area as Figure 7.8 shows and final used mesh is presented in Figure 7.9 to reach more accuracy.

The model width has great influence in the results accuracy has its low value may have two consequences: seismic waves reflection on boundaries, multiplying the seismic loading imposed to the soil, and lateral displacements may be restricted. However very wide models reach very high calculations time. Based on user experience, a 80 meters wide model was assumed and has its vertical boundaries further presented. Further presented results show that this model is not wide enough for a well calibrated outcome, as hereinafter

mentioned.

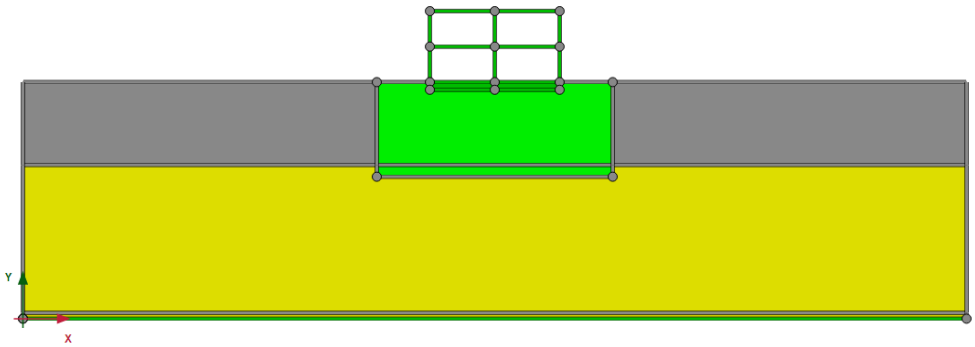

Figure 7.8: Different mesh coarseness areas

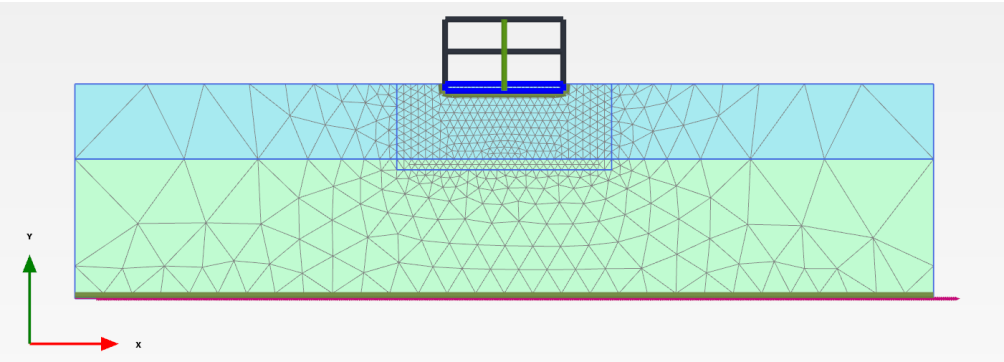

Figure 7.9: Final mesh used for the numerical simulation

7.7 PHASES

As proposed by the PLAXIS® manual [2], known to the common practice and specific to the present problem characteristics the simulation is made following 4 sequential phases explained and justified in present section.

7.7.1 INITIAL PHASE

To correctly generate the initial stress state it is needed to calculate the called ”initial phase” where the upper justified Hardening Soil constitutive model is used. This is a static phase and default fixities must be applied, resulting on normally fixed vertical boundaries for x_{min} and x_{max} and a fully fixed base at the bottom.

7.7.2 STATIC PHASE

This calculation step is used to ensure the initial stress field equilibrium and the occurrence of possible plastic points. In the present case this phase is needed to make the structure inclusion possible as well as the respective interfaces. The soil behaviour is also ruled by the Hardening Soil model.

In the end of the present phase the possible displacements induced by the structure activation must be set to zero so they have no influence in the forthcoming phases.

7.7.3 Dynamic phase

The most critical part of the simulation takes part in this phase as the liquefaction phenomena is simulated. The UBC3D-PLM soil constitutive model is used to simulate the creation of porewater pressure and the consequent decreasing of effective stress level. To properly simulate the wave propagation the boundaries must be readjusted in this phase: The vertical boundaries for x_{min} and x_{max} are given tied degrees of freedom to satisfy equal displacements of the two sides of the model as they have same depth and seismic loading.

The bottom boundary must be compliant base, in which case thin layer of rock formation should be introduced at the base of the model. This linear-elastic material absorbs the downward propagating waves, and thus allows for capturing the effect of continuation of seismic waves into the underlying deep soil.

7.7.4 Consolidation phase

After the rising of the porewater pressure as consequence of the seismic induced loading and to simulate the effects of post-consolidation volumetric settlements a consolidation phase is used.

Many consolidation options are available in PLAXIS$_{®}$ and the one used in this work is the Staged Construction one that makes possible to the user to set a specific time and the software will assume consolidation stops at that time independent of the still existing porewater pressure.

The boundary conditions must all be set as closed except for the top one which was kept open in order to grant porewater pressure dissipation through it, in order to have the consolidation indiced volumetric displacements.

7.8 NODES AND STRESS POINTS

To permit the generation of stress and displacement curves versus time with accuracy, nodes and stress points must be defined before calculation proceeds.

Figure 7.10 shows the relative location of the defined nodes and stress points summarised in Table 7.6.

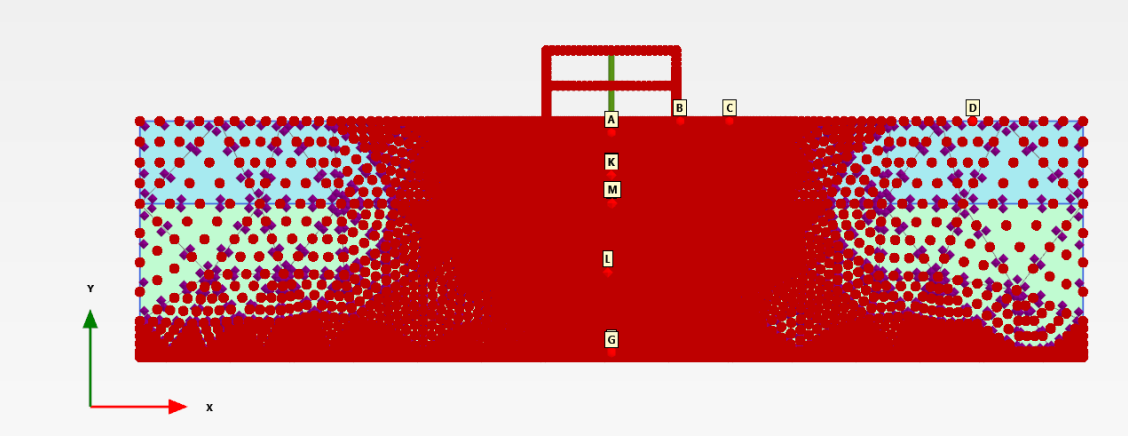

Figure 7.10: Nodes and stress points location and identification letter

Table 7.6: Nodes and stress points coordinates and description

Letter	Information	Coordinates	Description
A	Node	(40.00 ; 19.35)	Soil center of the building
B	Node	(45.50 ; 20.00)	Soil side of the building
C	Node	(50.00 ; 20.00)	Soil influenced by the building
D	Node	(70.64 ; 20.00)	Soil not influenced by the building
E	Node	(40.00 ; 13.00)	Soil units transition
F	Node	(40.00 ; 0.50)	Unit B transition to Rock
G	Node	(40.00 ; 0.00)	Base of the model
K	Stress Point	(40.00 ; 15.42)	Unit A center
L	Stress Point	(39.68 ; 7.18)	Unit B center
M	Stress Point	(40.06 ; 13.03)	Soil units transition

8
RESULTS ANALYSES AND DISCUSSION

Following Chapter 7, the present chapter outlines the simulation results and begins the discussion that is concluded in Chapter 9.

Although Plaxis® manual [2] accounts for a final consolidation phase for porewater pressure dissipation and consequent volumetric settlements to take place, this was not possible to achieve in present work. With an non-identified software or input parameters error and the approaching deadline, the consolidation phase does not present proper results. Nevertheless the achieved results are further presented.

8.1 NUMERICAL SIMULATION RESULTS

8.1.1 VERTICAL DISPLACEMENTS

In the present case study vertical displacements values are of major importance as it is the one parameter available for comparison with *in situ* observed results. Although the ”volumetric settlements” that take place when porewater pressure dissipates are not contemplated in the present results, the most important settlements are. As a result of the fact that in the presence of the structure loading, deviatoric induced displacements take place during seismic loading, even thought no drainage takes place and those are the most important displacements happening in present case study.

Figure 8.1 presents the vertical settlements consequence of the upper mentioned Static phase. In this phase, staged construction is applied to generate the stress field created by the structure construction. The settlements vary from zero to 0.220 centimetres and maximum values happen underneath the structure, which is to be expected.

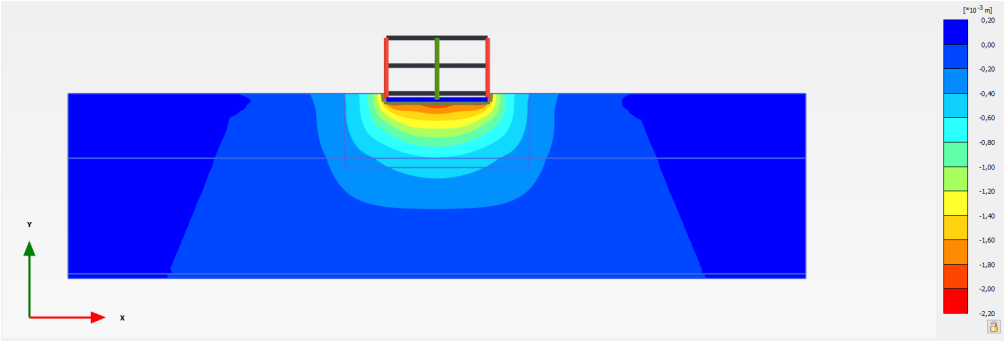

Figure 8.1: Vertical displacements after Static phase

When next phase takes place the previous settlements are rebooted to zero, so that there is no influence from the static phase. After the Dynamic phase, the upper mentioned deviatoric shear induced displacements take place as consequence of the structure presence. As shown by Figure 8.2 there are two different types of displacements taking place: settlements underneath the building and with its maximum values at the centre of it and heave close to the model vertical boundaries. The settlements values has its maximum in the centre of the building, reaching almost 40 centimetres and heave displaces for 16 centimetres.

These heave displacements above discribed are the consequence of an undrainded dynamic analyses, as no volumetric change is permited and the soil that is moved by the building punching tends to heave where there is no building influence.

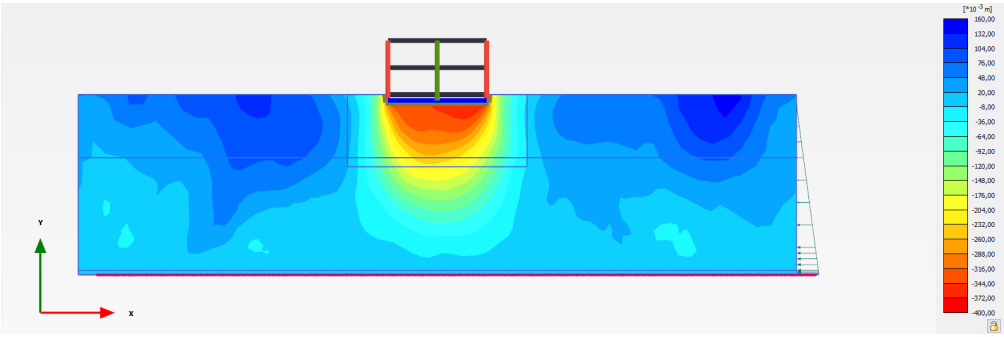

Figure 8.2: Vertical displacements after the dynamic phase

8.1.1.1 Vertical displacements generation curves

For better results analyses, three curves are drawn and further presented showing the vertical displacements evolution of three points during the dynamic analyses time of 40 seconds. The points coordinates and description are summarised in Table 7.6. Figure 8.3 shows the vertical displacements of stress points B, C and D plotted along the earthquake time.

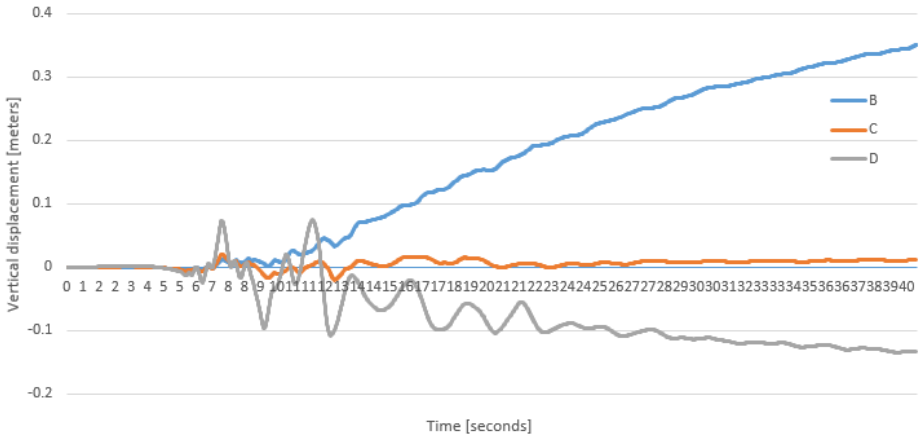

Figure 8.3: Vertical displacements during dynamic phase

Positive displacements refer to soil settlements and negative displacements refer to soil heave. Figure 8.3 makes the undrained conditions clear as the settlement of node B is atoned by the heave of D. The intermediate point C as no substantial change at the end of the shaking, although is influenced by the shaking during seismic loading.

Of particular importance is the fact that after first time interval of 20 seconds, where the highest acceleration of seismic signal takes place (Figure 7.1, the vertical settlements are still increasing, while stabilisation would be expected. This is understood as a consequence of the fact that during dynamic total stress phase on PLAXIS® substantial wave reflection on the model boundaries is taking place. As consequence of this wave reflection, higher seismic loading is imposed on the soil. This aspect would force porewatrer pressure to rise steadily during all period of seismic loading, and vertical settlements increasing accordingly.

Although it was not possible to model in this work the consolidation phase, the heave measured in point D would tend to disappear as the excess porewater pressure is dissipated.

8.1.2 LATERAL DISPLACEMENTS

One of the most damaging seismic induced liquefaction consequences on buildings are the lateral displacements. Not on the scope of this dissertation but the lateral displacements may introduce tension stresses on buildings with very damaging effects on its concrete structures.

The lateral displacements distribution is presented in Figure 8.4 where the highest values of almost 4 meters are observed underneath the building and compression values of 1.6 meters are to be found around the building, again confirming the building punching behaviour. Presented results also make clear the necessity of a wider model, where the vertical boundaries do not prevent lateral spreading from taking place. This question will be further discussed.

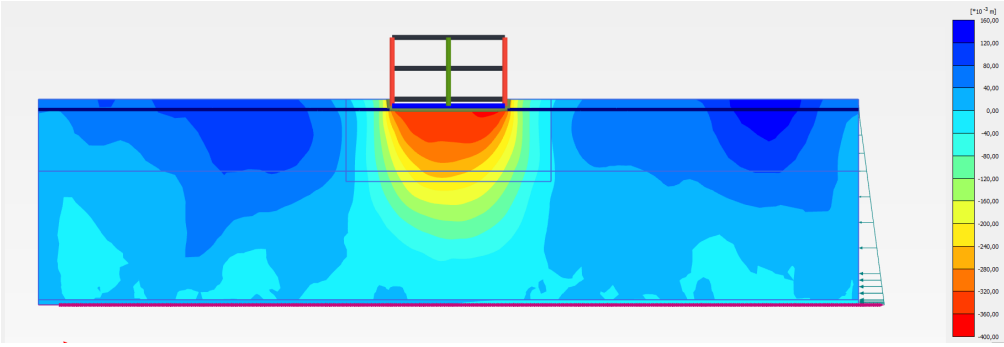

Figure 8.4: lateral displacements

8.1.2.1 Lateral displacements cross section

A cross section was drawn at four meters depth in the model and results are shown in Figure 8.5.

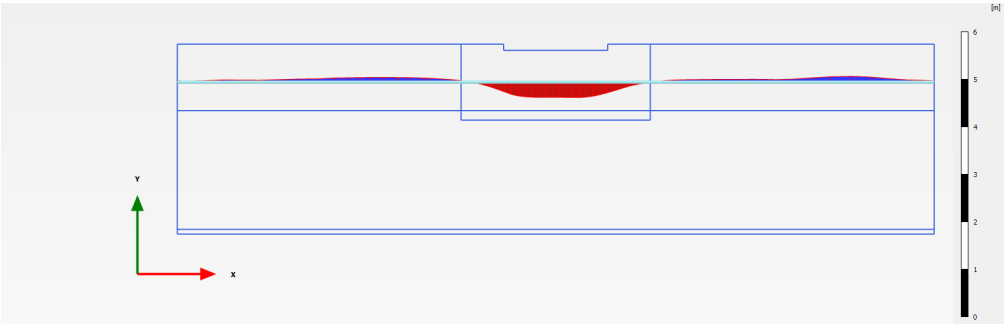

Figure 8.5: Cross section with lateral displacement values

8.1.3 Shear stress and deviatoric stress

Defining the relative shear strength as presented in Equation 8.1, this parameter can be used as a liquefaction triggering indicator.

$$\tau_{rel} = \frac{\tau_{mob}}{\tau_{max}} \tag{8.1}$$

where τ_{mob} is the mobilised shear stress and τ_{max} the maximum shear stress from the Mohr-Coulomb failure envelope. The relative shear strength τ_{rel} is the quotient of the two.

After the Dynamic phase τ_{rel} reaches highest values as porewater pressure is generated and no dissipation takes place. Figure 8.6 presents the final relative shear stress distribution. Results inacuracy is clear, probably caused by mesh coarseness.

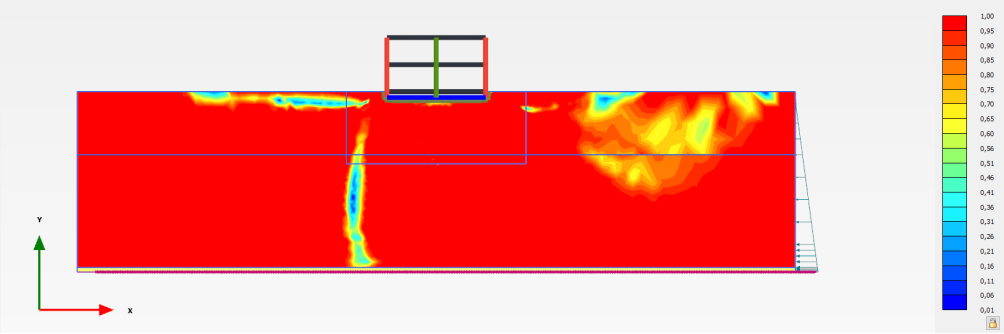

Figure 8.6: Relative shear strength after the Dynamic phase

Also important for this dissertation are the following results where the taking place of deviatoric shear stresses is made clear. As the present analyses is under undrained conditions all previously observed displacements are consequence of this deviatoric shear stresses.

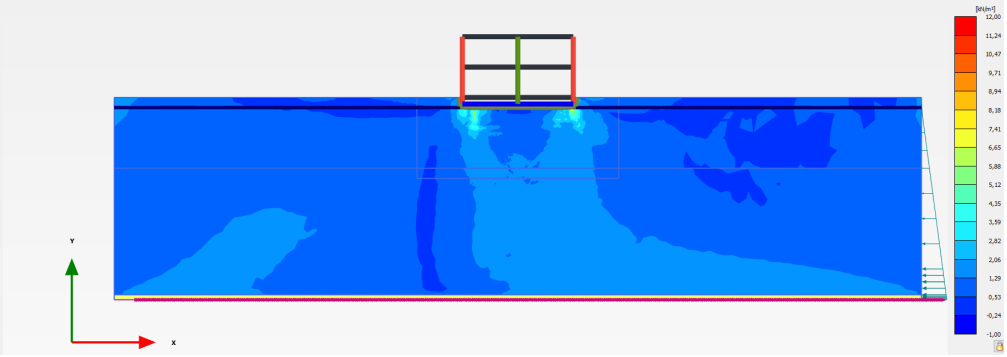

Figure 8.7: Mobilized shear stress distribution after dynamic phase

Figure 8.8 shows the distribution of the total deviatoric strain distribution with the maximum values located

underneath the building corners.

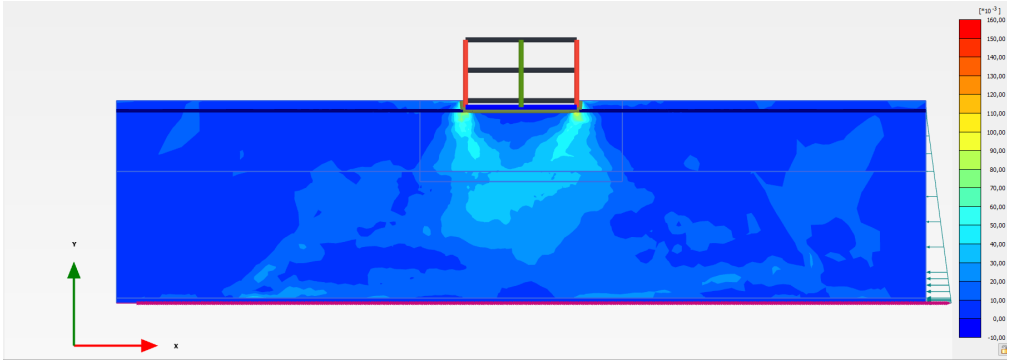

Figure 8.8: Total shear strain distribution

Figure 8.9 shows the incremental deviatoric strain dissemination where it is clear the formation of a rupture surface. Maximum values are located in the building corners and reach 1.5%, so colapse is not reached.

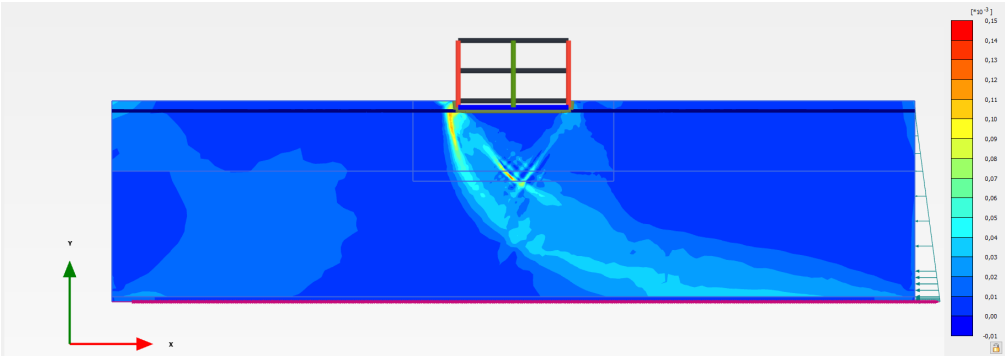

Figure 8.9: Incremental shear strain distribution

8.1.4 Excess porewater pressure generation curves

Figure 8.10 shows the excess porewater pressure generation plotted along the earthquake shaking time. Highest generation ratios take place in the interval from 4 to 18 seconds approximately, which resembles the highest amplitude acceleration spikes as in Figure 7.1. The four points coordinates and description are presented in Table 7.6.

Highest porewater pressure values take place in stress point L, as the one where initial effective stress is higher and bears more porewater pressure generation.

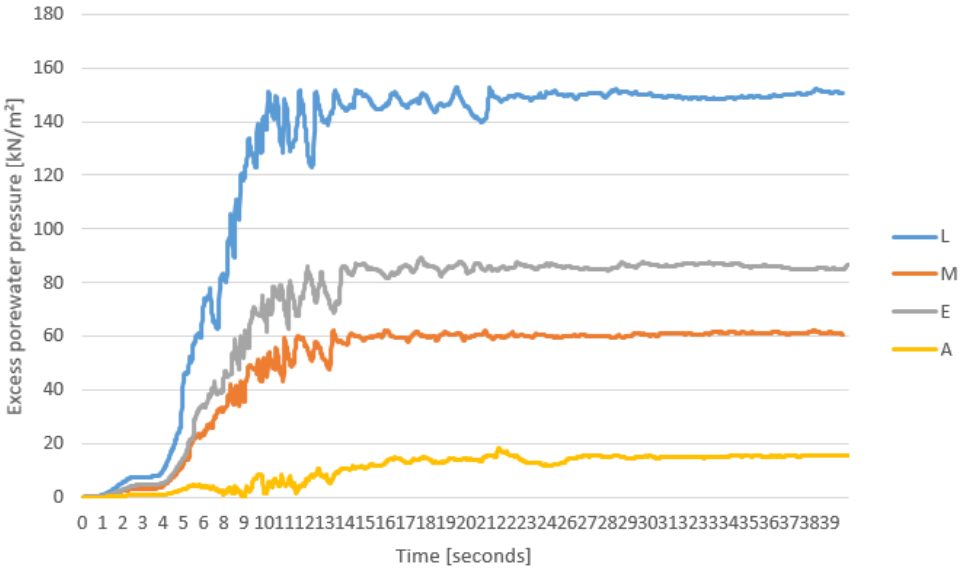

Figure 8.10: Porewater pressure evolution during dynamic phase

An expected diverse trend of steady increasing of the porewater pressure in the lateral points (B in the extreme corner of the foundation; C lateral and distanced from the foundation and D close to the vertical boundary) which can explain the continuous increase of settlements, mostly due to shear displacements, shown by Figure 8.3.

8.1.5 Undrained behaviour of dynamic phase

Figures 8.12 and 8.11 are not of major importance for results comparison but are essential as model results validation. The fact that the soils heaves near the vertical boundaries proves that the model width is not enough to ensure proper results. In a FF case there would be no vertical or lateral displacements during dynamic phase, as no volumetric change is possible without drainage. As for this model, the soil far enough from structural influence should have a FF like behaviour.

In this model it becomes clear through figures 8.11 and 8.12 that the structure influences all the model, as there are vertical displacements close to the vertical boundaries. Being so it must be concluded that boundary conditions are wrongly defined and the model requires enlarged horizontal dimension.

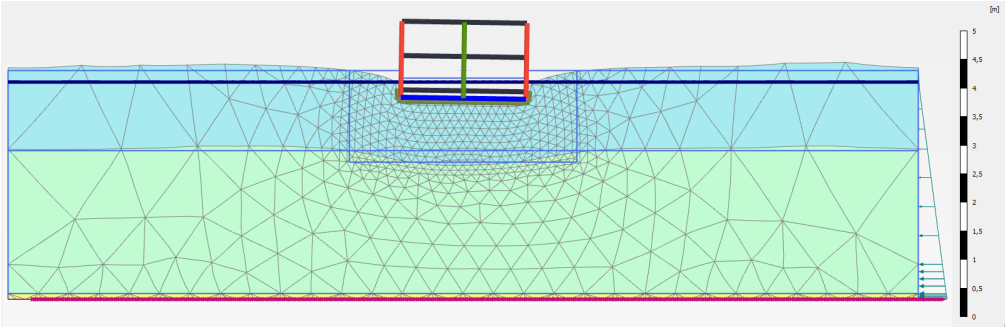

Figure 8.11: Enlarged scale model deformation 1

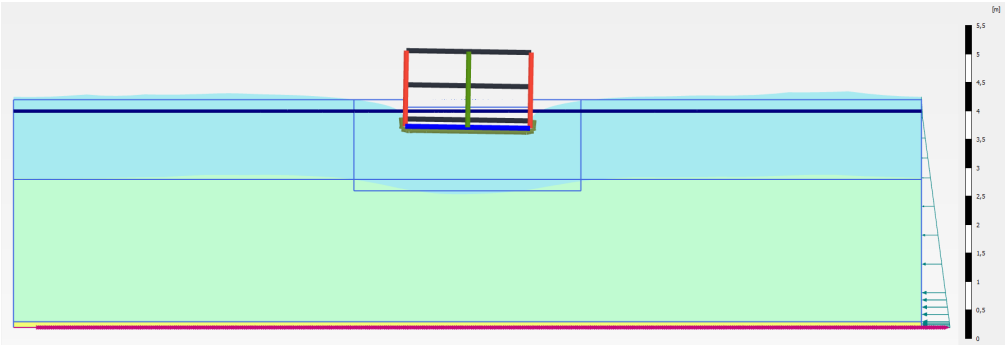

Figure 8.12: Enlarged scale model deformation 2

8.2 NUMERICAL SIMULATION RESULTS AND OBSERVED CONSEQUENCES

The present numerical simulations show that vertical settlements of 35 to 40 centimetres are to be expected underneath the building. Lateral displacements are expected to be of major importance as it reaches values up to 4 meters underneath the building. As shown by Figure 8.6, soil softening is to expected in all the simulated area. High heave values are predicted for the area in a 40 meters radius around the building perimeter.

These numerical results do not take into account the damaging tilting effects induced by the weight differential of the floors inside the building and the foundation system. The model also excludes the influence of nearby structures as the LS-I building and possible others around.

As the simulation performs an undrained analyses during the seismic loading and no porewater pressure dissipation is allowed on a following consolidation phase, potentially very important volumetric settlement values are not being estimated consequence of soil densification and sand ejecta to the surface.

Although all the limitations above stated, a parallel can be made between the values obtained from the numerical simulation and the ones observed in Christchurch. As stated in above chapters the vertical settlement is the focused parameter to compare estimated and observed results and although the difference is higher than 50% the values are of approximate dimensions.

9
CONCLUSIONS AND FUTURE DEVELOPMENTS

9.1 SYNOPSIS AND CONCLUSIONS

Much is now known about the negative consequences of seismic induced liquefaction on structures and mitigation measures are in constant development. But these mitigation measures are based on semi-empirical methods that can not take into account for all complex mechanism of this complicated apparition, specially in cases including SSI. Current engineering practice demands for numerical modelling capacity of the phenomena so that it is achievable to design based on structural performance.

This dissertation commences with a state of the art and practice on the liquefaction phenomena and its relation with the built environment. Chapter 2 provides an overview of the major cases in human history, presents the phenomena in the framework of soil mechanics and establishes the current state of research on the study and comprehension of SSI shear induced mechanisms. The third chapter, afterwards presents the current practice on liquefaction assessment trought the simplified procedure and semi-empirical methods to assess the liquefaction consequences on buildings. Chapter 4 introduces the UBC3D-PLM soil constitutive model and its PLAXIS® implementation as well as the proposed correlations further used on the present work.

In Chapter 5 the chosen case study is justified and seismic, geotechnical and structural data are presented. Chapter 6 uses this same input and CLIQ® software to estimate the liquefaction consequences on the site based on empirical analyses. This analyses assume FF soil behaviour so the comparison with the observed results proves the limitations of this kind of approach to the problem.

Chapters 7 and 8 follow from the numerical simulation procedure using PLAXIS® with the implemented UBC3D-PLM soil constitutive model to the presentation of results and final conclusions. The results are limited because of the many made assumptions and software incapacity to assume drainage during dynamic phase. The considered usage of CPT data for numerical simulation based on existing correlations has its limitations and potential advantages made clear throught this work.

9.2 FUTURE DEVELOPMENTS

From the work carried out and gained experience, future developments are further proposed.

The need for more validation on the correlations between results of *in situ* testing (CPT or SPT) to generate valid parameters to the UBC3D-PLM soil constitutive model, being this of great interest to engineering practice.

Due to the fact that PLAXIS® does not allow for drainage during dynamic phase it does not allows a true effective-stress analyses. This has high influence on the value of the overall settlements and lateral spreading, since a percentage of these increments also occur during shaking in view of the significant increment of shear stresses below the foundations. Still, extra analyses , with cross-checking of the evolution of settlement in undrained conditions in this dynamic phase, with the evolution of pore-pressure, in the horizontal plane, below soil surface, includinf the foundation borders, should be made to clarify observed behaviour stated in Figure 8.3 and upper stated.

Post-shaking consolidation phase, missing in this work, will have to be taken into consideration in future analyses, as it plays significant role in the induced settlements and lateral spreading.

The numerical model vertical boundaries distance has to be reevaluated and their absorbent boundaries characteristics reexamined in order to avoid reflections of the seismic waves.

BIBLIOGRAPHY

[1] Daftari A. *New approach in prediction of soil iquefaction*. PhD Thesis, Faculty of Geosciences, Geo-Engineering and Mining of the Technische Universität Bergakademie Freiberg, 2015.

[2] Laera A. and Brinkgreve R.B.J. *Site response analyses and liquefaction evaluation*. 2015.

[3] Makra A. *Evaluation of the UBC3D-PLM constitutive model for prediction of earthquake induced liquefaction on embankment dams*. Master Disserttaion, Delft University of Technology: 2013.

[4] Petalas A. and Galavi V. *Plaxis liquefaction model UBC3D-PLM*. 2012.

[5] Tsegaye A. *Plaxis liqueafaction model. report no. 1*. 2010.

[6] Bradley B.A. and Cubrinovski M. *Near-Source Ground Motions Observed in the 22 February 2011 Christchurch Earthquake.* 2011, pp. 853–865.

[7] Bradley B.A. and Hughes M. *Conditional Peak Ground Accelerations in the Canterbury Earthquakes for Conventional Liquefaction Assessment.* 2012, p. 22.

[8] Maurer B.W., Green R.A., Cubrinovski M.A., and Bradley B.A. *Assessment of CPT-Based Methods for Liquefaction Evaluation in a Liquefaction Potential Index (LPI) Framework*. 2015, pp. 328–336.

[9] Jorge C. *Zonamento do potencial de liquefacão. Tentativa de aplicacao a Portugal*. Master Dissertation, FCTUNL, Lisboa: 2014.

[10] Earthquake commission and GNS Science. *Geological hazard information for New Zealand*. URL: `https://www.geonet.org.nz/` (visited on 07/12/2017).

[11] Smyrou E., Tasiopoulou P., Bal I.E., and Gazetas G. *Ground Motions versus Geotechnical and Structural Damage in the February 2011 Christchurch Earthquake*. 2011, pp. 882–892.

[12] Zhang G., Robertson P.K., and Brachman R.W.I. *Estimating liquefaction-induced ground settlements from CPT for level ground*. 2002, pp. 1168–1180.

[13] Seed H.B. and Idriss I.M. *Ground motions and soil liquefaction during earthquakes.* 1982.

[14] Seed H.B. and Idriss I.M. *Simplified Procedure for Evaluating Soil Liquefaction Potential*. 1971, pp. 1249–1273.

[15] Idriss I.M. and Boulanger R.S. *Soil Liquefaction During Earthquakes*. 2008, pp. 1032–1051.

[16] Borozan J. *Numerical modelling of liquefaction effects on built structures*. Master Dissertation, FEUP, Porto: 2017.

[17] Bray J.D. and Frost D. *Geo-Engineering Reconnaissance of the February 27, 2010 Maule, Chile Earthquake.* 2010.

[18] Zupan J.D. *Seismic Performance of Buildings Subjected to Soil Liquefaction*. PhD Thesis, Civil and Environmental Engineering in the Graduate Division of the University of California, Berkeley, 2014.

[19] Ishiara K. *Stability of natural deposits during earthquakes.* 1985.

[20] Tokimatsu K. and Katsumata K. *Liquefaction-Induced Damage to Buildings in Urayasu City During the 2011 Tohoku Pacific Earthquake.* 2012.

[21] Cetin K.O., Seed R.B., Kiureghian A., Tokimatsu K., Harder L.F., Kayen R.E, and Moss R.E.S. *Standard Penetration Test-Based Probabilistic and Deterministic Assessment of Seismic Soil Liquefaction Potential*. 2004, pp. 1314–1340.

[22] Steven Kramer. *Geotechnical Earthquake Engineering*. Prentice Hall, 1996.

[23] Liu L. and Dobry R. *Seismic Response of Shallow Foundation on Liquefiable Sand*. 1997, pp. 557–567.

[24] Beca Carter Hollings Ferner Ltd. *Investigation into the Collapse of the Pyne Gould Corporation Building on 22nd February 2011.* 2011.

[25] Soares M. *Evaluation of soil liquefaction potential based on laboratory data: major factors and limit boundaries*. Faculty of Engineering of the University of Porto, Portugal: PhD Thesis, 2015.

[26] Beaty M.H. and Byrne P.M. *UBCSAND constitutive model version 904aR*. 2011.

[27] Beaty M.H. and Perlea V.G. *Several observations on advanced analyses with liquefiable materials, 21st Century Dam Design-Advances and Adaptations*. 2011.

[28] New Zealand Geotechnical Database NZGD. URL: `https://www.nzgd.org.nz.com/` (visited on 07/19/2017).

[29] Coelho P. *In situ densification as a liquefaction resistance measure for bridge foundations*. PhD Thesis, University of Cambridge, Department of engineering, 2007.

[30] Robertson P.K. and Wride C.E. *Evaluating Cyclic Liquefaction Potential Using the Cone Penetration Test.* 1998, pp. 442–459.

[31] Robertson P.K., Campanella R.G., and Wightman A. *SPT-CPT Correlations*. 1983.

[32] Seed R.B., Cetin K.O., Moss R.E.S., Kammerer A.M., Wu J., Pestana J.M., Riemer M.F., Sancio R.B., Bray J.D., Kayen R.E., and Faris A. *Recent Advances in Soil Liquefaction Engineering: A Unified and Consistent Framework*. 2003.

[33] Moss R.E.S., Seed R.B.and Kayen R.E., Stewart J.P., Kiureghian A., and Cetin K.O. *CPT-Based Probabilistic and Deterministic Assessment of In Situ Seismic Soil Liquefaction Potential.* 2006, pp. 1032–1051.

[34] Whitman R.V. and Lambe P.C. *Liquefaction: Consequences for a Structure*. 1982, pp. 941–949.

[35] Dashti S. *Toward evaluating building performance on softened ground.* PhD Thesis, University of California, Berkeley: 2009.

[36] Dashti S., Bray J.D., Pestana J.M., Riemer M.R., and Wilson D. *Mechanisms of seismically-induced settlement of buildings with shallow foundations on liquefiable soil.* 2010a, pp. 151–164.

[37] National Academies of Sciences Engineering and Medicine. *State of the Art and Practice in the Assessment of Earthquake-Induced Soil Liquefaction and Its Consequences*. 2016, doi:1017226/23474.

[38] Adachi T., Iwai S., and Yasui M. *Settlement and inclination of reinforced concrete buildings in Dagupan City due to liquefaction during the 1990 Philippine Earthquake*. 1992, pp. 147–152.

[39] Youd T.L., Idriss I.M., Andrus R.D., Arango I., Castro G., Christian J.T., Dobry R., Finn W.D.L., Harder L.F., Hynes M.E., Ishihara K., Koester J.P., Liao S.S.C., Marcuson W.F., Martin G.R., Mitchell J.K., Moriwaki Y., Power M.S., Robertson P.K., Seed R.B., and Stokoe K.H. *Liquefaction Resistance of Soils: Summary Report from the 1996 NCEER and 1998 NCEER/NSF Workshops on Evaluation of Liquefaction Resistance of Soils*. 2001, pp. 817–833.

[40] Galavi V., Petalas A., and Brinkgreve R.B.J. *Finite element modelling of seismic liquefaction in soils*. 2013, ISSN 0046-5828.

[41] Ishii Y. and Tokimatsu K. *Simplified procedures for the evaluation of settlements of structures during earthquakes.* 1988, pp. 95–100.

[42] Yoshimi Y. and Tokimatsu K. *Settlement of buildings on saturated sand during earthquakes.* 1977, pp. 23–38.

A

PGA PARAMETRIC STUDY USING CLIQ®

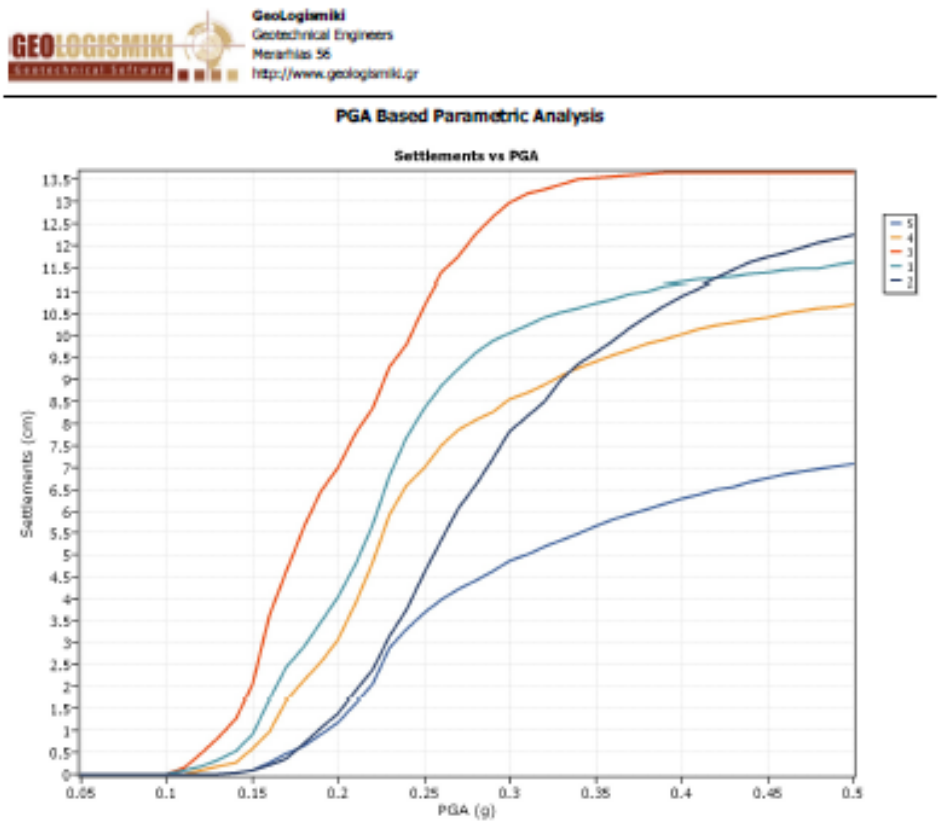

:: CPT main liquefaction parameters details ::

CPT Name	Assesment method	Earthquake Mag.	GWT in situ (m)	GWT earthq. (m)
5	NCEER (1998)	6.20	1.00	1.50
4	NCEER (1998)	6.20	1.00	1.50
3	NCEER (1998)	6.20	1.00	1.50
1	NCEER (1998)	6.20	1.00	1.50
2	NCEER (1998)	6.20	1.00	1.50

Figure A.1: PGA based parametric analyses from CLIQ®

B

CCCC SEISMIC STATION GEOLOGY

Nearby Faults	Pegasus1NW (c. 24 km)
Stability	Stable
ASNZS 1170	D, Deep or soft soil
NZS 4203	C, Flexible or deep soil
Ground Class Additional	deep
Geomatrix	D, Deep soil in broad canyon (soil greater than 20m thick)
Depth To Bedrock	800m. c. 800 m, effective bedrock possibly c. 55 m
Known Overburden	7 Layers. Cumulative thickness: 775.0m

Geology

Overburden Layer 1

Strength: soft

Description: silt with wood

Thickness: 3m

Notes: fluvial silt with wood (Springston Fm)

Overburden Layer 2

Strength: loose

Description: gravel & sand

Thickness: 9m

Notes: loose to medium dense fluvial gravel & sand (Springston Fm)

Overburden Layer 3

Strength: dense

Description: sand, silt

Thickness: 15m

Notes: marine /lagoonal sand, silt (Christchurch Fm)

Overburden Layer 4

Strength: dense

Description: gravel

Thickness: 10m

Notes: glacial outwash gravel (Riccarton Fm)

Overburden Layer 5

Strength: firm

Description: peat, silt, sand

Thickness: 18m

Notes: soft to stiff/ dense marine/ lagoonal/ swamp peat, silt, sand (Bromley Fm)

Overburden Layer 6

Strength: very dense

Description: gravel

Thickness: 20m

Notes: glacial outwash (Linwood gravel)

Overburden Layer 7

Strength: very dense

Description: gravels

Thickness: 700m

Notes: Tertiary rocks - effective bedrock

Bedrock Layer

Bedrock

Strength	strong
Type	basalt
Description	basalt (Lyttleton basalt)
References	Berrill, J.B., Davis, R.O., and McCahon, I.F. (1993). Christchurch seismic hazard pilot study. Bulln of the New Zealand National Society for Earthquake Engineering, 26(1): 14-27. ### Brown, L.J., and Weeber, J.H. (1992. Geology of the Christchurch Urban Area. Institute of Geological & Nuclear Sciences, 104pp, 1 map.

C

CLIQ® ANALYSES REPORT

GeoLogismiki
Geotechnical Engineers
Merarhias 56
http://www.geologismiki.gr

LIQUEFACTION ANALYSIS REPORT

Project title : **Location :**

CPT file : 5

Input parameters and analysis data

Analysis method:	NCEER (1998)	G.W.T. (in-situ):	1.00 m	Use fill:	No	Clay like behavior applied:	Sands only
Fines correction method:	NCEER (1998)	G.W.T. (earthq.):	1.50 m	Fill height:	N/A	Limit depth applied:	Yes
Points to test:	Based on Ic value	Average results interval:	3	Fill weight:	N/A	Limit depth:	20.00 m
Earthquake magnitude M_w:	6.20	Ic cut-off value:	2.60	Trans. detect. applied:	No	MSF method:	Method based
Peak ground acceleration:	0.50	Unit weight calculation:	Based on SBT	K_σ applied:	Yes		

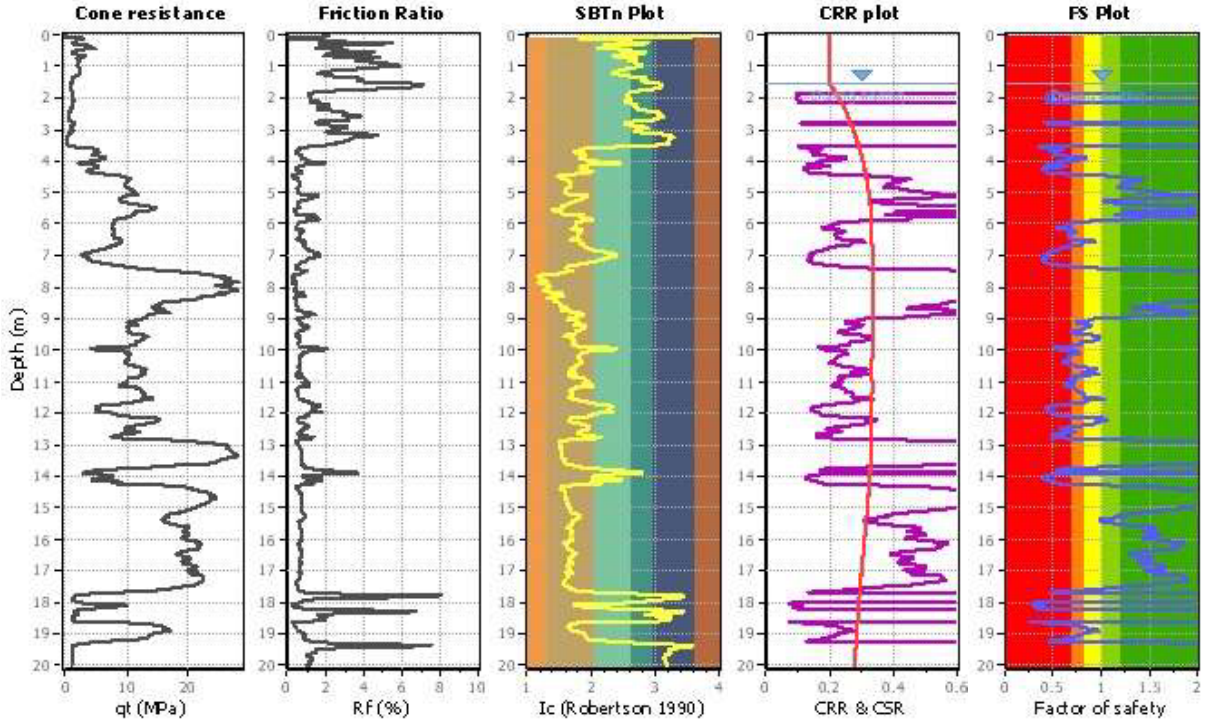

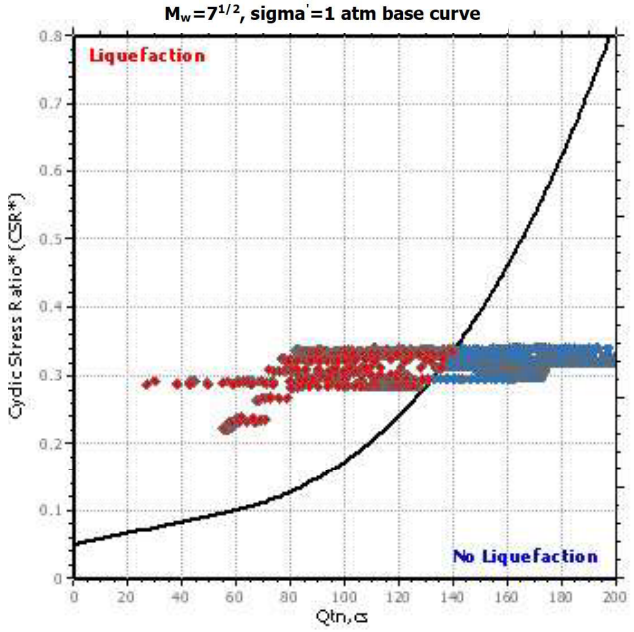

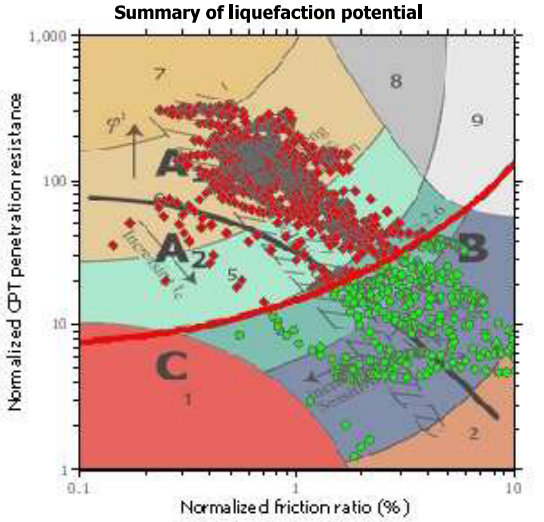

Zone A_1: Cyclic liquefaction likely depending on size and duration of cyclic loading
Zone A_2: Cyclic liquefaction and strength loss likely depending on loading and ground geometry
Zone B: Liquefaction and post-earthquake strength loss unlikely, check cyclic softening
Zone C: Cyclic liquefaction and strength loss possible depending on soil plasticity, brittleness/sensitivity, strain to peak undrained strength and ground geometry

CPT basic interpretation plo

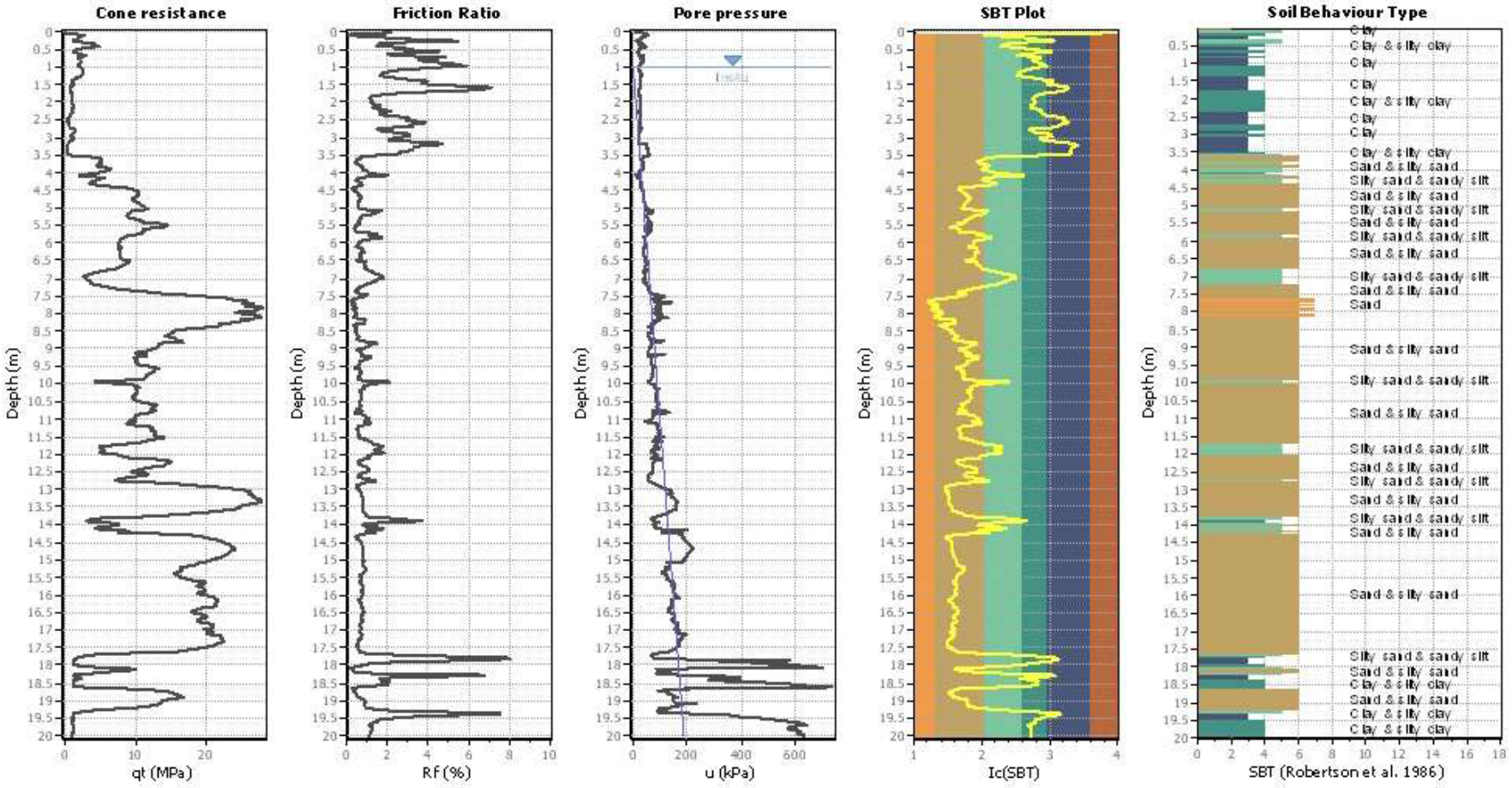

Input parameters and analysis data

Analysis method:	NCEER (1998)	Depth to water table (erthq.):	1.50 m	Fill weight:	N/A
Fines correction method:	NCEER (1998)	Average results interval:	3	Transition detect. applied:	No
Points to test:	Based on Ic value	Ic cut-off value:	2.60	K_σ applied:	Yes
Earthquake magnitude M_w:	6.20	Unit weight calculation:	Based on SBT	Clay like behavior applied:	Sands only
Peak ground acceleration:	0.50	Use fill:	No	Limit depth applied:	Yes
Depth to water table (insitu):	1.00 m	Fill height:	N/A	Limit depth:	20.00 m

SBT legend

1. Sensitive fine grained
2. Organic material
3. Clay to silty clay
4. Clayey silt to silty clay
5. Silty sand to sandy silt
6. Clean sand to silty sand
7. Gravely sand to sand
8. Very stiff sand to clayey sand
9. Very stiff fine grained

CPT basic interpretation plots (normaliz

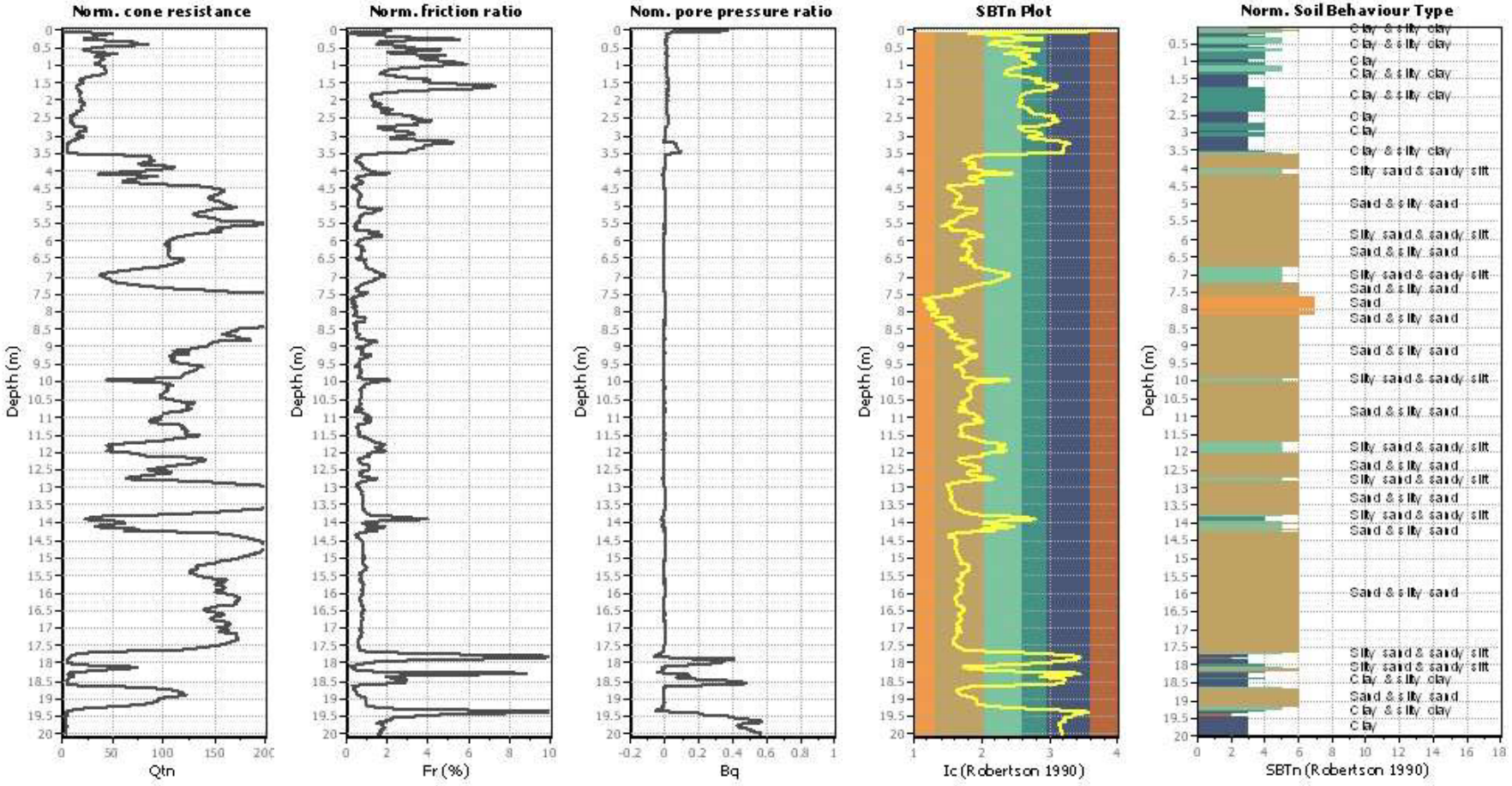

Input parameters and analysis data

Analysis method:	NCEER (1998)	Depth to water table (erthq.):	1.50 m	Fill weight:	N/A
Fines correction method:	NCEER (1998)	Average results interval:	3	Transition detect. applied:	No
Points to test:	Based on Ic value	Ic cut-off value:	2.60	K_σ applied:	Yes
Earthquake magnitude M_w:	6.20	Unit weight calculation:	Based on SBT	Clay like behavior applied:	Sands only
Peak ground acceleration:	0.50	Use fill:	No	Limit depth applied:	Yes
Depth to water table (insitu):	1.00 m	Fill height:	N/A	Limit depth:	20.00 m

SBTn legend

1. Sensitive fine grained
2. Organic material
3. Clay to silty clay
4. Clayey silt to silty clay
5. Silty sand to sandy silt
6. Clean sand to silty sand
7. Gravely sand to sand
8. Very stiff sand to clayey sand
9. Very stiff fine grained

Liquefaction analysis overall plots (intermediate resu

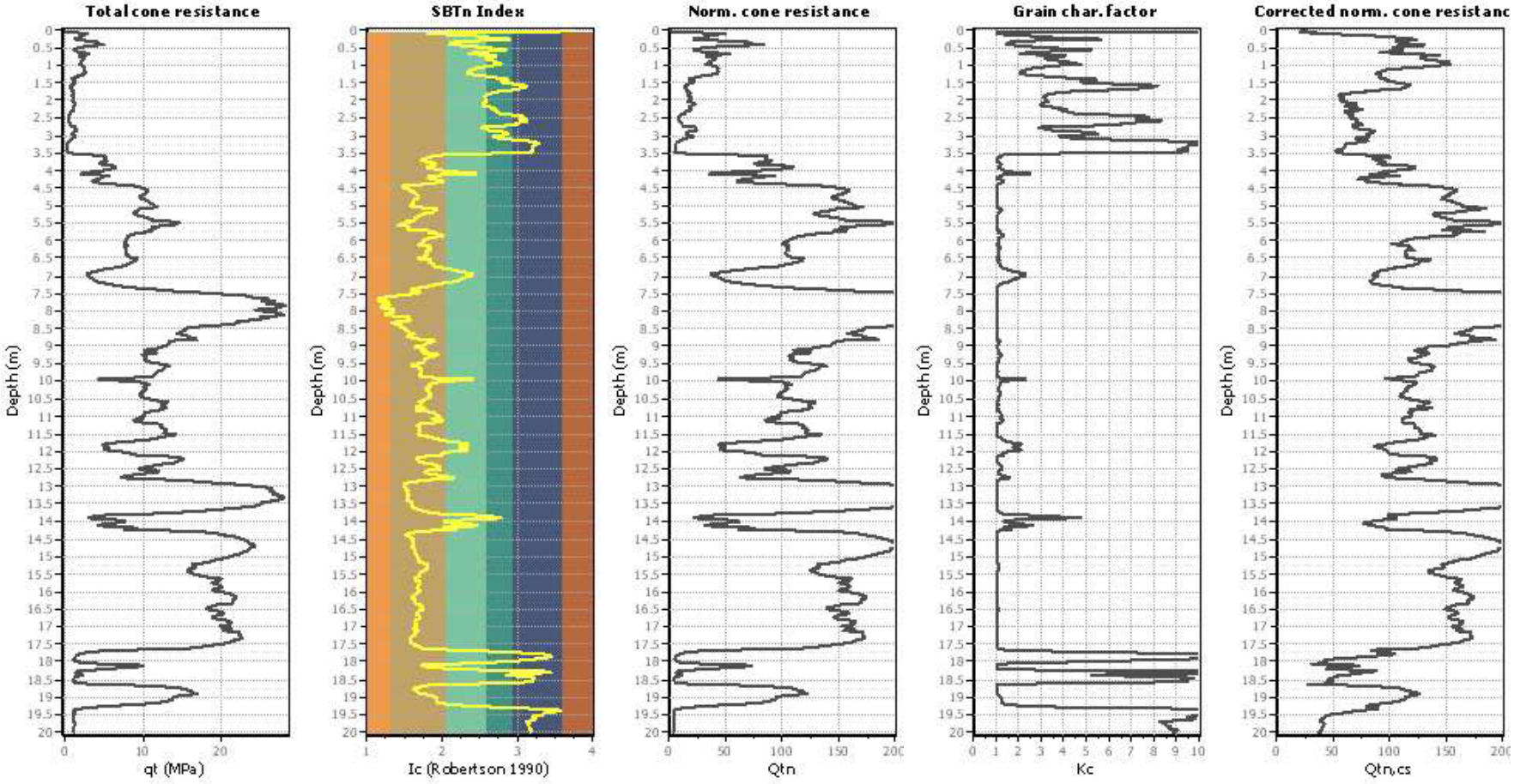

Input parameters and analysis data

Analysis method:	NCEER (1998)	Depth to water table (erthq.):	1.50 m	Fill weight:	N/A
Fines correction method:	NCEER (1998)	Average results interval:	3	Transition detect. applied:	No
Points to test:	Based on Ic value	Ic cut-off value:	2.60	K_σ applied:	Yes
Earthquake magnitude M_w:	6.20	Unit weight calculation:	Based on SBT	Clay like behavior applied:	Sands only
Peak ground acceleration:	0.50	Use fill:	No	Limit depth applied:	Yes
Depth to water table (insitu):	1.00 m	Fill height:	N/A	Limit depth:	20.00 m

Liquefaction analysis overall plot

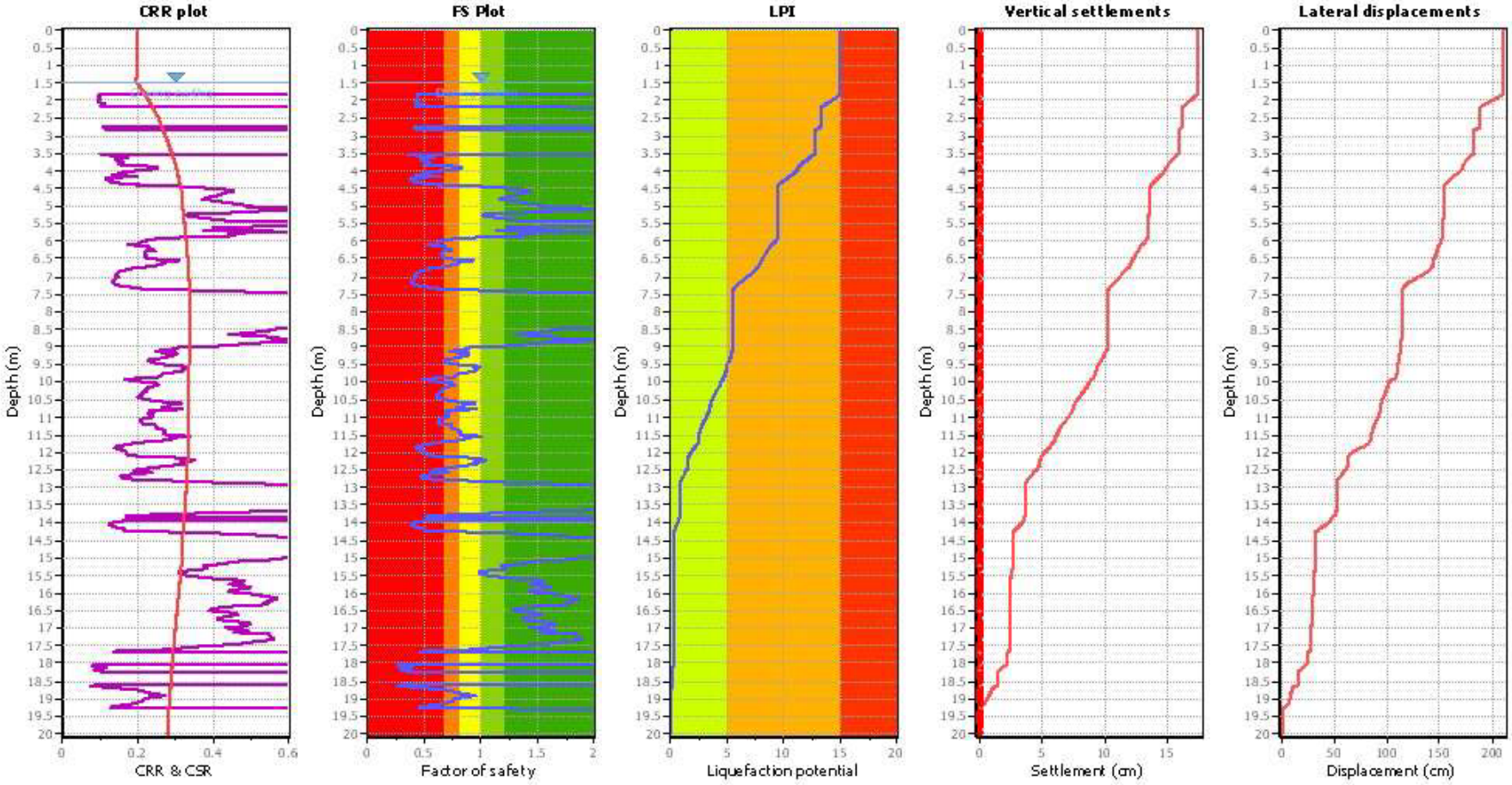

Input parameters and analysis data

Analysis method:	NCEER (1998)	Depth to water table (erthq.):	1.50 m	Fill weight:	N/A
Fines correction method:	NCEER (1998)	Average results interval:	3	Transition detect. applied:	No
Points to test:	Based on Ic value	Ic cut-off value:	2.60	K_σ applied:	Yes
Earthquake magnitude M_w:	6.20	Unit weight calculation:	Based on SBT	Clay like behavior applied:	Sands only
Peak ground acceleration:	0.50	Use fill:	No	Limit depth applied:	Yes
Depth to water table (insitu):	1.00 m	Fill height:	N/A	Limit depth:	20.00 m

F.S. color scheme

- Almost certain it will liquefy
- Very likely to liquefy
- Liquefaction and no liq. are equally likely
- Unlike to liquefy
- Almost certain it will not liquefy

LPI color scheme

- Very high risk
- High risk
- Low risk

Liquefaction analysis summary plo

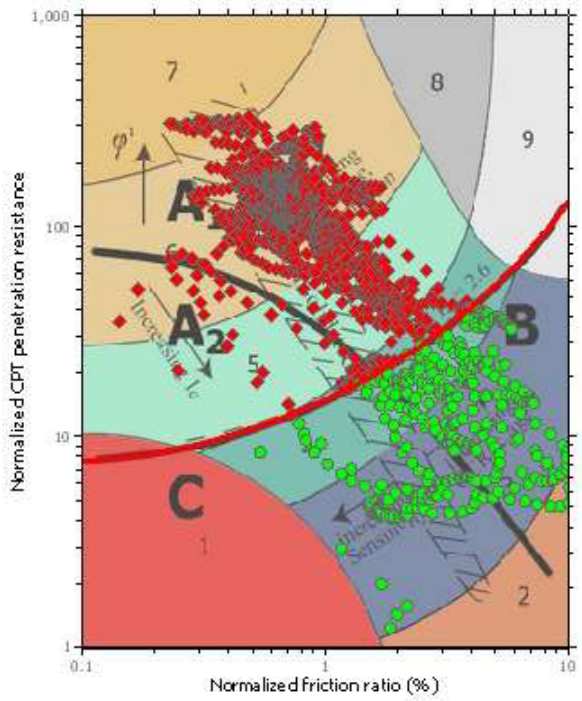

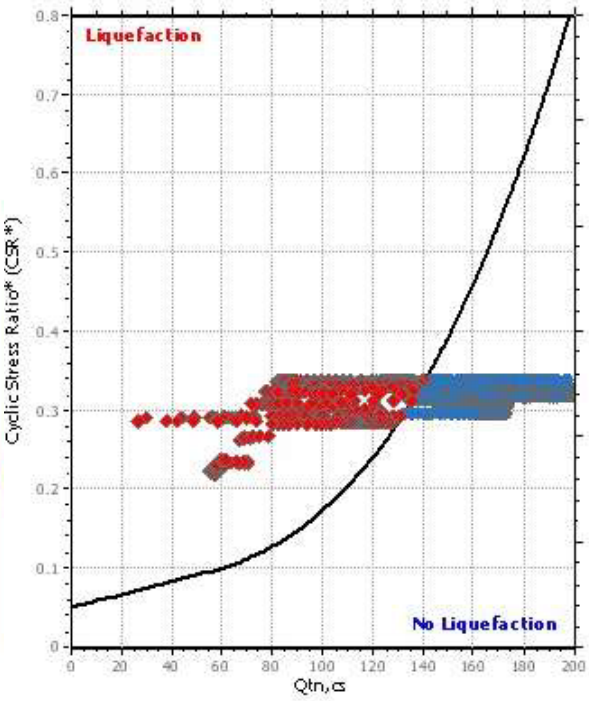

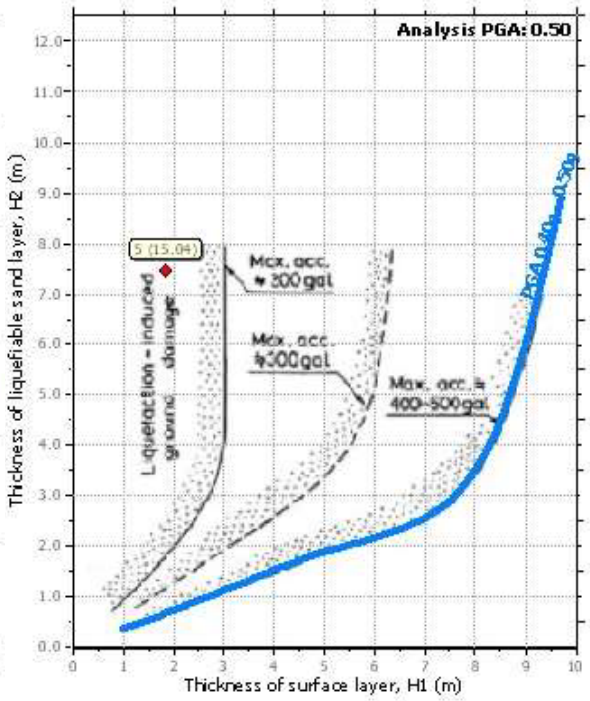

Input parameters and analysis data

Analysis method:	NCEER (1998)	Depth to water table (erthq.):	1.50 m	Fill weight:	N/A
Fines correction method:	NCEER (1998)	Average results interval:	3	Transition detect. applied:	No
Points to test:	Based on Ic value	Ic cut-off value:	2.60	K_σ applied:	Yes
Earthquake magnitude M_w:	6.20	Unit weight calculation:	Based on SBT	Clay like behavior applied:	Sands only
Peak ground acceleration:	0.50	Use fill:	No	Limit depth applied:	Yes
Depth to water table (insitu):	1.00 m	Fill height:	N/A	Limit depth:	20.00 m

Check for strength loss plots (Robertson (2010))

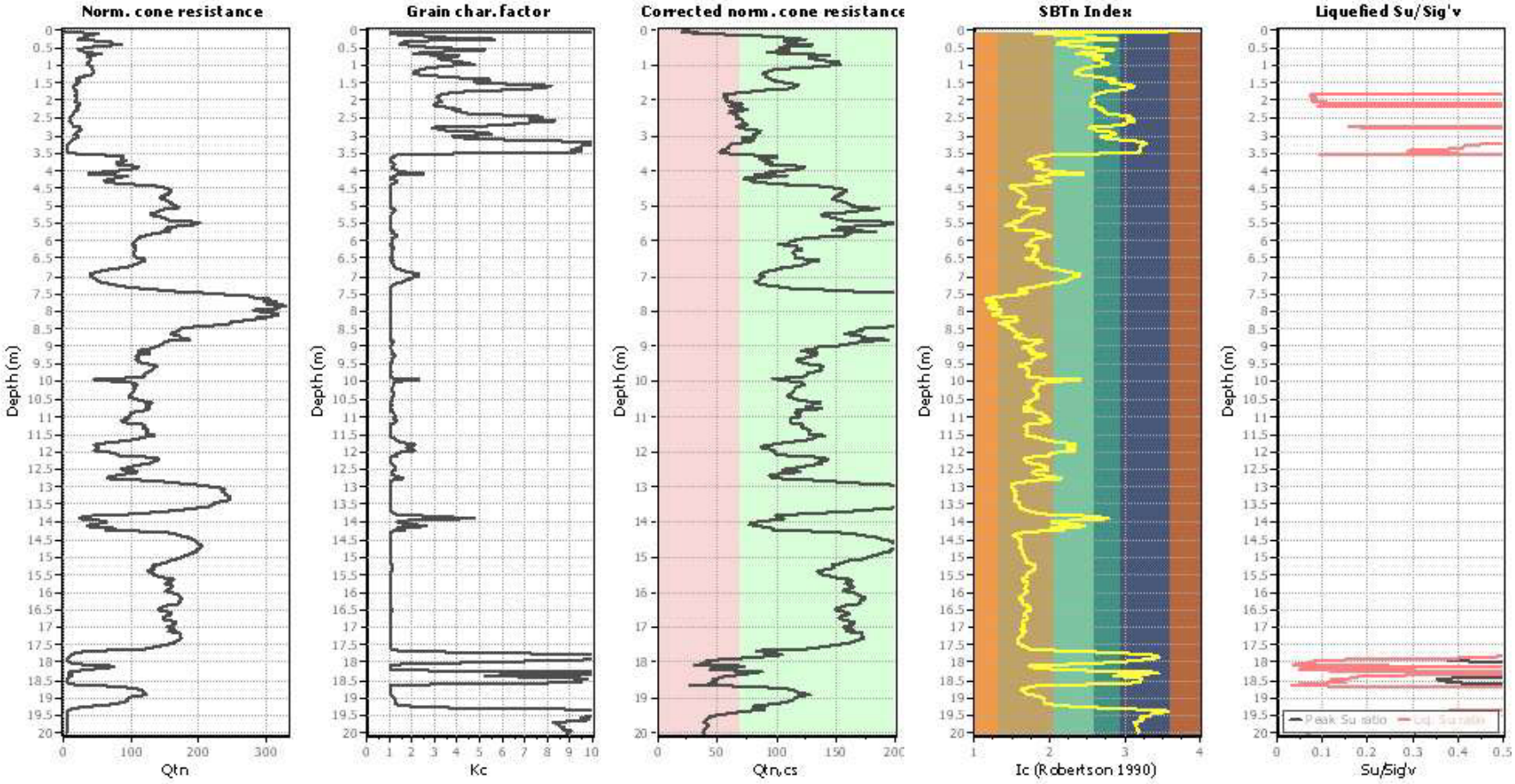

Input parameters and analysis data

Analysis method:	NCEER (1998)	Depth to water table (erthq.):	1.50 m	Fill weight:	N/A
Fines correction method:	NCEER (1998)	Average results interval:	3	Transition detect. applied:	No
Points to test:	Based on Ic value	Ic cut-off value:	2.60	K_σ applied:	Yes
Earthquake magnitude M_w:	6.20	Unit weight calculation:	Based on SBT	Clay like behavior applied:	Sands only
Peak ground acceleration:	0.50	Use fill:	No	Limit depth applied:	Yes
Depth to water table (insitu):	1.00 m	Fill height:	N/A	Limit depth:	20.00 m

GeoLogismiki
Geotechnical Engineers
Merarhias 56
http://www.geologismiki.gr

LIQUEFACTION ANALYSIS REPORT

Project title : **Location :**

CPT file : 4

Input parameters and analysis data

Analysis method:	NCEER (1998)	G.W.T. (in-situ):	1.00 m	Use fill:	No	Clay like behavior applied:	Sands only
Fines correction method:	NCEER (1998)	G.W.T. (earthq.):	1.50 m	Fill height:	N/A	Limit depth applied:	Yes
Points to test:	Based on Ic value	Average results interval:	3	Fill weight:	N/A	Limit depth:	20.00 m
Earthquake magnitude M_w:	6.20	Ic cut-off value:	2.60	Trans. detect. applied:	No	MSF method:	Method based
Peak ground acceleration:	0.50	Unit weight calculation:	Based on SBT	K_σ applied:	Yes		

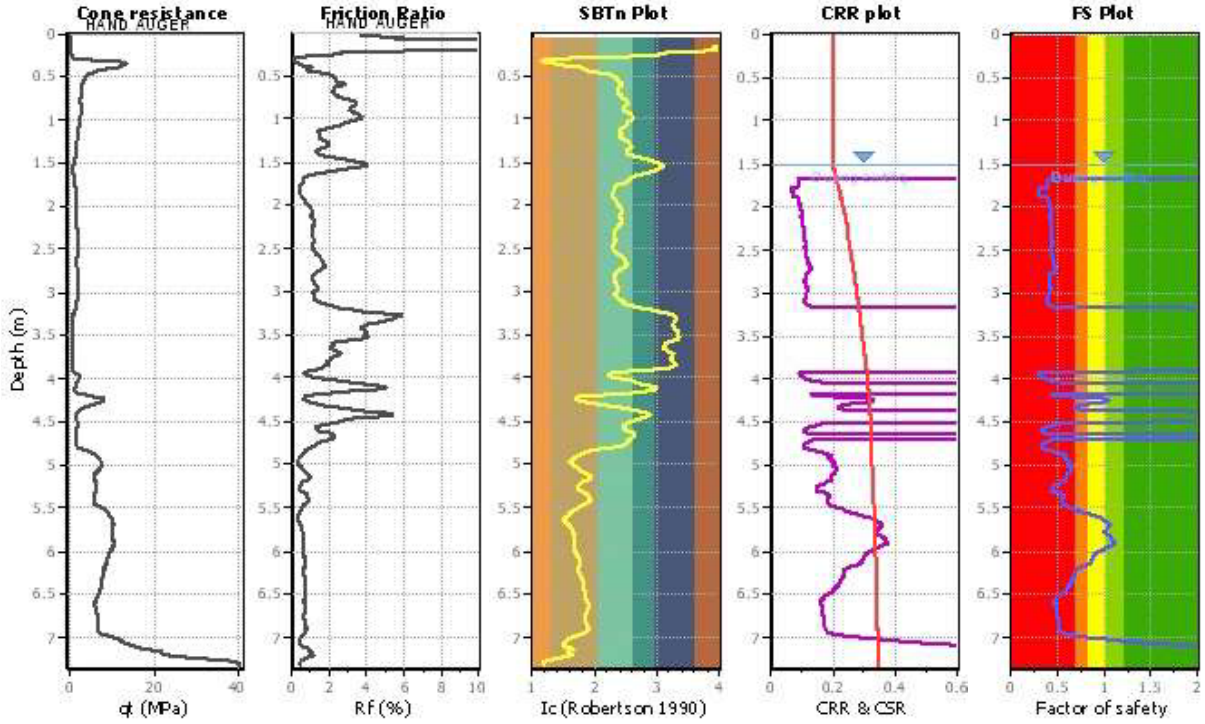

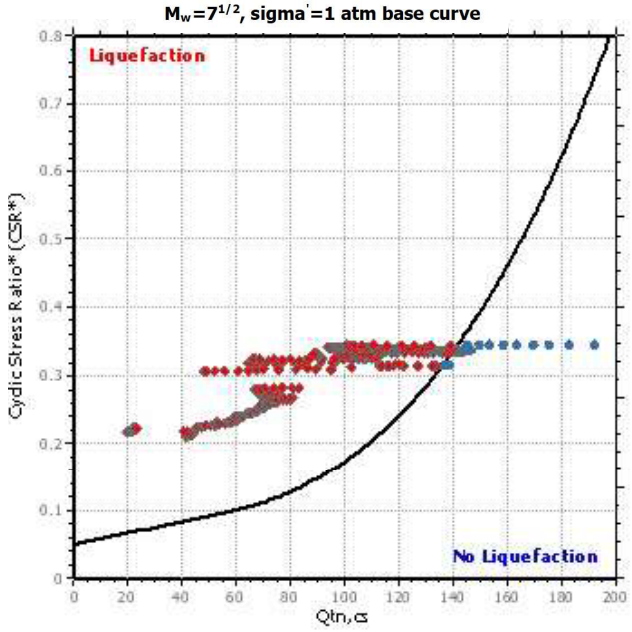

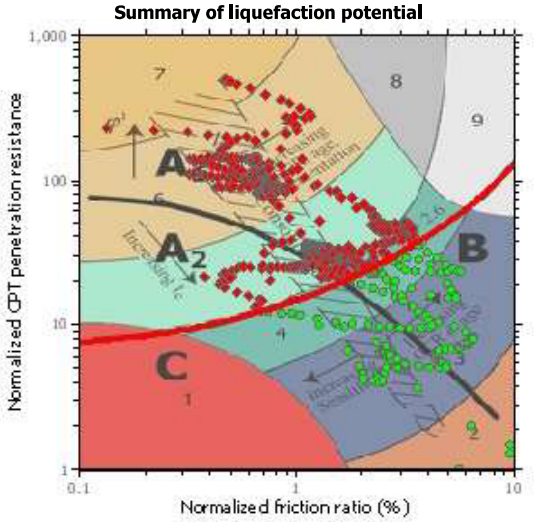

Zone A_1: Cyclic liquefaction likely depending on size and duration of cyclic loading
Zone A_2: Cyclic liquefaction and strength loss likely depending on loading and ground geometry
Zone B: Liquefaction and post-earthquake strength loss unlikely, check cyclic softening
Zone C: Cyclic liquefaction and strength loss possible depending on soil plasticity, brittleness/sensitivity, strain to peak undrained strength and ground geometry

CPT basic interpretation plo

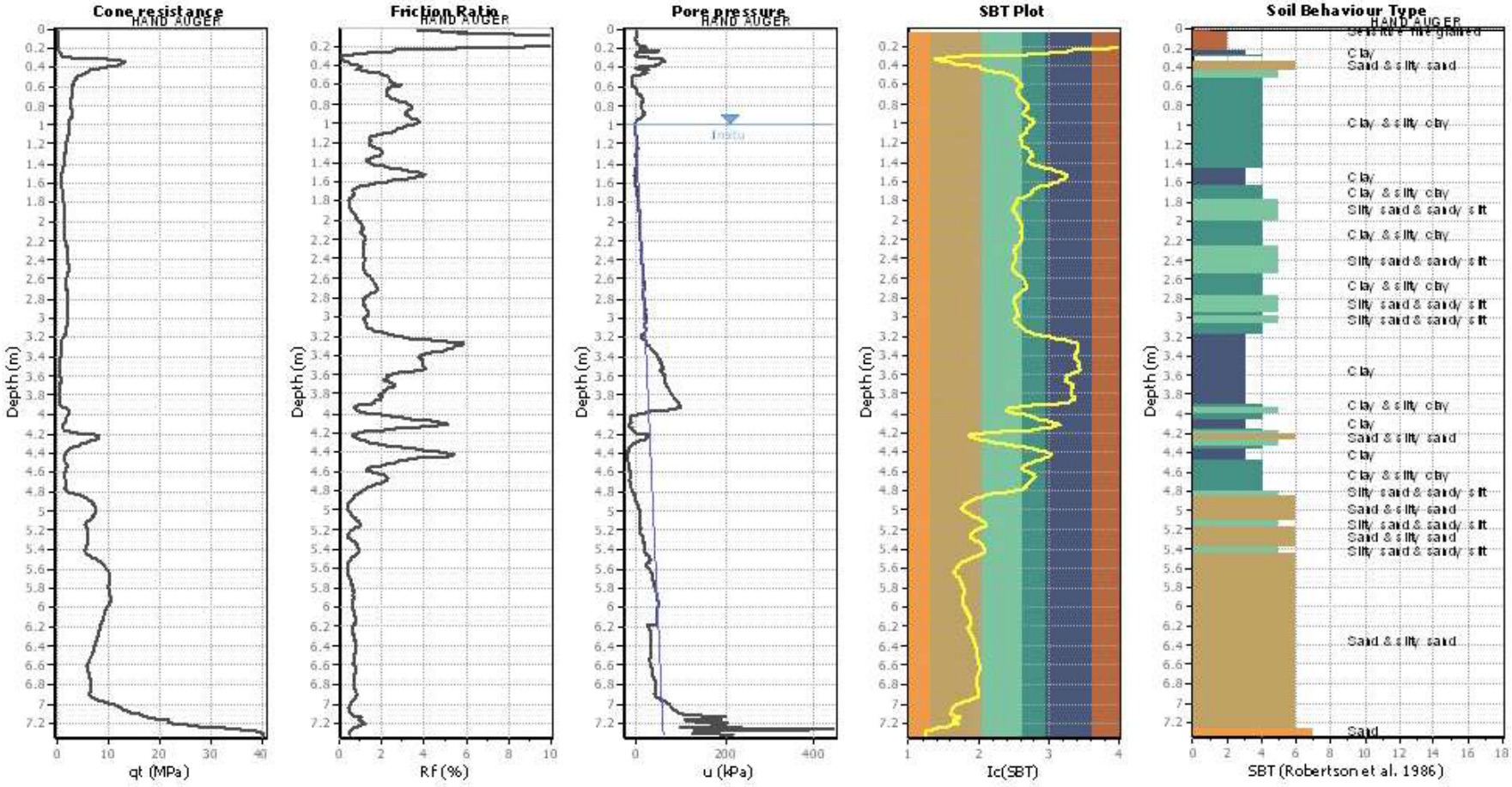

Input parameters and analysis data

Analysis method:	NCEER (1998)	Depth to water table (erthq.):	1.50 m	Fill weight:	N/A
Fines correction method:	NCEER (1998)	Average results interval:	3	Transition detect. applied:	No
Points to test:	Based on Ic value	Ic cut-off value:	2.60	K_σ applied:	Yes
Earthquake magnitude M_w:	6.20	Unit weight calculation:	Based on SBT	Clay like behavior applied:	Sands only
Peak ground acceleration:	0.50	Use fill:	No	Limit depth applied:	Yes
Depth to water table (insitu):	1.00 m	Fill height:	N/A	Limit depth:	20.00 m

SBT legend

1. Sensitive fine grained
2. Organic material
3. Clay to silty clay
4. Clayey silt to silty clay
5. Silty sand to sandy silt
6. Clean sand to silty sand
7. Gravely sand to sand
8. Very stiff sand to clayey sand
9. Very stiff fine grained

CPT basic interpretation plots (normaliz

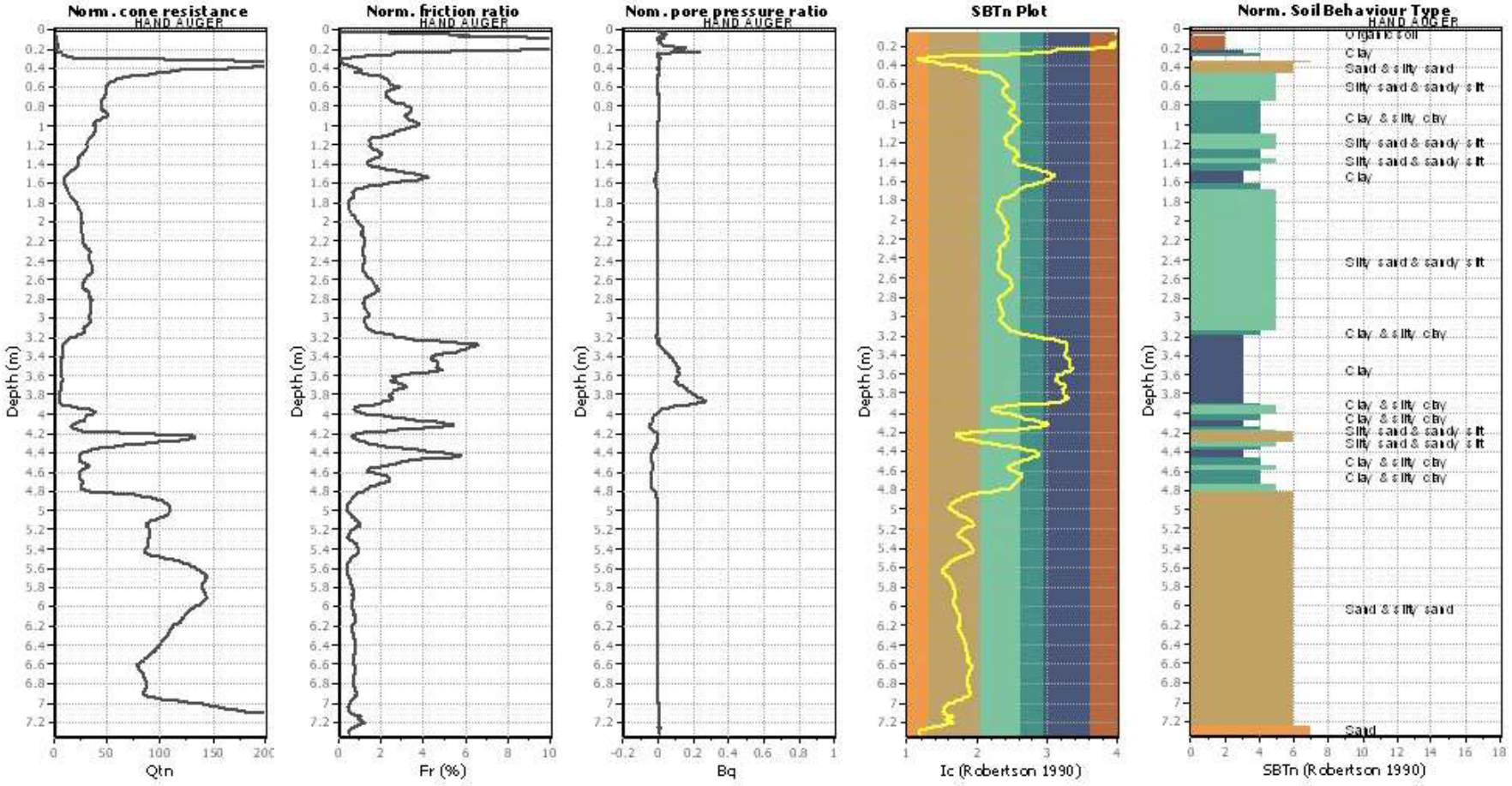

Input parameters and analysis data

Analysis method:	NCEER (1998)	Depth to water table (erthq.):	1.50 m	Fill weight:	N/A
Fines correction method:	NCEER (1998)	Average results interval:	3	Transition detect. applied:	No
Points to test:	Based on Ic value	Ic cut-off value:	2.60	K_σ applied:	Yes
Earthquake magnitude M_w:	6.20	Unit weight calculation:	Based on SBT	Clay like behavior applied:	Sands only
Peak ground acceleration:	0.50	Use fill:	No	Limit depth applied:	Yes
Depth to water table (insitu):	1.00 m	Fill height:	N/A	Limit depth:	20.00 m

SBTn legend

1. Sensitive fine grained
2. Organic material
3. Clay to silty clay
4. Clayey silt to silty clay
5. Silty sand to sandy silt
6. Clean sand to silty sand
7. Gravely sand to sand
8. Very stiff sand to clayey sand
9. Very stiff fine grained

Liquefaction analysis overall plots (intermediate resu

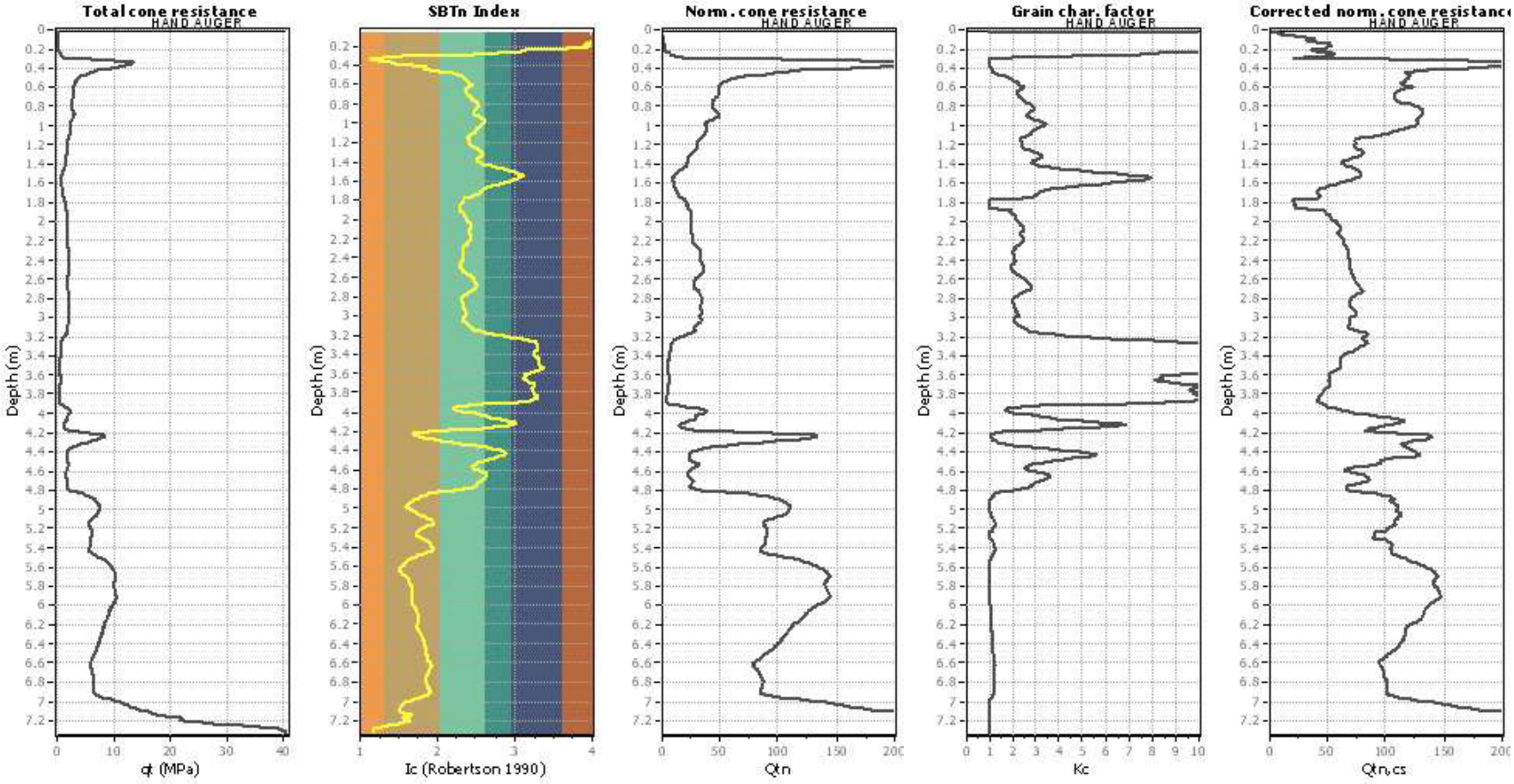

Input parameters and analysis data

Analysis method:	NCEER (1998)	Depth to water table (erthq.):	1.50 m	Fill weight:	N/A
Fines correction method:	NCEER (1998)	Average results interval:	3	Transition detect. applied:	No
Points to test:	Based on Ic value	Ic cut-off value:	2.60	K_σ applied:	Yes
Earthquake magnitude M_w:	6.20	Unit weight calculation:	Based on SBT	Clay like behavior applied:	Sands only
Peak ground acceleration:	0.50	Use fill:	No	Limit depth applied:	Yes
Depth to water table (insitu):	1.00 m	Fill height:	N/A	Limit depth:	20.00 m

Liquefaction analysis overall plot

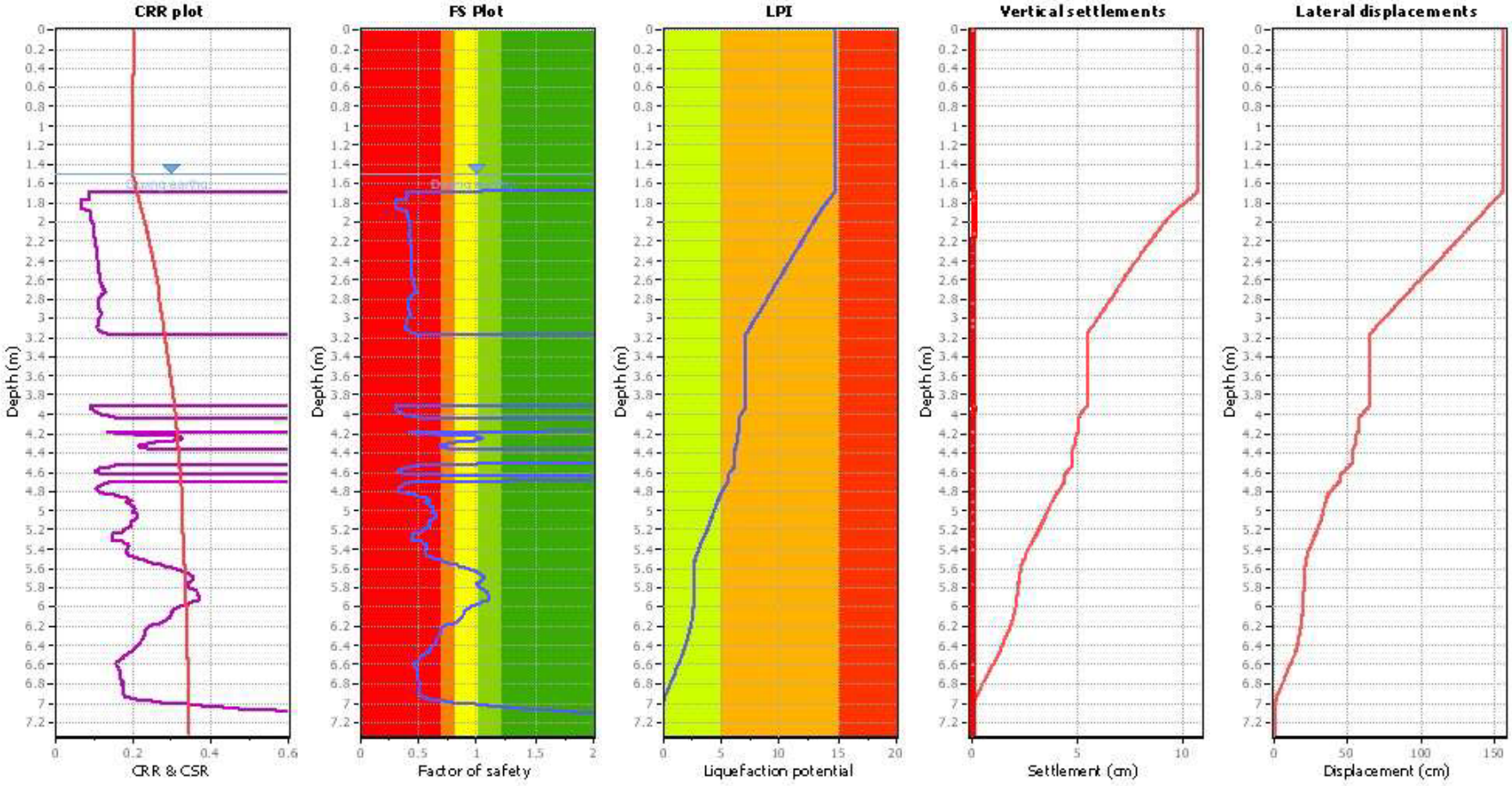

Input parameters and analysis data

Analysis method:	NCEER (1998)	Depth to water table (erthq.):	1.50 m	Fill weight:	N/A
Fines correction method:	NCEER (1998)	Average results interval:	3	Transition detect. applied:	No
Points to test:	Based on Ic value	Ic cut-off value:	2.60	K_σ applied:	Yes
Earthquake magnitude M_w:	6.20	Unit weight calculation:	Based on SBT	Clay like behavior applied:	Sands only
Peak ground acceleration:	0.50	Use fill:	No	Limit depth applied:	Yes
Depth to water table (insitu):	1.00 m	Fill height:	N/A	Limit depth:	20.00 m

F.S. color scheme

- Almost certain it will liquefy
- Very likely to liquefy
- Liquefaction and no liq. are equally likely
- Unlike to liquefy
- Almost certain it will not liquefy

LPI color scheme

- Very high risk
- High risk
- Low risk

Liquefaction analysis summary plo

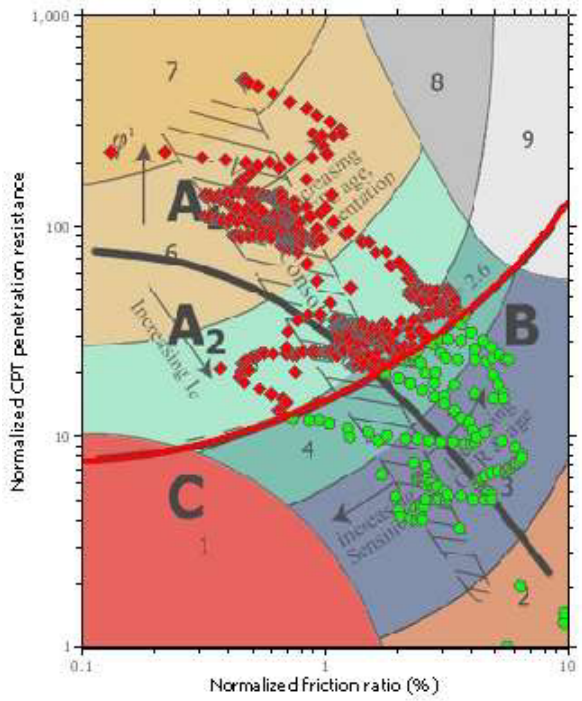

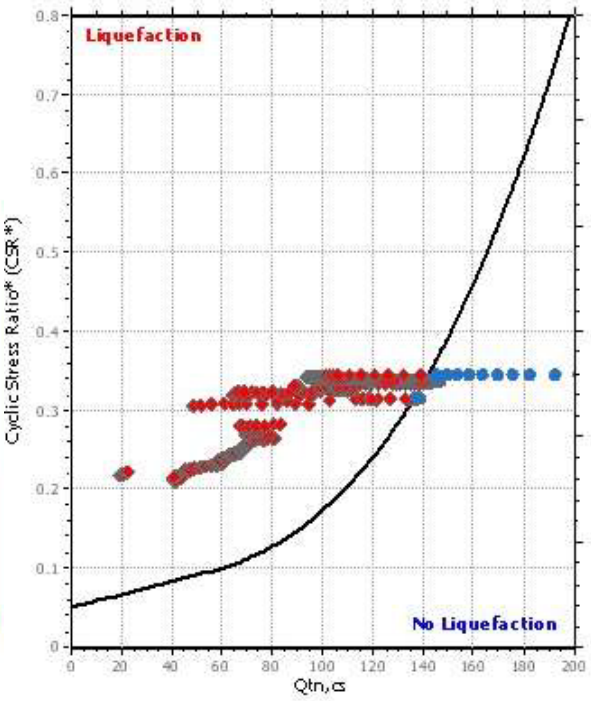

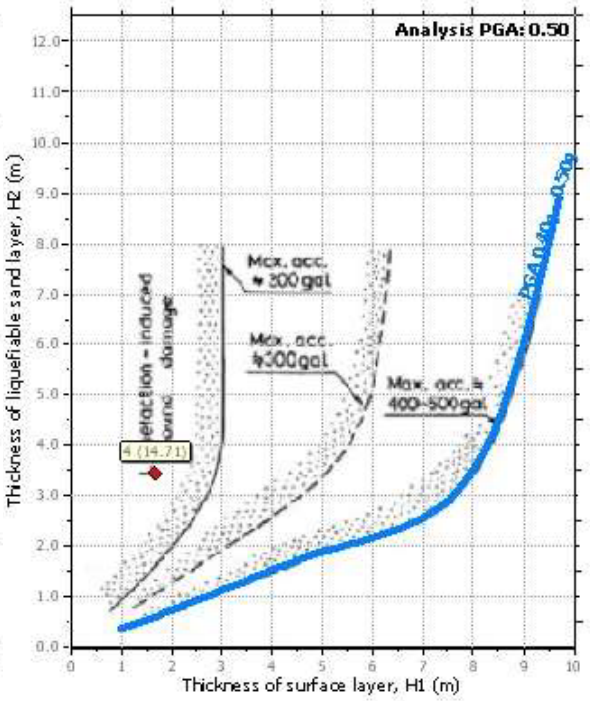

Input parameters and analysis data

Analysis method:	NCEER (1998)	Depth to water table (erthq.):	1.50 m	Fill weight:	N/A
Fines correction method:	NCEER (1998)	Average results interval:	3	Transition detect. applied:	No
Points to test:	Based on Ic value	Ic cut-off value:	2.60	K_σ applied:	Yes
Earthquake magnitude M_w:	6.20	Unit weight calculation:	Based on SBT	Clay like behavior applied:	Sands only
Peak ground acceleration:	0.50	Use fill:	No	Limit depth applied:	Yes
Depth to water table (insitu):	1.00 m	Fill height:	N/A	Limit depth:	20.00 m

Check for strength loss plots (Robertson (2010))

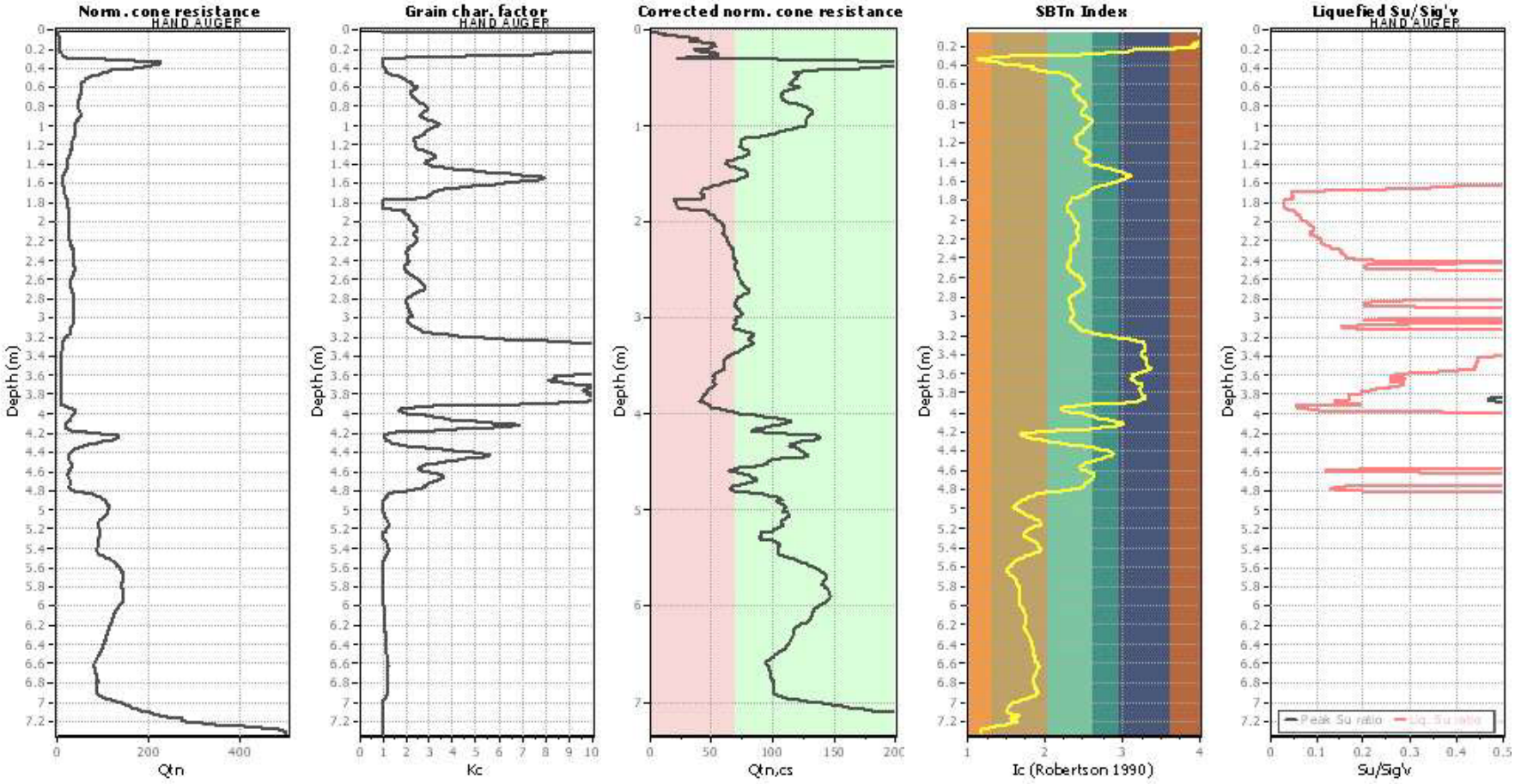

Input parameters and analysis data

Analysis method:	NCEER (1998)	Depth to water table (erthq.):	1.50 m	Fill weight:	N/A
Fines correction method:	NCEER (1998)	Average results interval:	3	Transition detect. applied:	No
Points to test:	Based on Ic value	Ic cut-off value:	2.60	K_σ applied:	Yes
Earthquake magnitude M_w:	6.20	Unit weight calculation:	Based on SBT	Clay like behavior applied:	Sands only
Peak ground acceleration:	0.50	Use fill:	No	Limit depth applied:	Yes
Depth to water table (insitu):	1.00 m	Fill height:	N/A	Limit depth:	20.00 m

GeoLogismiki
Geotechnical Engineers
Merarhias 56
http://www.geologismiki.gr

LIQUEFACTION ANALYSIS REPORT

Project title : **Location :**

CPT file : 3

Input parameters and analysis data

Analysis method:	NCEER (1998)	G.W.T. (in-situ):	1.00 m	Use fill:	No	Clay like behavior applied:	Sands only
Fines correction method:	NCEER (1998)	G.W.T. (earthq.):	1.50 m	Fill height:	N/A	Limit depth applied:	Yes
Points to test:	Based on Ic value	Average results interval:	3	Fill weight:	N/A	Limit depth:	20.00 m
Earthquake magnitude M_w:	6.20	Ic cut-off value:	2.60	Trans. detect. applied:	No	MSF method:	Method based
Peak ground acceleration:	0.50	Unit weight calculation:	Based on SBT	K_σ applied:	Yes		

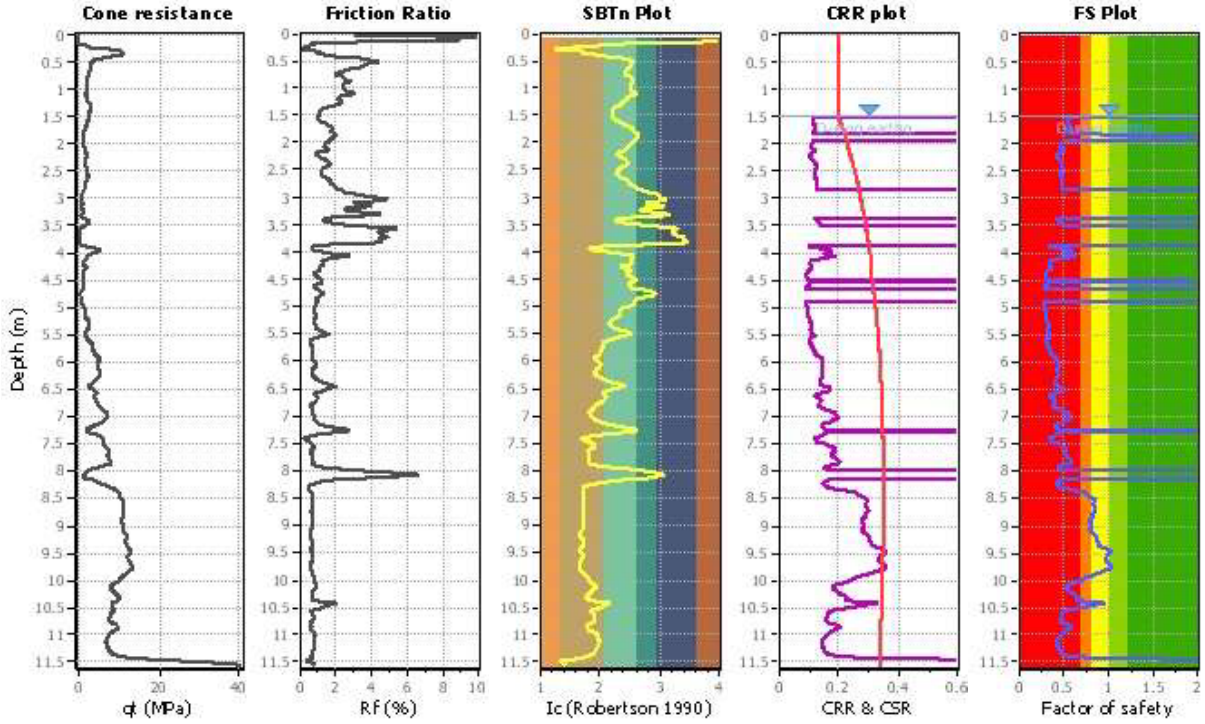

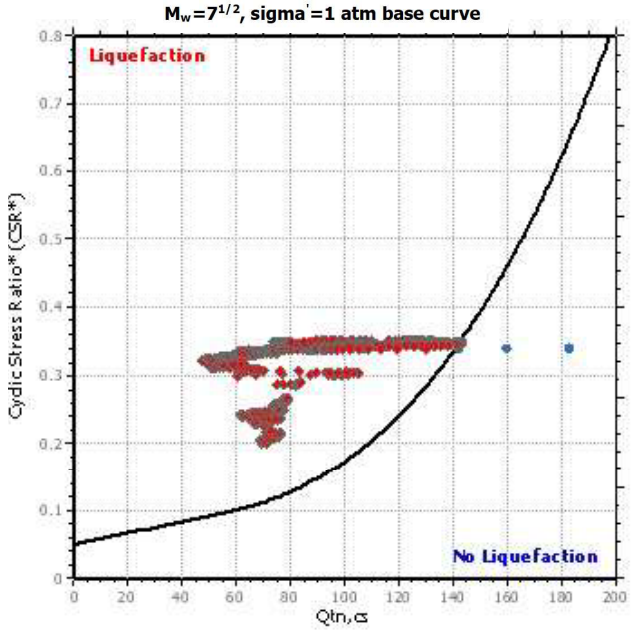

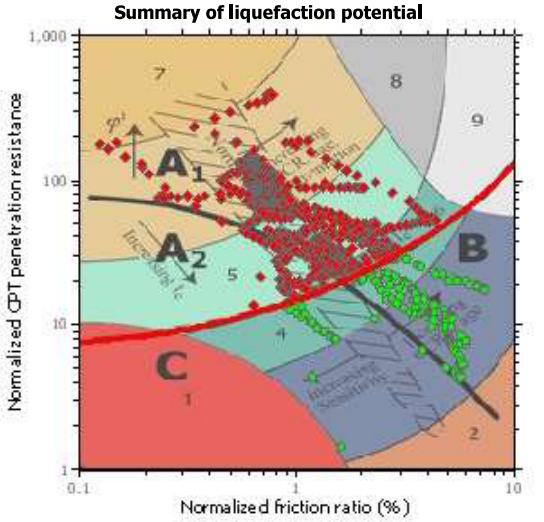

Zone A_1: Cyclic liquefaction likely depending on size and duration of cyclic loading
Zone A_2: Cyclic liquefaction and strength loss likely depending on loading and ground geometry
Zone B: Liquefaction and post-earthquake strength loss unlikely, check cyclic softening
Zone C: Cyclic liquefaction and strength loss possible depending on soil plasticity, brittleness/sensitivity, strain to peak undrained strength and ground geometry

CPT basic interpretation plo

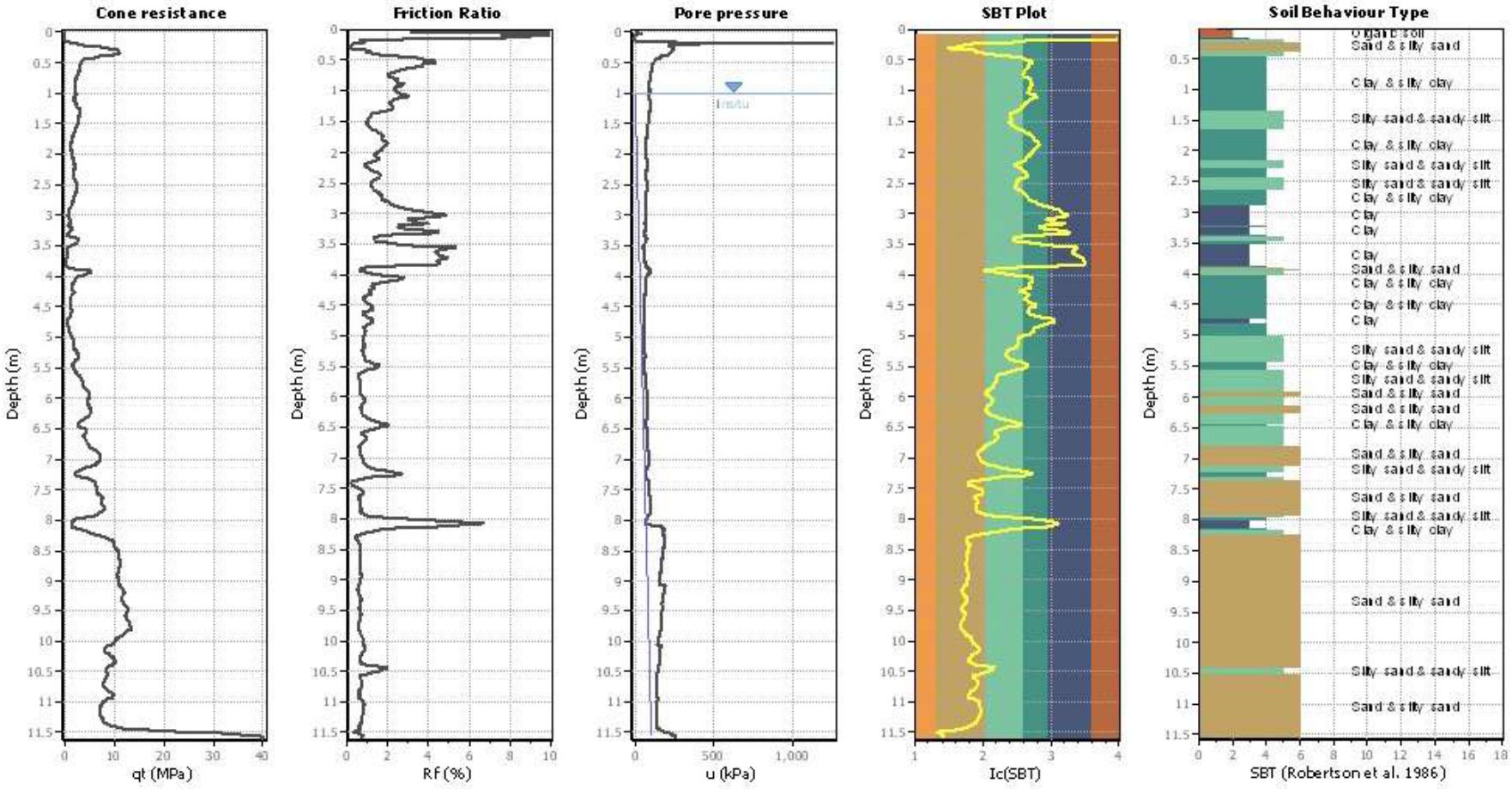

Input parameters and analysis data

Analysis method:	NCEER (1998)	Depth to water table (erthq.):	1.50 m	Fill weight:	N/A
Fines correction method:	NCEER (1998)	Average results interval:	3	Transition detect. applied:	No
Points to test:	Based on Ic value	Ic cut-off value:	2.60	K_σ applied:	Yes
Earthquake magnitude M_w:	6.20	Unit weight calculation:	Based on SBT	Clay like behavior applied:	Sands only
Peak ground acceleration:	0.50	Use fill:	No	Limit depth applied:	Yes
Depth to water table (insitu):	1.00 m	Fill height:	N/A	Limit depth:	20.00 m

SBT legend

1. Sensitive fine grained
2. Organic material
3. Clay to silty clay
4. Clayey silt to silty clay
5. Silty sand to sandy silt
6. Clean sand to silty sand
7. Gravely sand to sand
8. Very stiff sand to clayey sand
9. Very stiff fine grained

CPT basic interpretation plots (normaliz

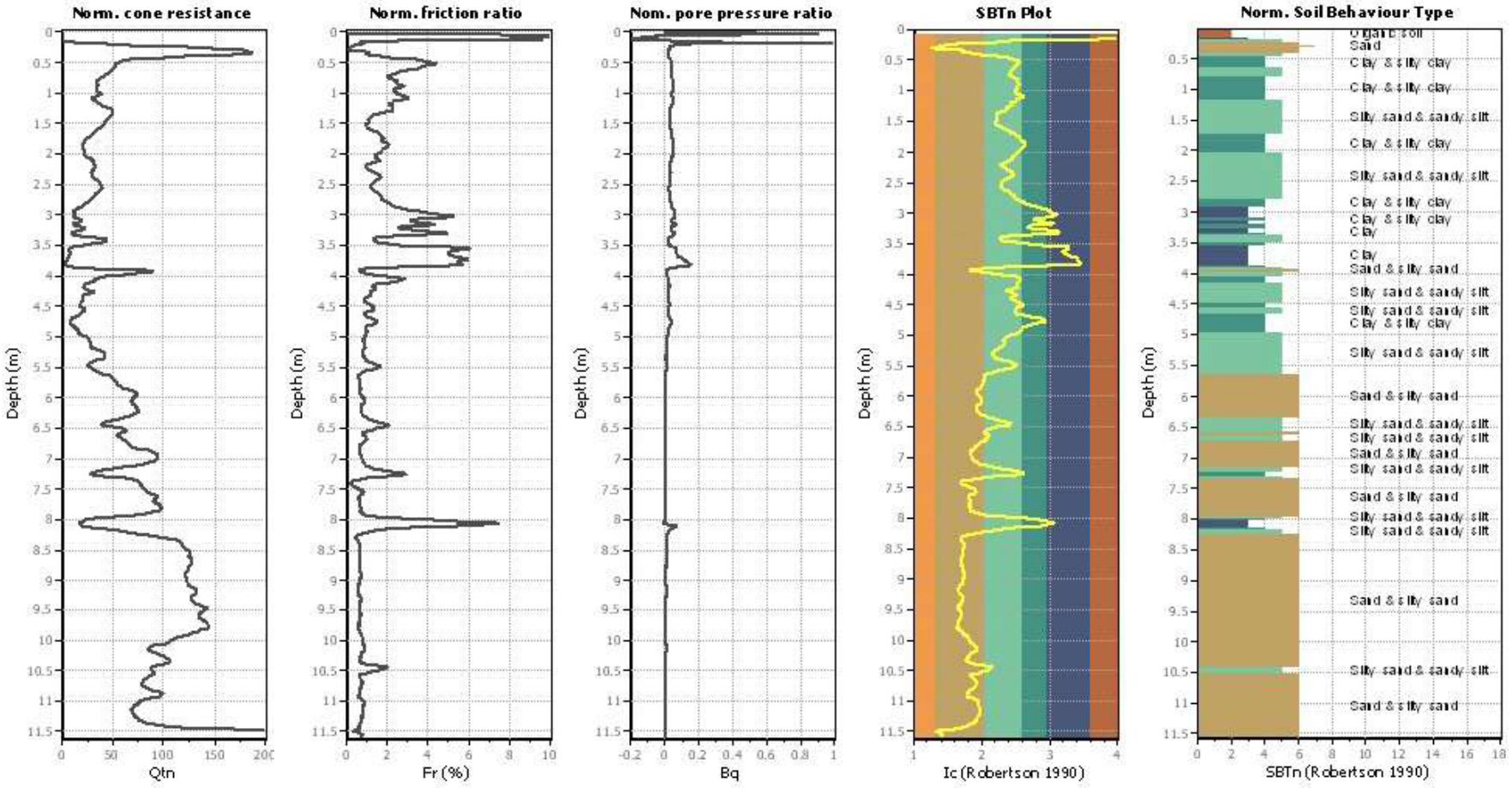

Input parameters and analysis data

Analysis method:	NCEER (1998)	Depth to water table (erthq.):	1.50 m	Fill weight:	N/A
Fines correction method:	NCEER (1998)	Average results interval:	3	Transition detect. applied:	No
Points to test:	Based on Ic value	Ic cut-off value:	2.60	K_σ applied:	Yes
Earthquake magnitude M_w:	6.20	Unit weight calculation:	Based on SBT	Clay like behavior applied:	Sands only
Peak ground acceleration:	0.50	Use fill:	No	Limit depth applied:	Yes
Depth to water table (insitu):	1.00 m	Fill height:	N/A	Limit depth:	20.00 m

SBTn legend

1. Sensitive fine grained
2. Organic material
3. Clay to silty clay
4. Clayey silt to silty clay
5. Silty sand to sandy silt
6. Clean sand to silty sand
7. Gravely sand to sand
8. Very stiff sand to clayey sand
9. Very stiff fine grained

Liquefaction analysis overall plots (intermediate resu

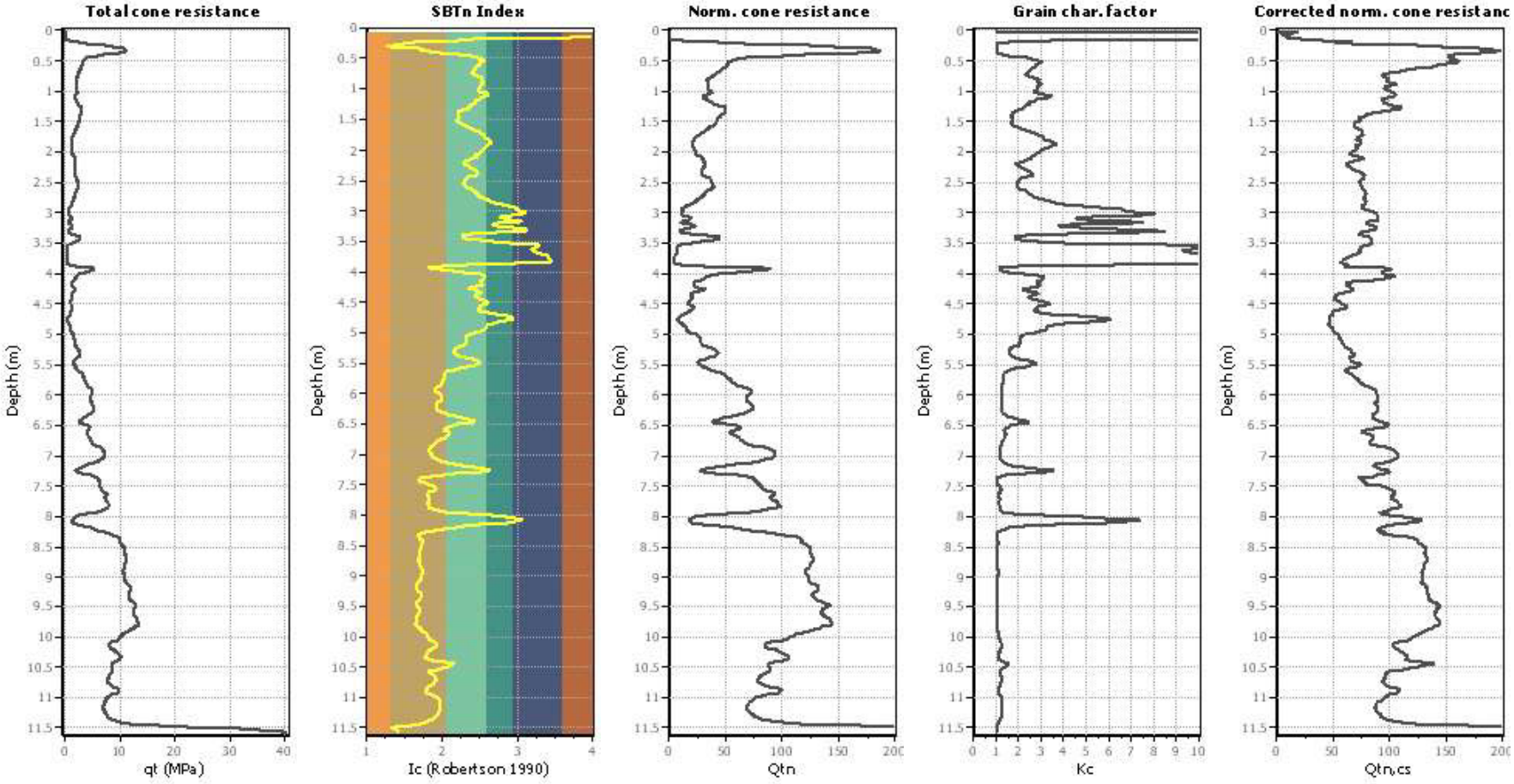

Input parameters and analysis data

Analysis method:	NCEER (1998)	Depth to water table (erthq.):	1.50 m	Fill weight:	N/A
Fines correction method:	NCEER (1998)	Average results interval:	3	Transition detect. applied:	No
Points to test:	Based on Ic value	Ic cut-off value:	2.60	K_σ applied:	Yes
Earthquake magnitude M_w:	6.20	Unit weight calculation:	Based on SBT	Clay like behavior applied:	Sands only
Peak ground acceleration:	0.50	Use fill:	No	Limit depth applied:	Yes
Depth to water table (insitu):	1.00 m	Fill height:	N/A	Limit depth:	20.00 m

Liquefaction analysis overall plot

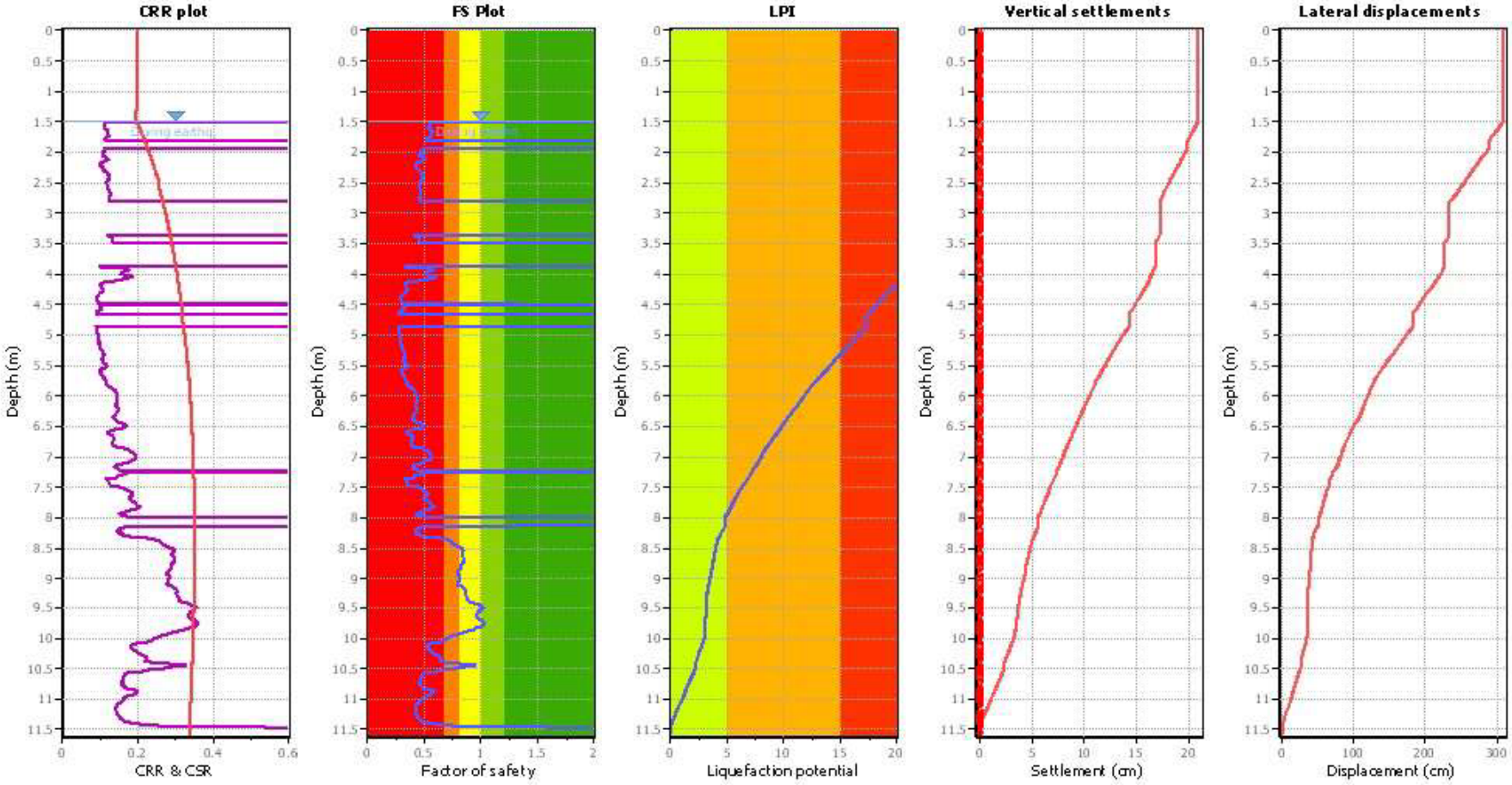

Input parameters and analysis data

Analysis method:	NCEER (1998)	Depth to water table (erthq.):	1.50 m	Fill weight:	N/A
Fines correction method:	NCEER (1998)	Average results interval:	3	Transition detect. applied:	No
Points to test:	Based on Ic value	Ic cut-off value:	2.60	K_σ applied:	Yes
Earthquake magnitude M_w:	6.20	Unit weight calculation:	Based on SBT	Clay like behavior applied:	Sands only
Peak ground acceleration:	0.50	Use fill:	No	Limit depth applied:	Yes
Depth to water table (insitu):	1.00 m	Fill height:	N/A	Limit depth:	20.00 m

F.S. color scheme

- Almost certain it will liquefy
- Very likely to liquefy
- Liquefaction and no liq. are equally likely
- Unlike to liquefy
- Almost certain it will not liquefy

LPI color scheme

- Very high risk
- High risk
- Low risk

Liquefaction analysis summary plo

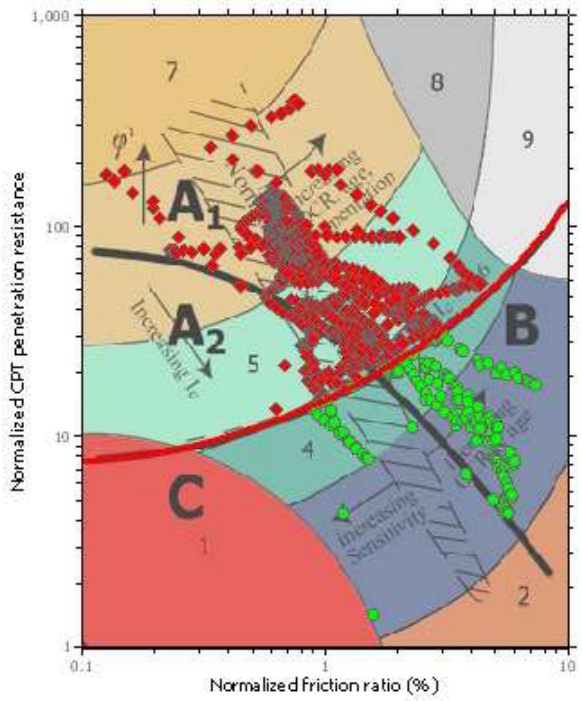

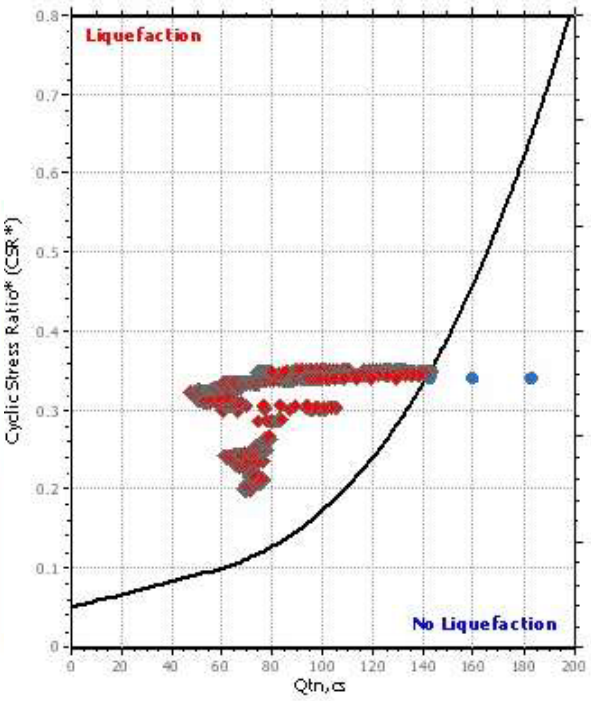

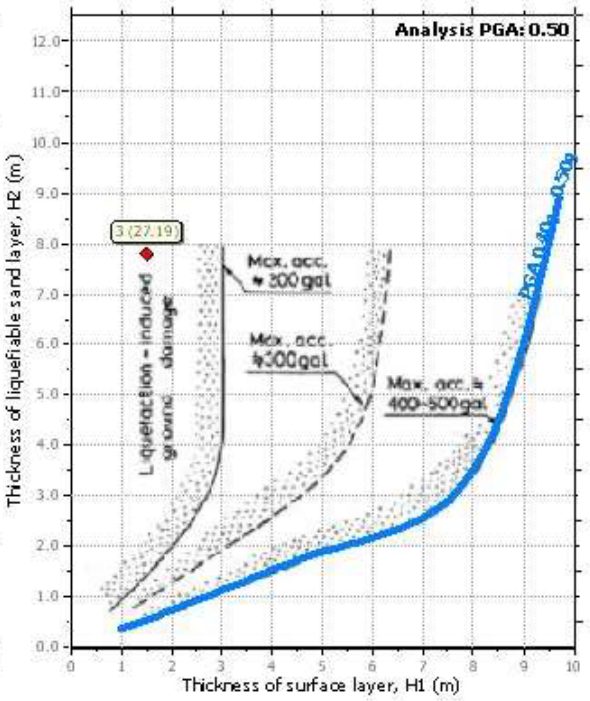

Input parameters and analysis data

Analysis method:	NCEER (1998)	Depth to water table (erthq.):	1.50 m	Fill weight:	N/A
Fines correction method:	NCEER (1998)	Average results interval:	3	Transition detect. applied:	No
Points to test:	Based on Ic value	Ic cut-off value:	2.60	K_σ applied:	Yes
Earthquake magnitude M_w:	6.20	Unit weight calculation:	Based on SBT	Clay like behavior applied:	Sands only
Peak ground acceleration:	0.50	Use fill:	No	Limit depth applied:	Yes
Depth to water table (insitu):	1.00 m	Fill height:	N/A	Limit depth:	20.00 m

Check for strength loss plots (Robertson (2010))

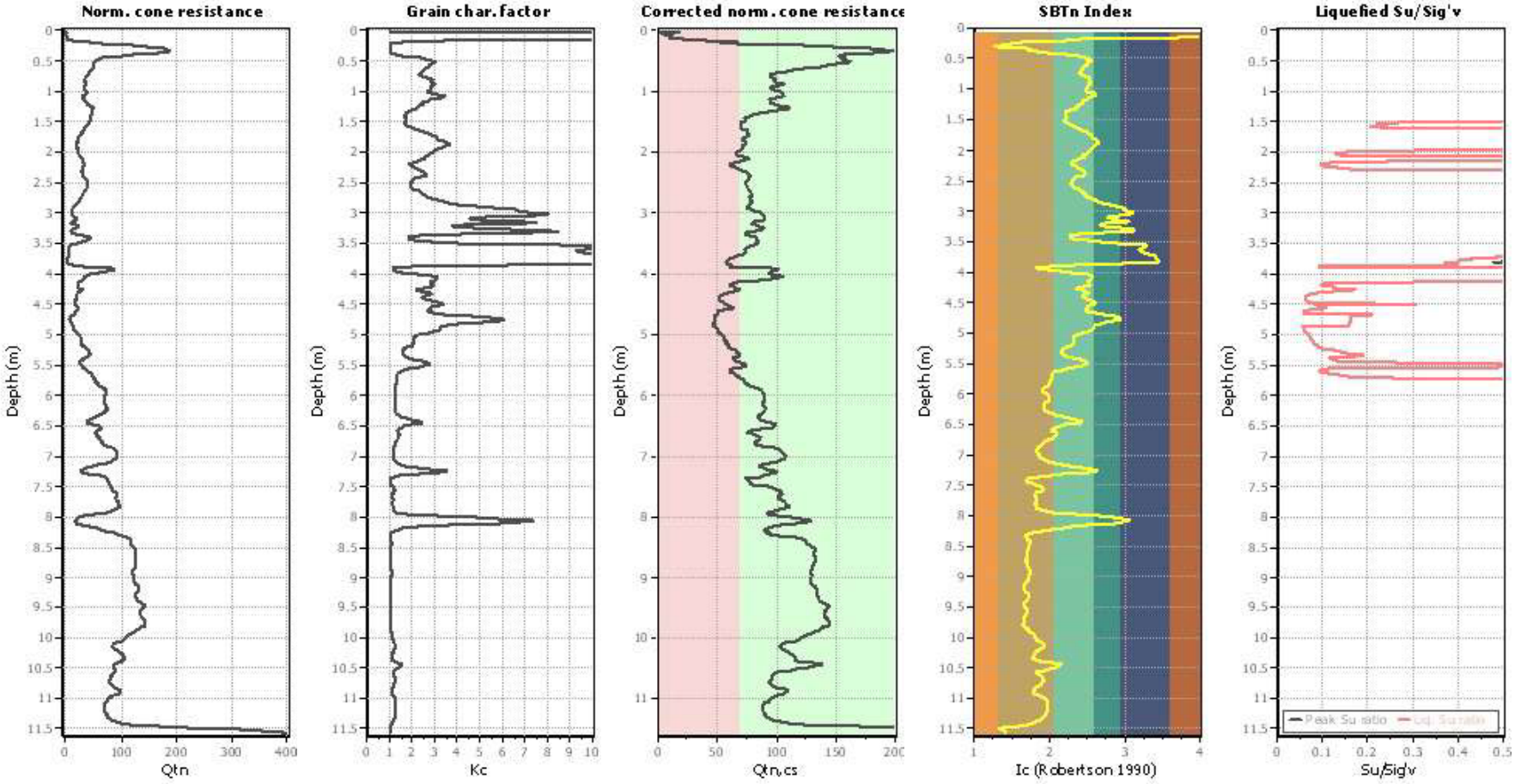

Input parameters and analysis data

Analysis method:	NCEER (1998)	Depth to water table (erthq.):	1.50 m	Fill weight:	N/A
Fines correction method:	NCEER (1998)	Average results interval:	3	Transition detect. applied:	No
Points to test:	Based on Ic value	Ic cut-off value:	2.60	K_σ applied:	Yes
Earthquake magnitude M_w:	6.20	Unit weight calculation:	Based on SBT	Clay like behavior applied:	Sands only
Peak ground acceleration:	0.50	Use fill:	No	Limit depth applied:	Yes
Depth to water table (insitu):	1.00 m	Fill height:	N/A	Limit depth:	20.00 m

GeoLogismiki
Geotechnical Engineers
Merarhias 56
http://www.geologismiki.gr

LIQUEFACTION ANALYSIS REPORT

Project title : **Location :**

CPT file : 1

Input parameters and analysis data

Analysis method:	NCEER (1998)	G.W.T. (in-situ):	1.00 m	Use fill:	No	Clay like behavior applied:	Sands only
Fines correction method:	NCEER (1998)	G.W.T. (earthq.):	1.50 m	Fill height:	N/A	Limit depth applied:	Yes
Points to test:	Based on Ic value	Average results interval:	3	Fill weight:	N/A	Limit depth:	20.00 m
Earthquake magnitude M_w:	6.20	Ic cut-off value:	2.60	Trans. detect. applied:	No	MSF method:	Method based
Peak ground acceleration:	0.50	Unit weight calculation:	Based on SBT	K_σ applied:	Yes		

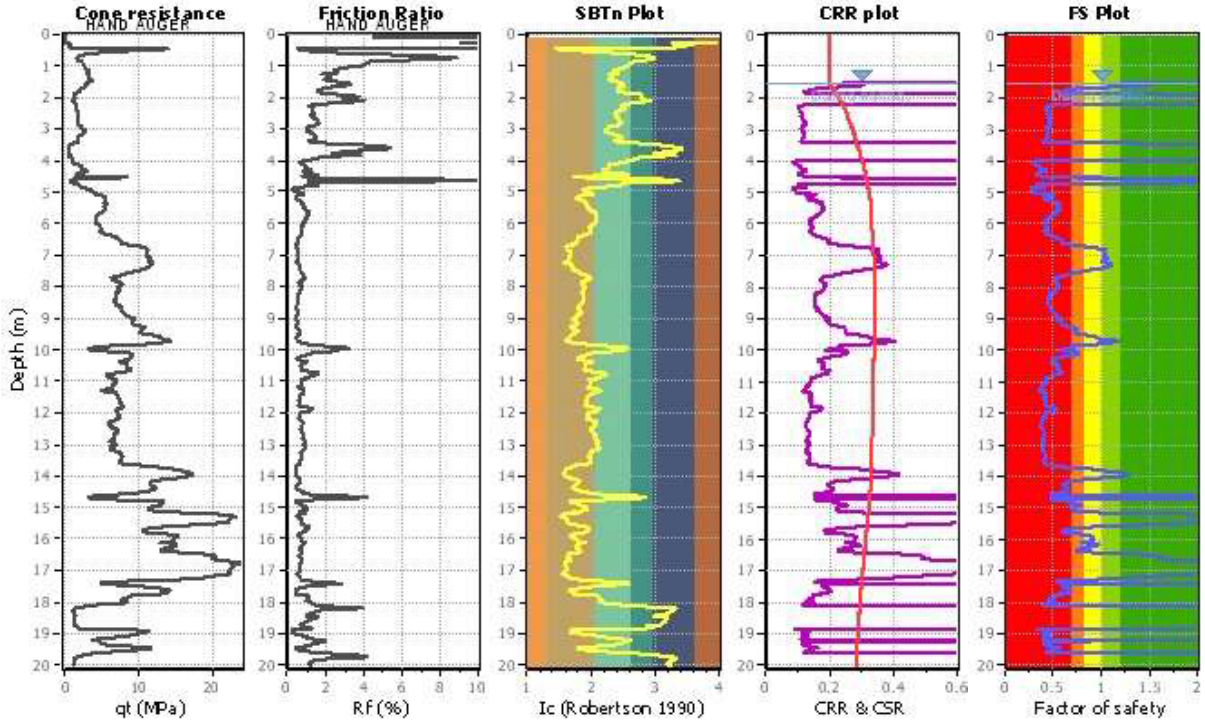

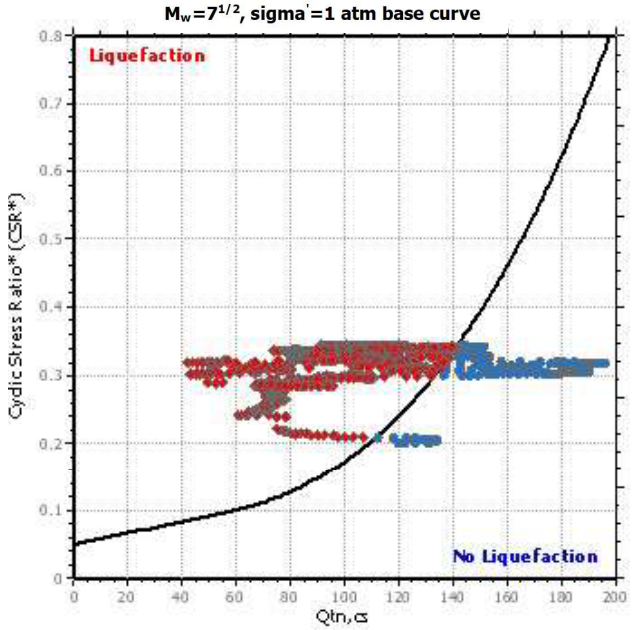

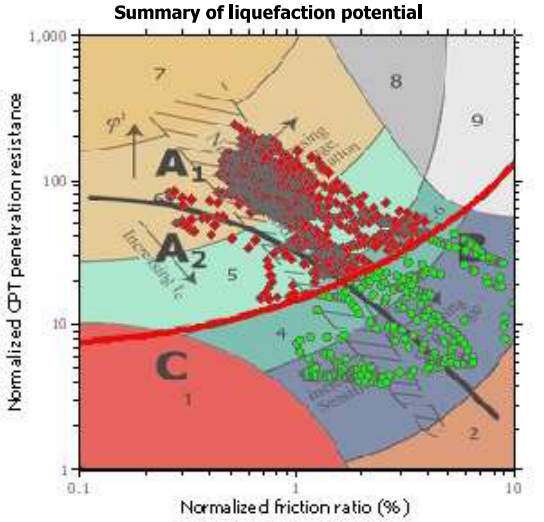

Zone A_1: Cyclic liquefaction likely depending on size and duration of cyclic loading
Zone A_2: Cyclic liquefaction and strength loss likely depending on loading and ground geometry
Zone B: Liquefaction and post-earthquake strength loss unlikely, check cyclic softening
Zone C: Cyclic liquefaction and strength loss possible depending on soil plasticity, brittleness/sensitivity, strain to peak undrained strength and ground geometry

CPT basic interpretation plo

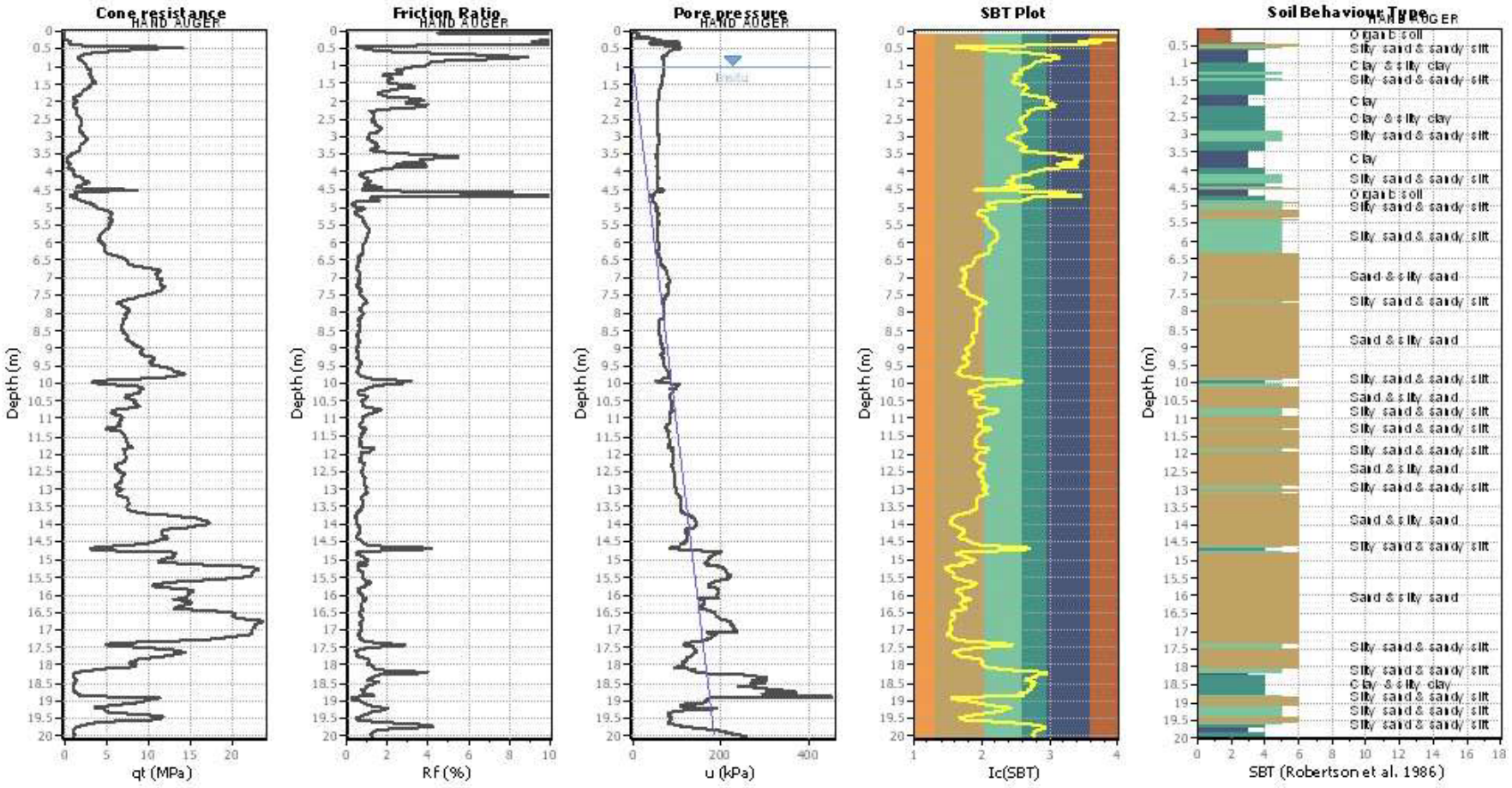

Input parameters and analysis data

Analysis method:	NCEER (1998)	Depth to water table (erthq.):	1.50 m	Fill weight:	N/A
Fines correction method:	NCEER (1998)	Average results interval:	3	Transition detect. applied:	No
Points to test:	Based on Ic value	Ic cut-off value:	2.60	K_σ applied:	Yes
Earthquake magnitude M_w:	6.20	Unit weight calculation:	Based on SBT	Clay like behavior applied:	Sands only
Peak ground acceleration:	0.50	Use fill:	No	Limit depth applied:	Yes
Depth to water table (insitu):	1.00 m	Fill height:	N/A	Limit depth:	20.00 m

SBT legend

1. Sensitive fine grained
2. Organic material
3. Clay to silty clay
4. Clayey silt to silty clay
5. Silty sand to sandy silt
6. Clean sand to silty sand
7. Gravely sand to sand
8. Very stiff sand to clayey sand
9. Very stiff fine grained

CPT basic interpretation plots (normaliz

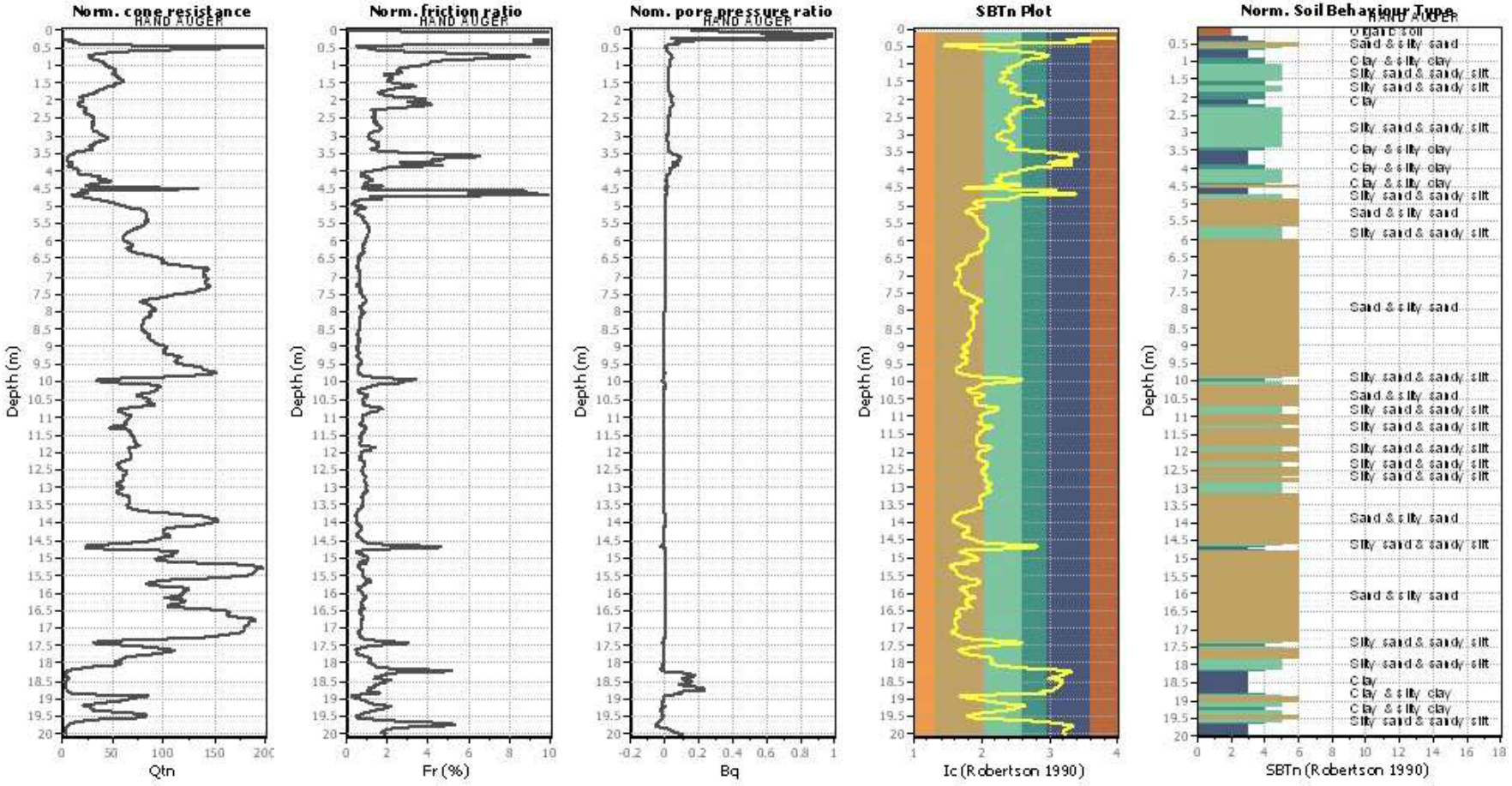

Input parameters and analysis data

Analysis method:	NCEER (1998)	Depth to water table (erthq.):	1.50 m	Fill weight:	N/A
Fines correction method:	NCEER (1998)	Average results interval:	3	Transition detect. applied:	No
Points to test:	Based on Ic value	Ic cut-off value:	2.60	K_σ applied:	Yes
Earthquake magnitude M_w:	6.20	Unit weight calculation:	Based on SBT	Clay like behavior applied:	Sands only
Peak ground acceleration:	0.50	Use fill:	No	Limit depth applied:	Yes
Depth to water table (insitu):	1.00 m	Fill height:	N/A	Limit depth:	20.00 m

SBTn legend

1. Sensitive fine grained
2. Organic material
3. Clay to silty clay
4. Clayey silt to silty clay
5. Silty sand to sandy silt
6. Clean sand to silty sand
7. Gravely sand to sand
8. Very stiff sand to clayey sand
9. Very stiff fine grained

Liquefaction analysis overall plots (intermediate resu

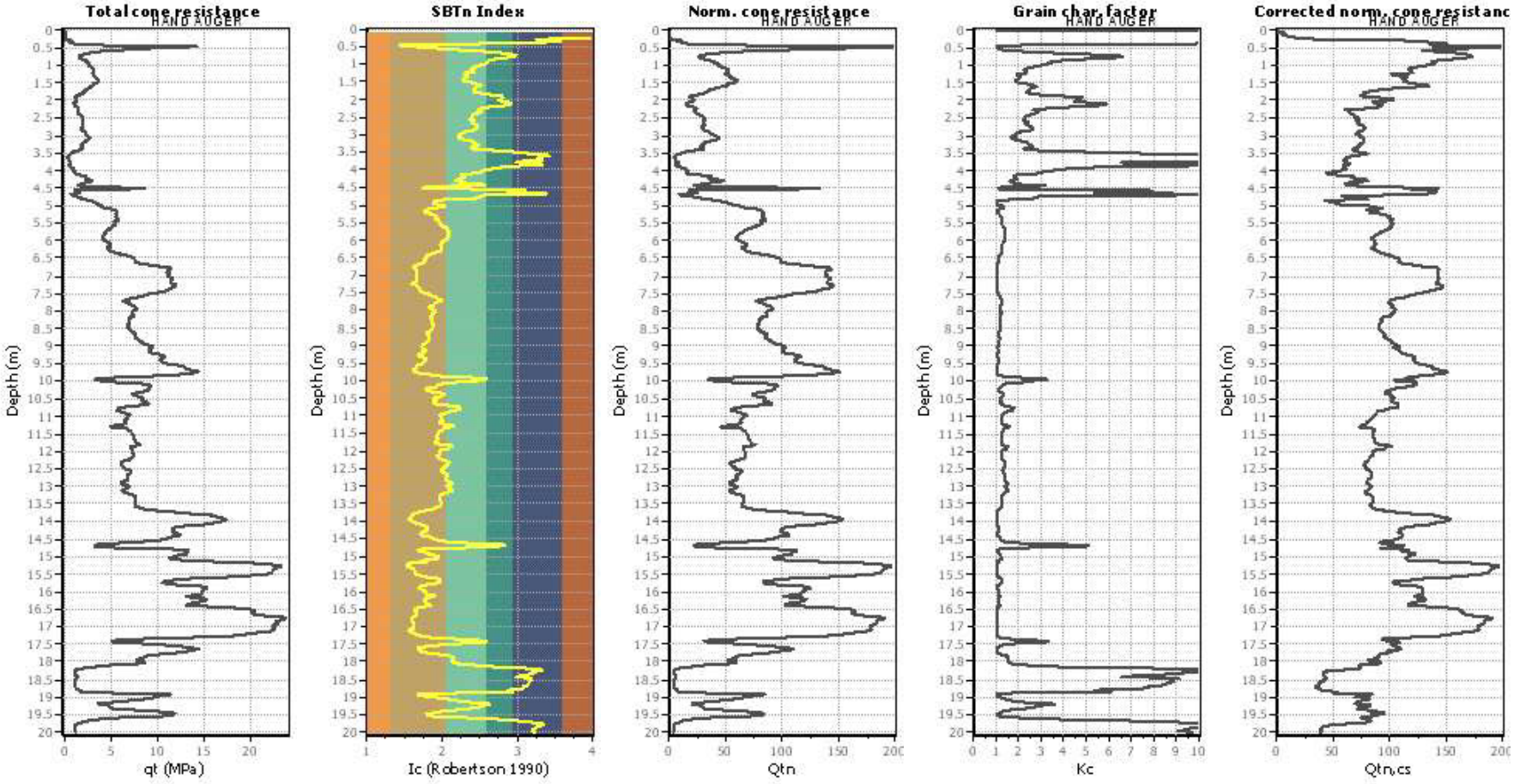

Input parameters and analysis data

Analysis method:	NCEER (1998)	Depth to water table (erthq.):	1.50 m	Fill weight:	N/A
Fines correction method:	NCEER (1998)	Average results interval:	3	Transition detect. applied:	No
Points to test:	Based on Ic value	Ic cut-off value:	2.60	K_σ applied:	Yes
Earthquake magnitude M_w:	6.20	Unit weight calculation:	Based on SBT	Clay like behavior applied:	Sands only
Peak ground acceleration:	0.50	Use fill:	No	Limit depth applied:	Yes
Depth to water table (insitu):	1.00 m	Fill height:	N/A	Limit depth:	20.00 m

Liquefaction analysis overall plot

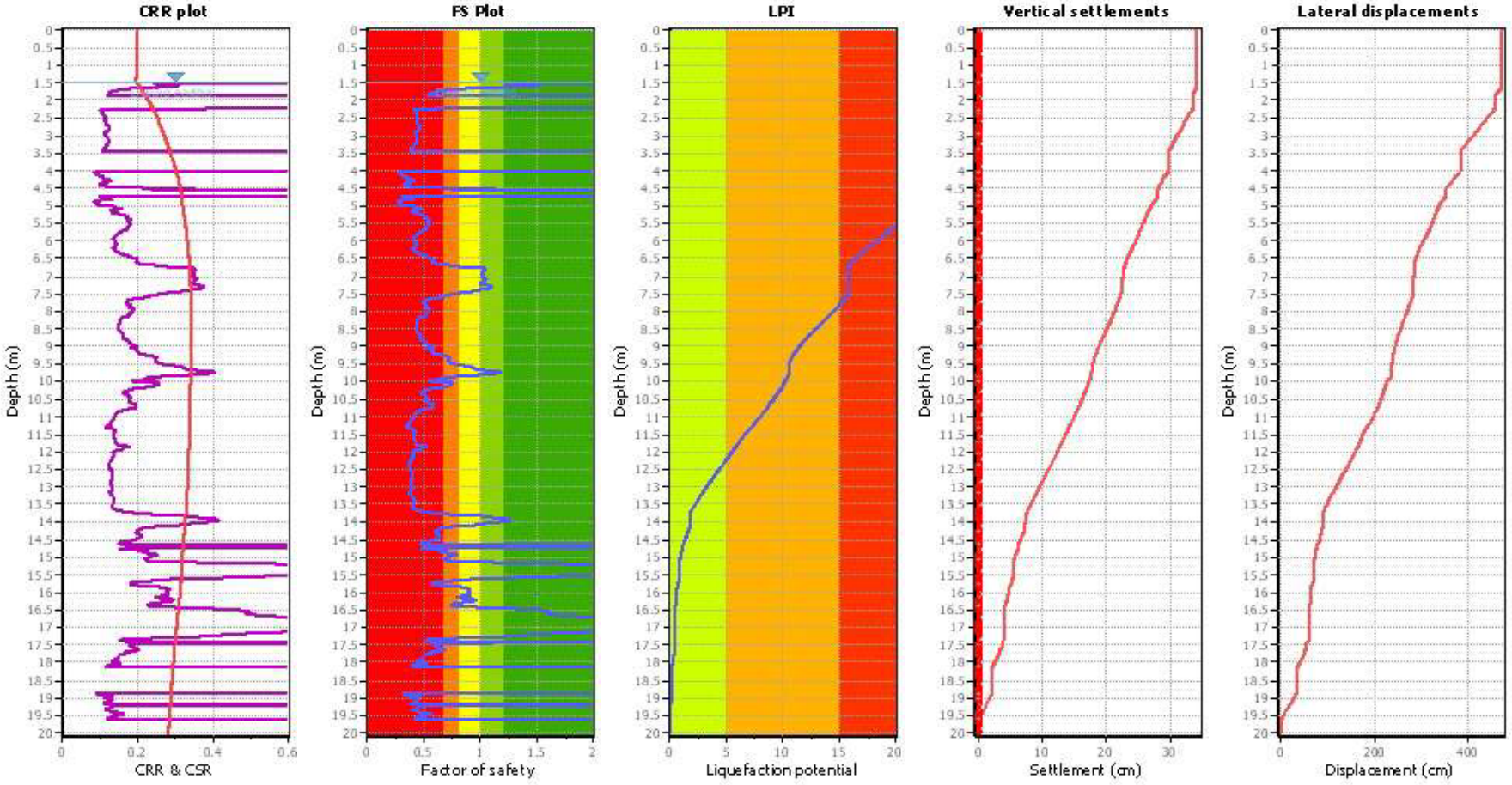

Input parameters and analysis data

Analysis method:	NCEER (1998)	Depth to water table (erthq.):	1.50 m	Fill weight:	N/A
Fines correction method:	NCEER (1998)	Average results interval:	3	Transition detect. applied:	No
Points to test:	Based on Ic value	Ic cut-off value:	2.60	K_σ applied:	Yes
Earthquake magnitude M_w:	6.20	Unit weight calculation:	Based on SBT	Clay like behavior applied:	Sands only
Peak ground acceleration:	0.50	Use fill:	No	Limit depth applied:	Yes
Depth to water table (insitu):	1.00 m	Fill height:	N/A	Limit depth:	20.00 m

F.S. color scheme

- Almost certain it will liquefy
- Very likely to liquefy
- Liquefaction and no liq. are equally likely
- Unlike to liquefy
- Almost certain it will not liquefy

LPI color scheme

- Very high risk
- High risk
- Low risk

Liquefaction analysis summary plo

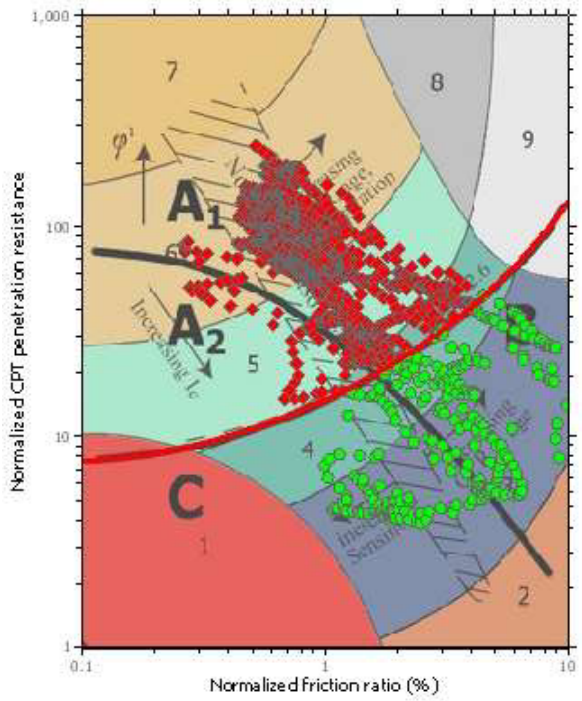

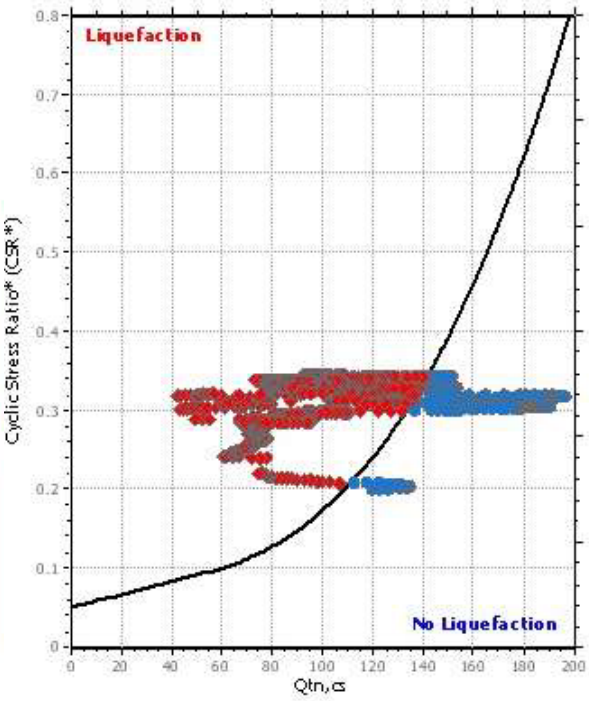

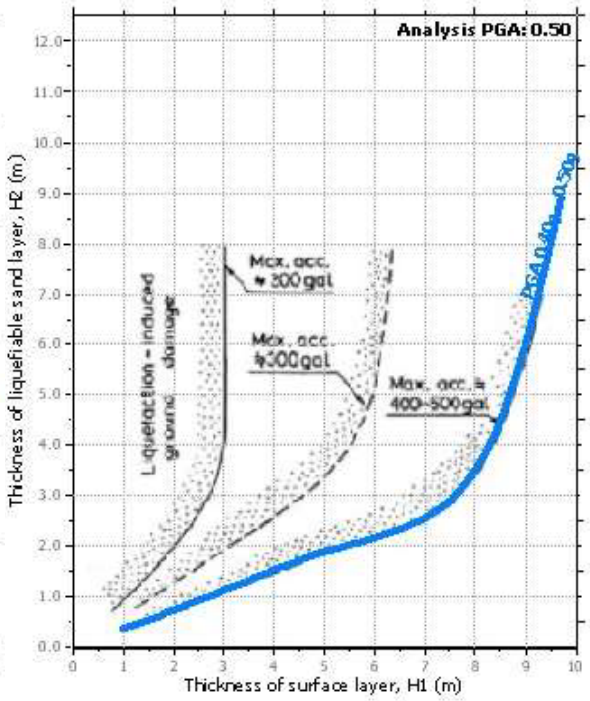

Input parameters and analysis data

Analysis method:	NCEER (1998)	Depth to water table (erthq.):	1.50 m	Fill weight:	N/A
Fines correction method:	NCEER (1998)	Average results interval:	3	Transition detect. applied:	No
Points to test:	Based on Ic value	Ic cut-off value:	2.60	K_σ applied:	Yes
Earthquake magnitude M_w:	6.20	Unit weight calculation:	Based on SBT	Clay like behavior applied:	Sands only
Peak ground acceleration:	0.50	Use fill:	No	Limit depth applied:	Yes
Depth to water table (insitu):	1.00 m	Fill height:	N/A	Limit depth:	20.00 m

Check for strength loss plots (Robertson (2010))

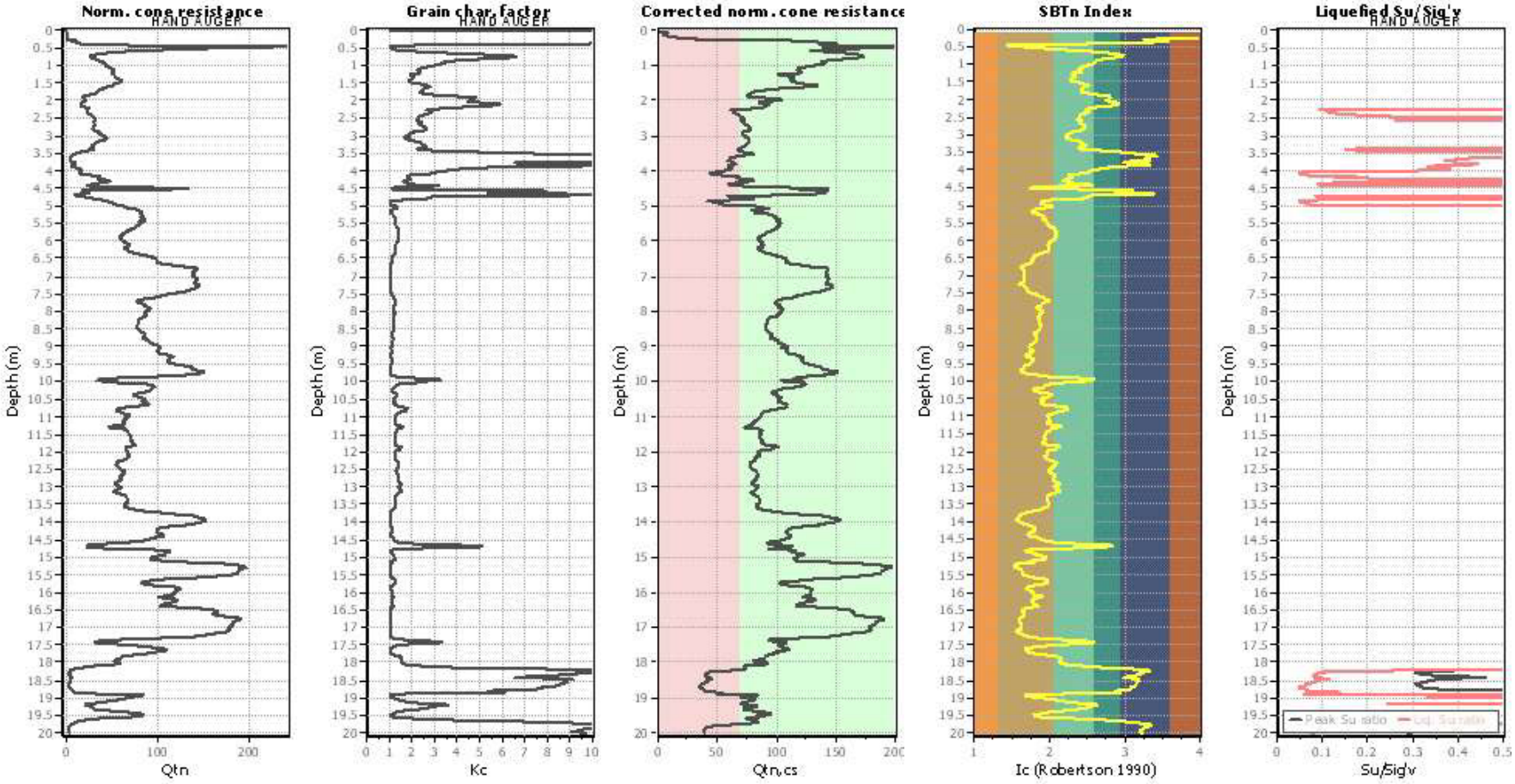

Input parameters and analysis data

Analysis method:	NCEER (1998)	Depth to water table (erthq.):	1.50 m	Fill weight:	N/A
Fines correction method:	NCEER (1998)	Average results interval:	3	Transition detect. applied:	No
Points to test:	Based on Ic value	Ic cut-off value:	2.60	K_σ applied:	Yes
Earthquake magnitude M_w:	6.20	Unit weight calculation:	Based on SBT	Clay like behavior applied:	Sands only
Peak ground acceleration:	0.50	Use fill:	No	Limit depth applied:	Yes
Depth to water table (insitu):	1.00 m	Fill height:	N/A	Limit depth:	20.00 m

GeoLogismiki
Geotechnical Engineers
Merarhias 56
http://www.geologismiki.gr

LIQUEFACTION ANALYSIS REPORT

Project title : **Location :**

CPT file : 2

Input parameters and analysis data

Analysis method:	NCEER (1998)	G.W.T. (in-situ):	1.00 m	Use fill:	No	Clay like behavior applied:	Sands only
Fines correction method:	NCEER (1998)	G.W.T. (earthq.):	1.50 m	Fill height:	N/A		
Points to test:	Based on Ic value	Average results interval:	3	Fill weight:	N/A	Limit depth applied:	Yes
Earthquake magnitude M_w:	6.20	Ic cut-off value:	2.60	Trans. detect. applied:	No	Limit depth:	20.00 m
Peak ground acceleration:	0.50	Unit weight calculation:	Based on SBT	K_σ applied:	Yes	MSF method:	Method based

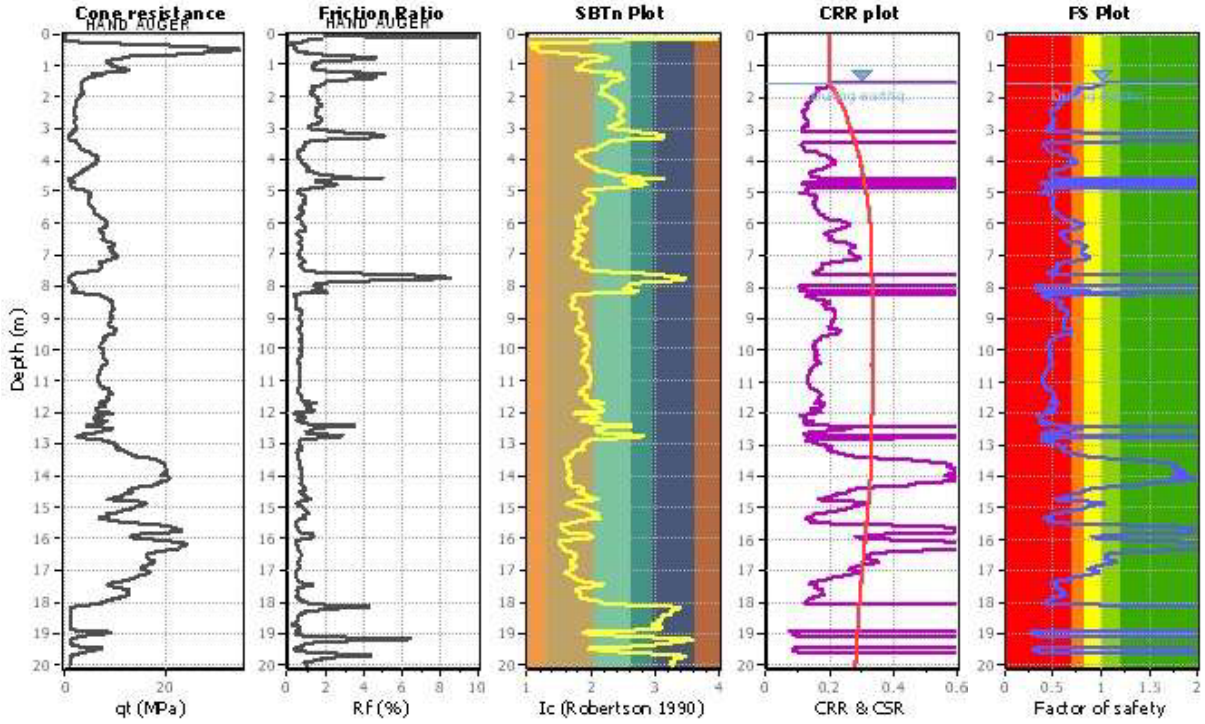

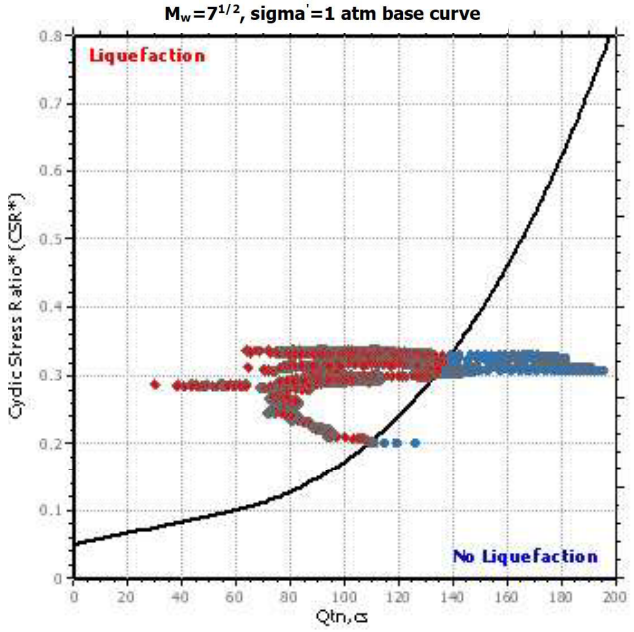

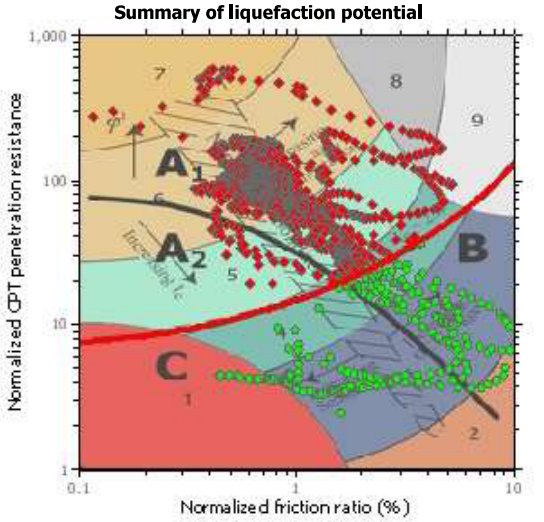

Zone A_1: Cyclic liquefaction likely depending on size and duration of cyclic loading
Zone A_2: Cyclic liquefaction and strength loss likely depending on loading and ground geometry
Zone B: Liquefaction and post-earthquake strength loss unlikely, check cyclic softening
Zone C: Cyclic liquefaction and strength loss possible depending on soil plasticity, brittleness/sensitivity, strain to peak undrained strength and ground geometry

CPT basic interpretation plo

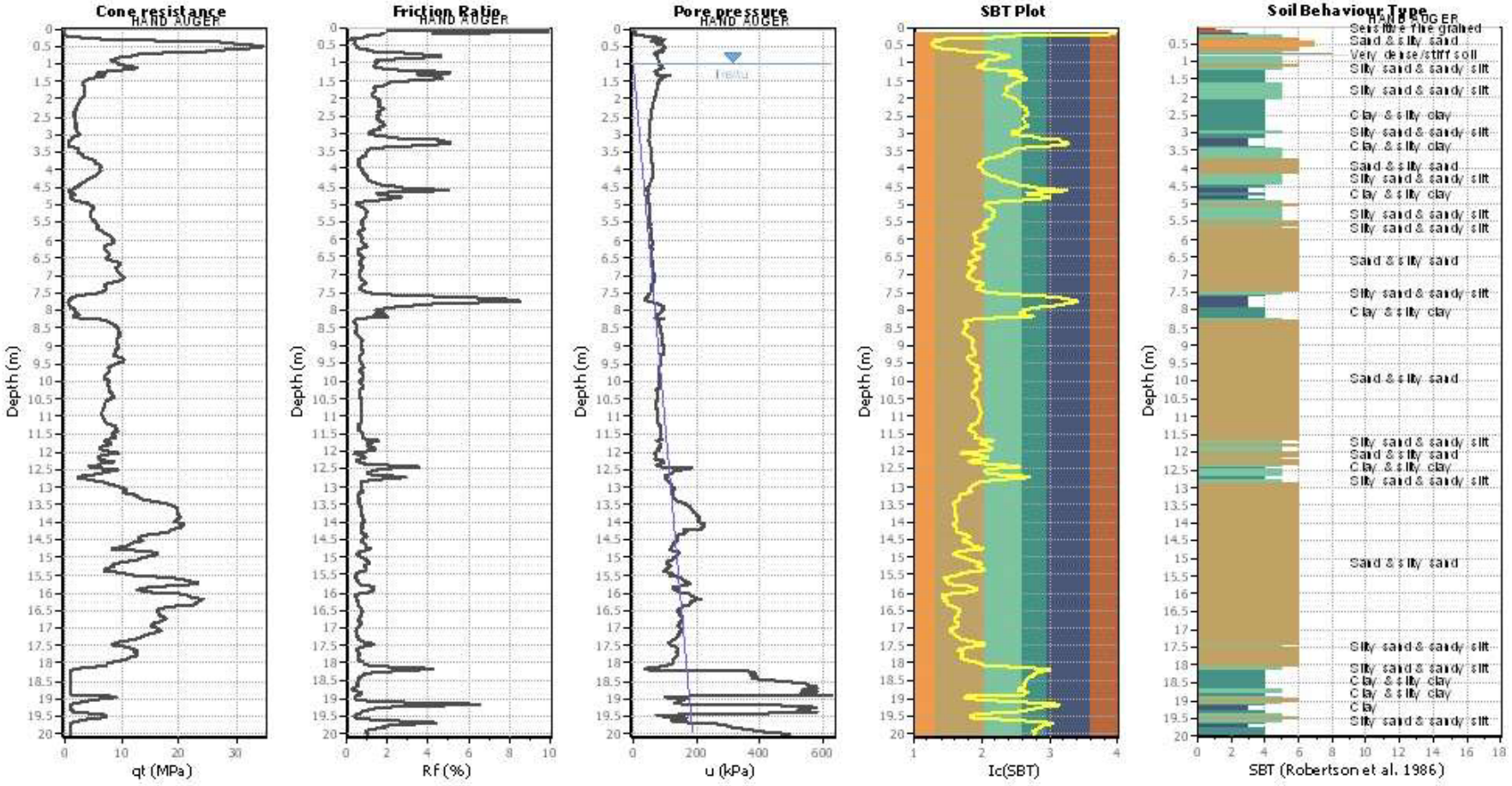

Input parameters and analysis data

Analysis method:	NCEER (1998)	Depth to water table (erthq.):	1.50 m	Fill weight:	N/A
Fines correction method:	NCEER (1998)	Average results interval:	3	Transition detect. applied:	No
Points to test:	Based on Ic value	Ic cut-off value:	2.60	K_σ applied:	Yes
Earthquake magnitude M_w:	6.20	Unit weight calculation:	Based on SBT	Clay like behavior applied:	Sands only
Peak ground acceleration:	0.50	Use fill:	No	Limit depth applied:	Yes
Depth to water table (insitu):	1.00 m	Fill height:	N/A	Limit depth:	20.00 m

SBT legend

1. Sensitive fine grained
2. Organic material
3. Clay to silty clay
4. Clayey silt to silty clay
5. Silty sand to sandy silt
6. Clean sand to silty sand
7. Gravely sand to sand
8. Very stiff sand to clayey sand
9. Very stiff fine grained

CPT basic interpretation plots (normaliz

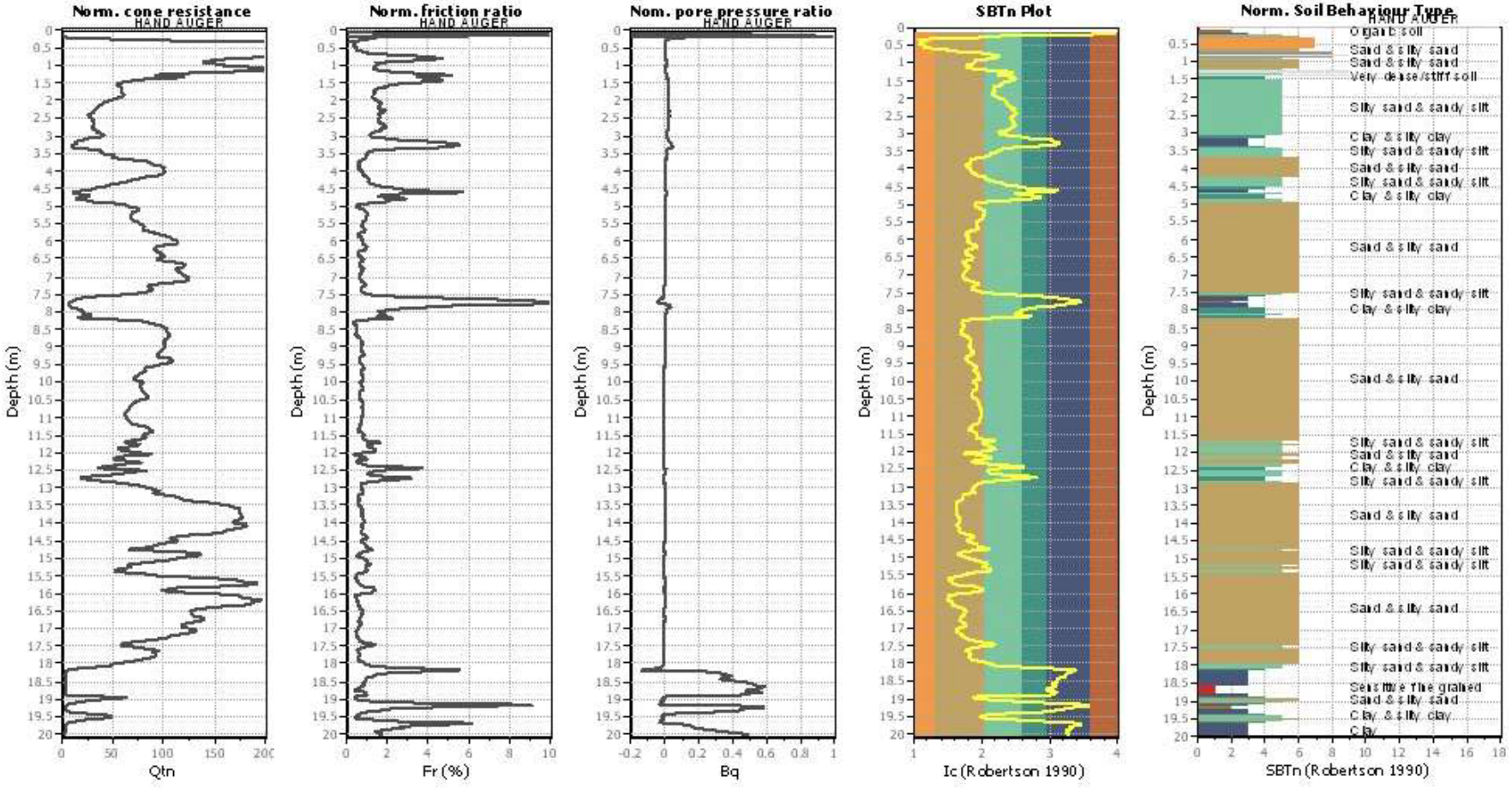

Input parameters and analysis data

Analysis method:	NCEER (1998)	Depth to water table (erthq.):	1.50 m	Fill weight:	N/A
Fines correction method:	NCEER (1998)	Average results interval:	3	Transition detect. applied:	No
Points to test:	Based on Ic value	Ic cut-off value:	2.60	K_σ applied:	Yes
Earthquake magnitude M_w:	6.20	Unit weight calculation:	Based on SBT	Clay like behavior applied:	Sands only
Peak ground acceleration:	0.50	Use fill:	No	Limit depth applied:	Yes
Depth to water table (insitu):	1.00 m	Fill height:	N/A	Limit depth:	20.00 m

SBTn legend

1. Sensitive fine grained
2. Organic material
3. Clay to silty clay
4. Clayey silt to silty clay
5. Silty sand to sandy silt
6. Clean sand to silty sand
7. Gravely sand to sand
8. Very stiff sand to clayey sand
9. Very stiff fine grained

Liquefaction analysis overall plots (intermediate resu

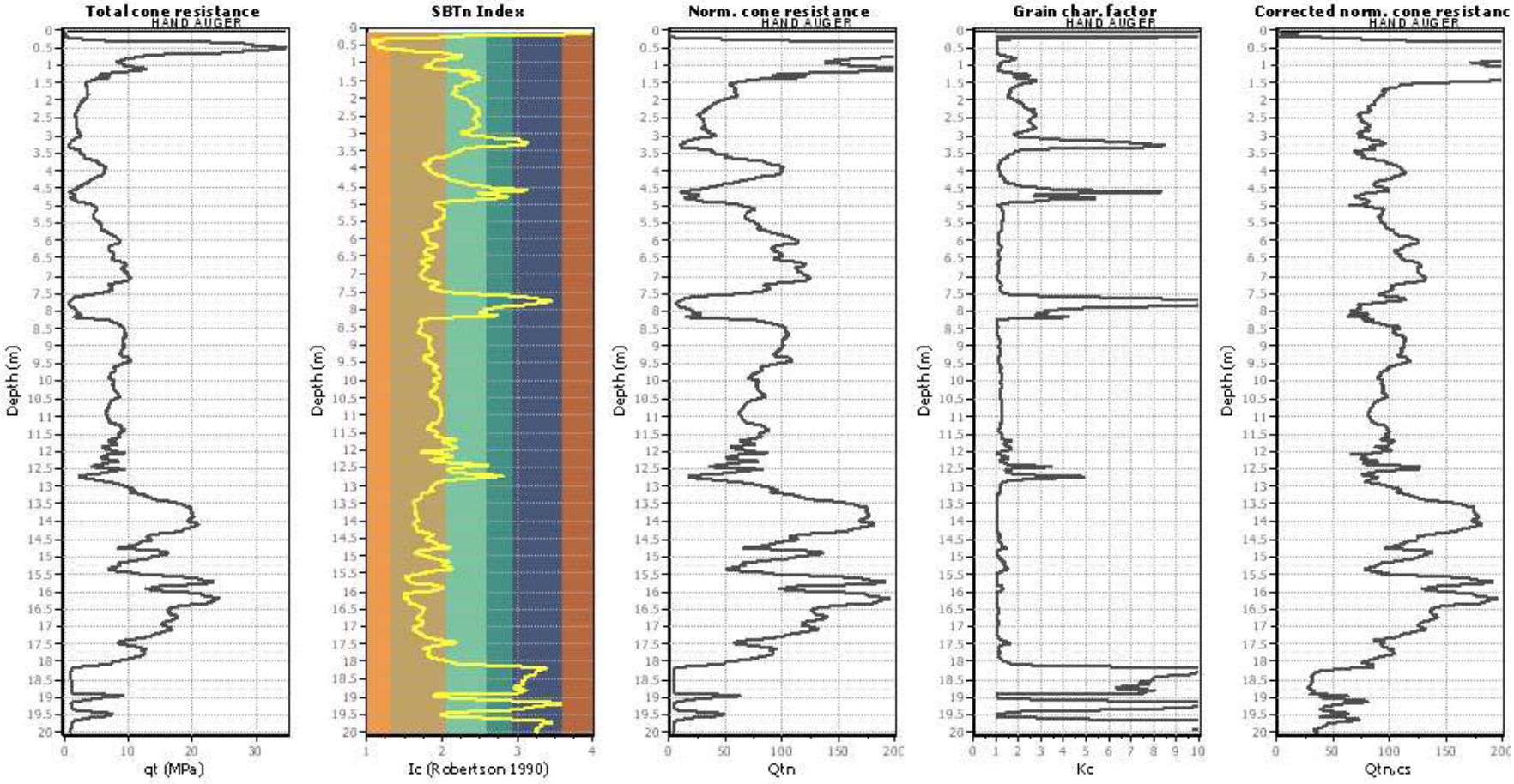

Input parameters and analysis data

Analysis method:	NCEER (1998)	Depth to water table (erthq.):	1.50 m	Fill weight:	N/A
Fines correction method:	NCEER (1998)	Average results interval:	3	Transition detect. applied:	No
Points to test:	Based on Ic value	Ic cut-off value:	2.60	K_σ applied:	Yes
Earthquake magnitude M_w:	6.20	Unit weight calculation:	Based on SBT	Clay like behavior applied:	Sands only
Peak ground acceleration:	0.50	Use fill:	No	Limit depth applied:	Yes
Depth to water table (insitu):	1.00 m	Fill height:	N/A	Limit depth:	20.00 m

Liquefaction analysis overall plot

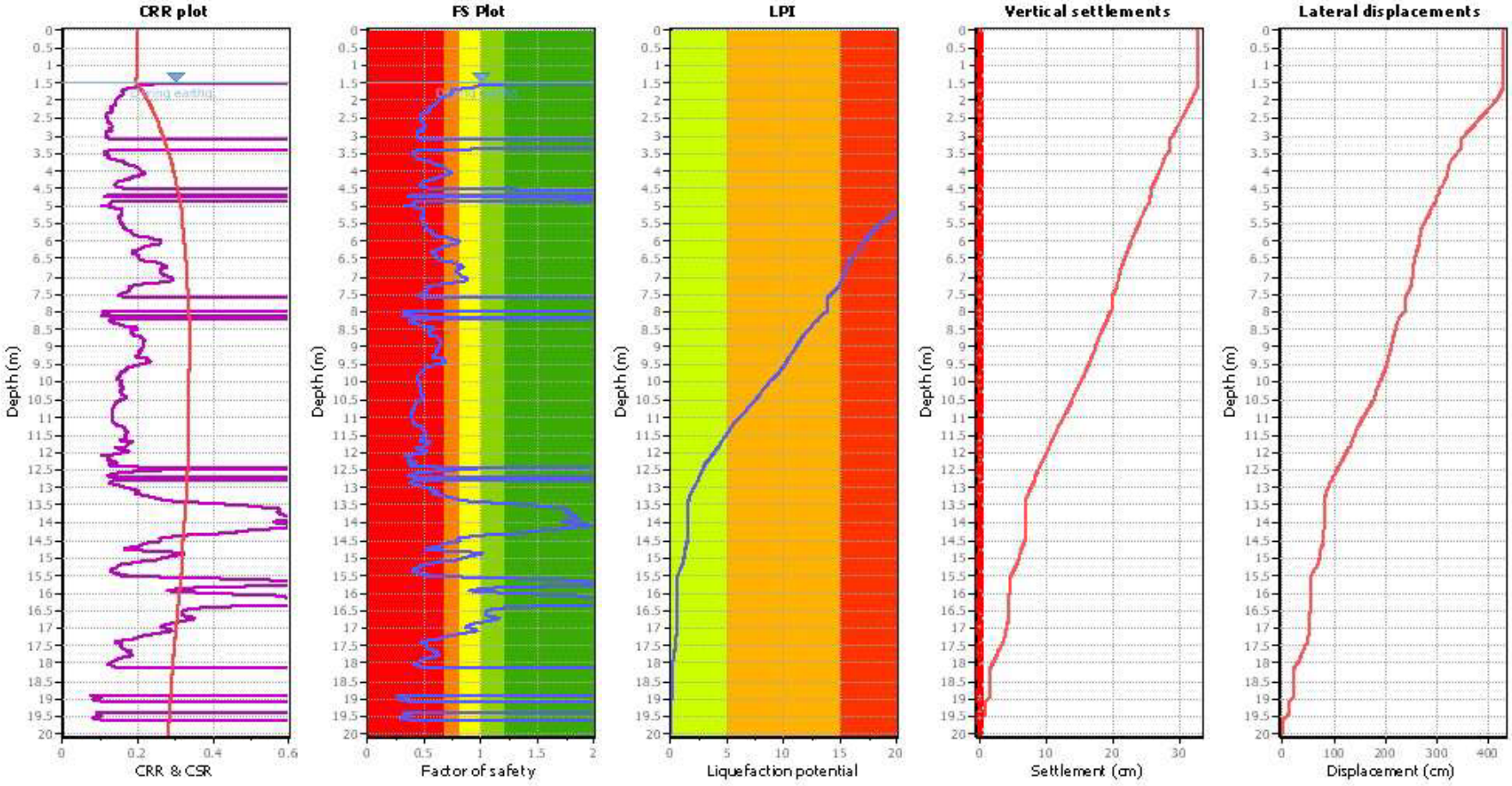

Input parameters and analysis data

Analysis method:	NCEER (1998)	Depth to water table (erthq.):	1.50 m	Fill weight:	N/A
Fines correction method:	NCEER (1998)	Average results interval:	3	Transition detect. applied:	No
Points to test:	Based on Ic value	Ic cut-off value:	2.60	K_σ applied:	Yes
Earthquake magnitude M_w:	6.20	Unit weight calculation:	Based on SBT	Clay like behavior applied:	Sands only
Peak ground acceleration:	0.50	Use fill:	No	Limit depth applied:	Yes
Depth to water table (insitu):	1.00 m	Fill height:	N/A	Limit depth:	20.00 m

F.S. color scheme

- Almost certain it will liquefy
- Very likely to liquefy
- Liquefaction and no liq. are equally likely
- Unlike to liquefy
- Almost certain it will not liquefy

LPI color scheme

- Very high risk
- High risk
- Low risk

Liquefaction analysis summary plo

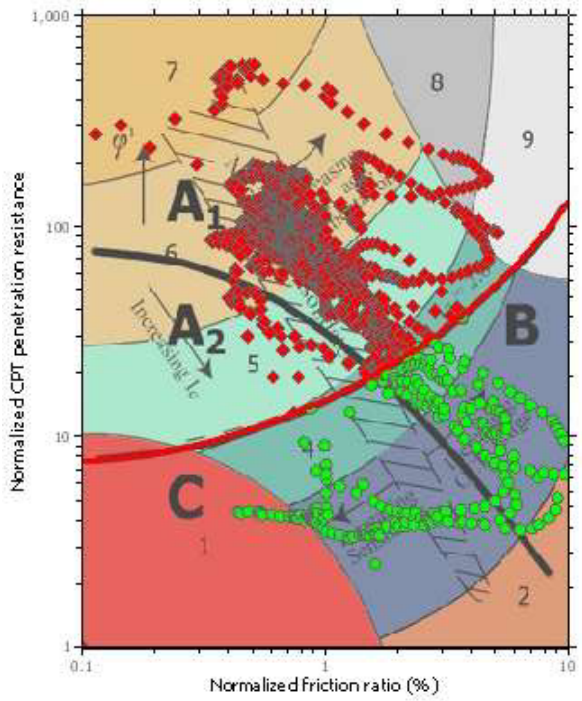

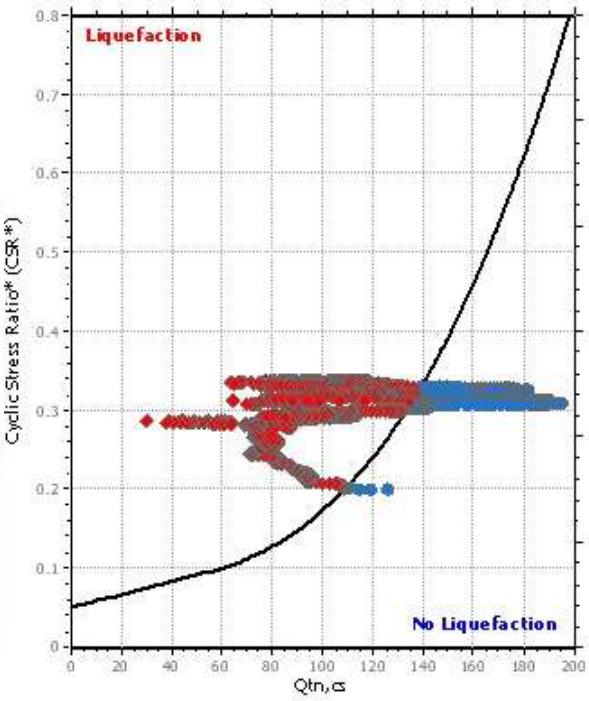

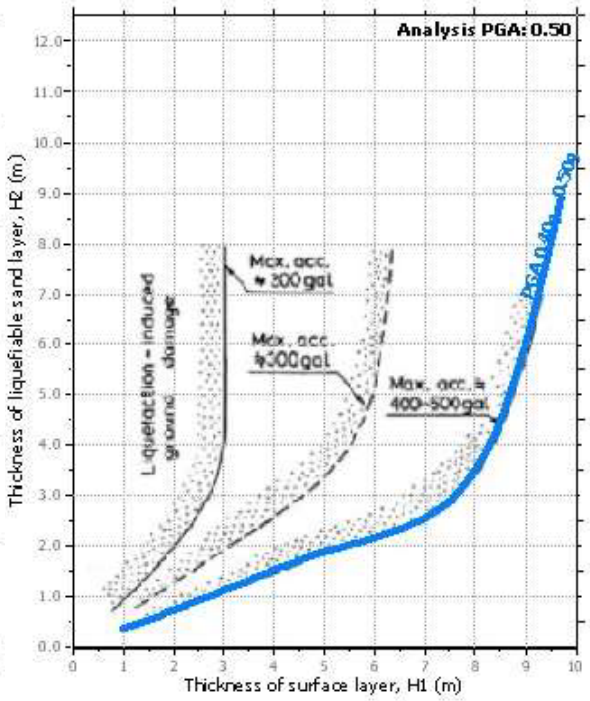

Input parameters and analysis data

Analysis method:	NCEER (1998)	Depth to water table (erthq.):	1.50 m	Fill weight:	N/A
Fines correction method:	NCEER (1998)	Average results interval:	3	Transition detect. applied:	No
Points to test:	Based on Ic value	Ic cut-off value:	2.60	K_σ applied:	Yes
Earthquake magnitude M_w:	6.20	Unit weight calculation:	Based on SBT	Clay like behavior applied:	Sands only
Peak ground acceleration:	0.50	Use fill:	No	Limit depth applied:	Yes
Depth to water table (insitu):	1.00 m	Fill height:	N/A	Limit depth:	20.00 m

Check for strength loss plots (Robertson (2010))

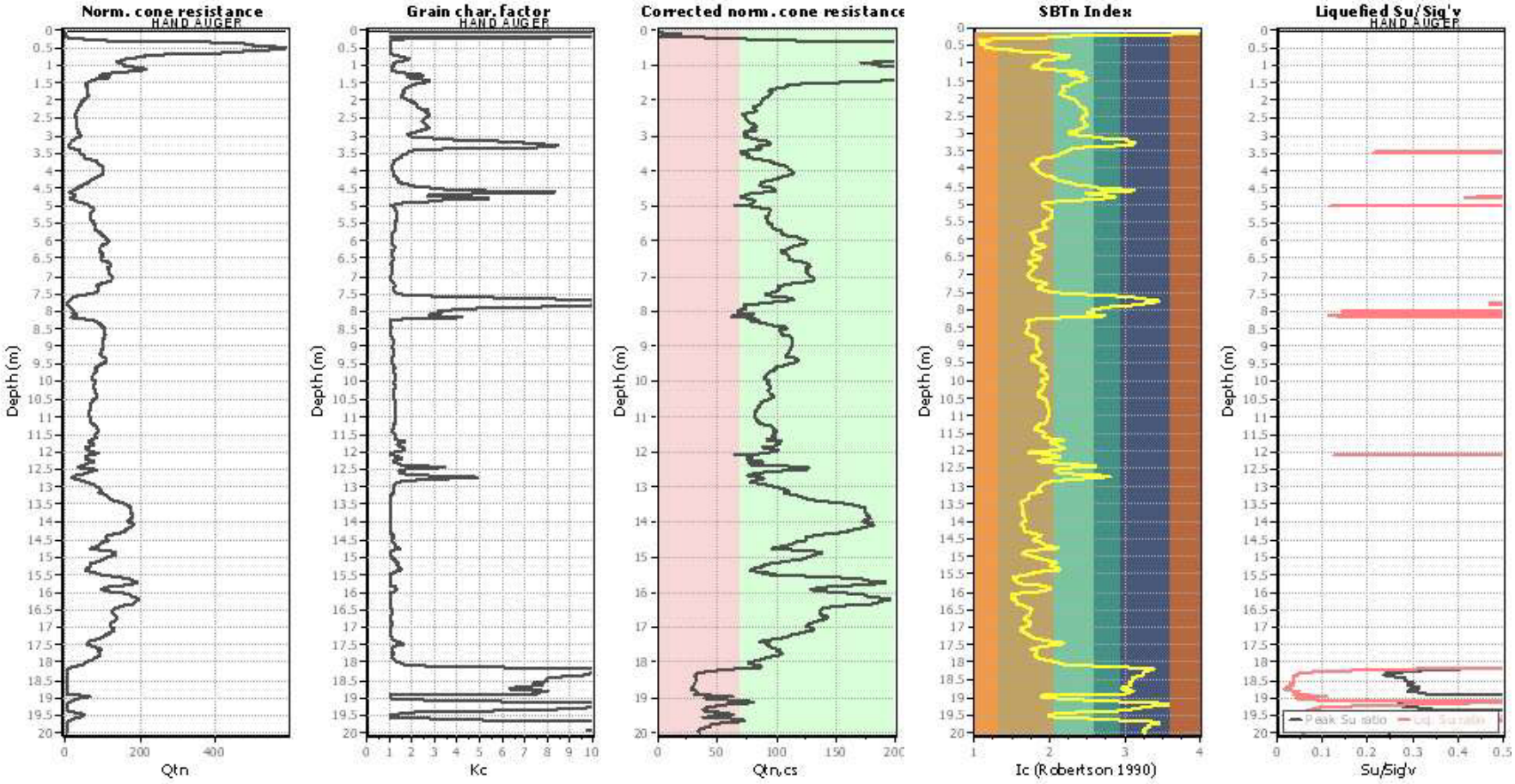

Input parameters and analysis data

Analysis method:	NCEER (1998)	Depth to water table (erthq.):	1.50 m	Fill weight:	N/A
Fines correction method:	NCEER (1998)	Average results interval:	3	Transition detect. applied:	No
Points to test:	Based on Ic value	Ic cut-off value:	2.60	K_σ applied:	Yes
Earthquake magnitude M_w:	6.20	Unit weight calculation:	Based on SBT	Clay like behavior applied:	Sands only
Peak ground acceleration:	0.50	Use fill:	No	Limit depth applied:	Yes
Depth to water table (insitu):	1.00 m	Fill height:	N/A	Limit depth:	20.00 m